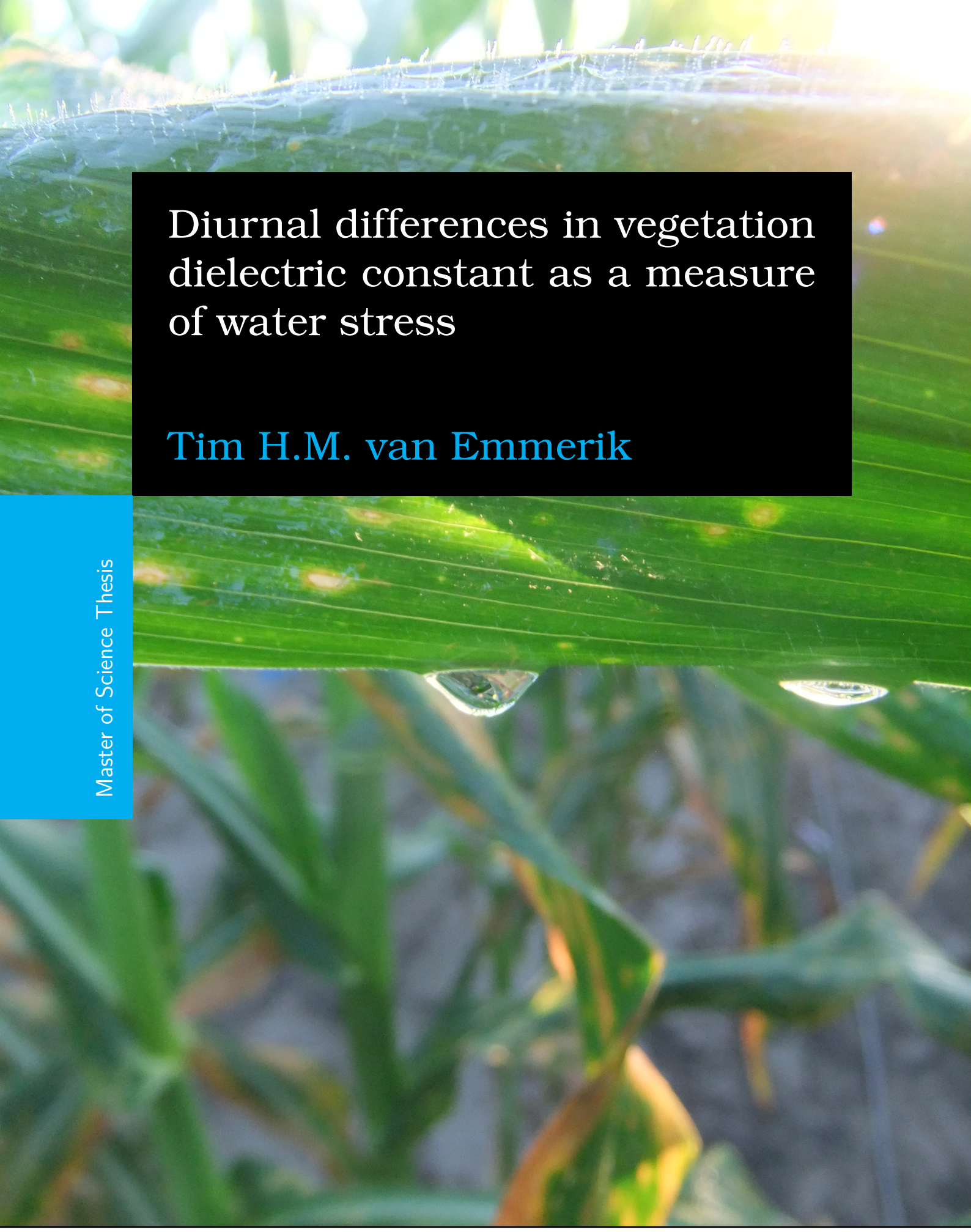

Diurnal differences in vegetation dielectric constant as a measure of water stress

Tim H.M. van Emmerik

Master of Science Thesis

TU Delft Delft University of Technology

Diurnal differences in vegetation dielectric constant as a measure of water stress

Master of Science Thesis

For the degree of Master of Science in Civil Engineering at Delft University of Technology

Tim H.M. van Emmerik

March 13, 2013

Committee
Prof.dr.ir. N.C. van de Giesen — Delft University of Technology
Dr.ir. S.C. Steele-Dunne — Delft University of Technology
Dr. J. Judge — University of Florida
Prof.dr. M. Menenti — Delft University of Technology

Faculty of Civil Engineering and Geosciences (CEG) · Delft University of Technology

Abstract

Currently, vegetation is considered a barrier to soil moisture retrieval by both passive and active remote sensing missions. Microwave emission and backscattering of vegetation is driven by the vegetation dielectric constant, which is a function of vegetation water content. The latter is a measure of root zone water availability. Understanding the variation in dielectric properties of vegetation will contribute to soil moisture retrieval using microwaves in vegetated areas. This study presents a unique dataset of the diurnal pattern of the leaf dielectric properties, which was linked to vegetation water content and water stress.

Using a microstrip line sensor, in-vivo dielectric property measurements were conducted on three maize leaves (leaf 8, 10 and 12) from 8 to 19 October 2012. A correlation was found between the resonant frequency of the microstrip line and the leaf water content of maize. This showed that a decrease of leaf water content during the day led to an increase of the resonant frequency.

Water stress was quantified by calculating the evaporation deficit and by measuring the soil water tension at 30cm and 50cm depth. It was found that the diurnal difference in resonant frequency of the sensor at leaf 8 increased in similar fashion as the soil tension and evaporation deficit, which indicates a correlation between water stress and vegetation dielectric properties. The upper leaves 10 and 12 responded differently to increased water stress. The diurnal difference in resonant frequency of the sensor at leaf 10 and 12 decreased or was non-existent. The dielectric measurements revealed the complex reaction of vegetation to water stress and pointed out many opportunities for further research.

The water-cloud model was used to demonstrate the impact of changing water content at different frequencies and polarizations. For L-,C-,X-,K_u- and K_a-band the sensitivity of radar backscatter to soil moisture and vegetation water content was modeled. This showed that at L-band, for low volumetric soil moisture (<0.2) vegetation is the main contributor to total backscatter. At higher frequencies backscatter was mainly sensitive to leaf water content.

Time series analysis of modeled radar backscatter, based on field measurements of vegetation water content and soil moisture, showed that using the standard water-cloud model, the simulated diurnal difference in backscatter was small (0.05 dB). A modified water-cloud model was formulated that takes into account leaf and stalk water content separately. This model

simulated a higher diurnal difference in backscatter (0.8 dB) and corresponded better to the trend in decreasing leaf water content and increasing water stress.

This study presented interesting results that will hopefully stimulate follow up research projects. As a first step, it already revealed possibilities of using vegetation as an indicator for soil moisture, vegetation water status and water stress. The eventual possibilities of monitoring this at a global scale will lead to new innovative applications that will contribute to improving the state of the world.

Table of Contents

List of Figures

List of Tables

Acknowledgements

There are so many people to thank that I don't know where to start. Let's start by dividing them into a number of categories: (1) supervisors, (2) facilitators and (3) supporters.

Research wise the people from the first category are most important, so let's begin with them. As the main supervisor and master mind behind this research, I want to thank Susan Steele-Dunne for giving me the opportunity to work on this topic. I have learned a lot about conducting research, fieldwork, writing, remote sensing and Ireland. Thanks to professor Nick van de Giesen for trusting me in bringing this study to a successful ending. Nick already sent me all around the globe, but the fieldwork in Florida was an experience of a lifetime. Furthermore, I'm grateful to professor Massimo Menenti for all his useful critique from the remote sensing point of view.

In the twilight zone between category (1) and (2), I want to thank Jasmeet Judge. Without her the fieldwork in Florida wouldn't have been possible. I'm also thankful for her comments throughout the fieldwork campaign and as a supervisor while writing my thesis. From the Center of Remote Sensing at the University of Florida I want to thank Pat, Daniel, Pang, Karthik, Tara, Sherry and Ella for allowing me to play along in the football league, my birthday cake and all their help during the fieldwork. In particular I'd like to thank Pat for the best last day of fieldwork ever (and yes, I made it home). A special thanks to Heather Christian who offered me a fine room throughout my entire stay in Gainesville. Not only did she let me stay in her awesome house, she also made sure I had the perfect all American experience! With county fairs, BBQ, fried butter and bowling it was a success.

Then the last group, the supporters. From category (3) I like to thank everybody from the 'old' room 4.84 (i.e. members of the 4.84 Facebook page). Thanks Dirk, Emma, Franca, Laurene, Marleen and Wouter for making coffee, getting tea, brining lunch, motivating & distracting me, the laughs, cries and beers. Special thanks to Emma for her endless efforts to correct this thesis. Finally I want to thank the ZAB, the best house I could ever wish for. Arie, Floor, Gerben, Marte, Ruben, Piers and Sylvia, thanks for the occasional karaoke & cocktail get-togethers. They were very inspirational and definitely helped me getting through the graduation process. Last but not least thanks to all of those whose name I'm forgetting.

Chapter 1

Introduction

This thesis is about a first step in exploring the potential of using vegetation as a source of information for soil moisture retrieval and water stress monitoring by means of microwave remote sensing. The findings of this research are based on field measurements of the dielectric properties of maize. This chapter will first discuss the importance of soil moisture in hydrology, flood and drought prediction and vegetation. Second, it will be shortly discussed how soil moisture is retrieved using microwave remote sensing and how vegetation is seen as a barrier in this. However, vegetation can actually be a source of information rather than an obstruction, which will be discussed in the following section. Subsequently, a more complete theoretical background will be presented on the relations between remote sensing, soil moisture, vegetation and water stress. Finally, the scope of this research, the research questions and the hypotheses are presented.

1-1 Importance of soil moisture

Soil moisture is considered as the water present in the unsaturated zone [1] and is one of the most important variables within the hydrological cycle. Not only is its availability crucial for the livelihood of vegetation, it also plays a prominent role in the water and energy balances. Soil moisture has a significant influence on temperature, precipitation, evaporation, transpiration and hence the climate [2]. The amount of soil moisture determines the probability of the occurrence of flood and droughts. For seasonal climate forecasting soil moisture is rather crucial [3]. Including information on soil moisture anomalies result in better forecasts of e.g. precipitation and air temperature.

Climate, food security, occurrence of floods and water availability are all connected to soil moisture. However, to reveal which processes are linking them, a better understanding of soil moisture behavior is required. To summarize, global soil moisture data will (1) contribute to understanding and estimating water, energy and carbon cycles, (2) improve weather and climate forecasting and (3) open possibilities for flood prediction and drought monitoring on a global scale.

Water and energy balance

Soil moisture is one of the few directly observable hydrological variables that has an important role in both the surface energy and water balance [4]. Soil moisture is a main source for evaporation and hence a key variable in the land energy and water balance [5],[6], because root zone soil moisture is the water that goes into the atmosphere via e.g. vegetation.

Soil moisture influences near-surface air temperature and limits the total energy to be used by latent heat [7], and thus determines how much energy is availably for sensible heating (i.e. changing near-surface air temperature). Because soil moisture has impact on the latent heat flux (i.e. evaporation), soil moisture and precipitation are indirectly coupled, a hypothesis confirmed by recent studies (e.g. [8]; [9]). Soil moisture influences evaporation, on which precipitation is depending. The amount of precipitation fallen again influences soil moisture. The albedo is influenced by soil moisture. This dependency consists of three mechanisms [7], i.e. changes in bare soil albedo with soil moisture content, changes in vegetation albedo with soil moisture content and changes in exposed bare soil fraction due to drought impacts on vegetation (orientation and total area of leaves).

Both albedo (reflection of short wave radiation) and long wave radiation emission are depending on the surface type, vegetation and soil moisture content. Hence, if the amount of water present in the unsaturated zone changes, the surface radiation balance will change, causing an alteration of the energy budget.

In parsimonious hydrological rainfall-runoff models, often no forcing or validation data is available considering soil moisture content. If this information would be available, a better prediction of the to-be-expected runoff mechanisms could be made [10]. Soil moisture controls the partitioning of rainfall in runoff and infiltration, which has a major impact on runoff responses in catchments [11]. How much precipitation infiltrates or runs off due to saturated soil could be forecasted and floods could be predicted, when soil moisture is monitored more closely.

Besides applications on global scale or in our own (developed) environment, a broad range of opportunities for developing countries arises. In developed areas, policy regarding food security, flood protection and use of surface- and groundwater sources are based on in-situ measurements of precipitation, evaporation, river flow and groundwater levels. However, a lack of gauging stations can be found in developing countries. With the number of remote sensing application rising, monitoring of soil moisture would be a great contribution. Eventually, most important water and energy fluxes can be monitored, also in typical ungauged basins (mostly in developing countries) (e.g.[12],[13],[14]). This means that areas where famines, floods, droughts and aquifer depletion are most occurring, new strategies to fight these challenges can be based on remote sensing data.

Vegetation and water stress

The unsaturated (or vadose) zone is also the layer from which roots of vegetation take up water. When a lack of water occurs in the root zone, we speak of water stress. In that case vegetation cannot take as much water up as required. Water stress can have significant impact on the growth and development of plants and for agricultural crops, water stress might result in a decreased yield. Many ecosystems suffer from water stress, which is controlled by the

temporal fluctuations of soil moisture ([15],[16]). Although other sources of stress affect plant development as well (e.g. salinity, temperature, nutrient availability, light), soil moisture is the most important resource that affects vegetation growth and development ([15],[16]). Reduced water availability in the root zone decreases plant transpiration, leading to a drop in turgor pressure, causing serious irreversible damage to vegetation. A more detailed description of the effect of water stress on vegetation will be presented later on.

Accurate estimates of root zone water availability for vegetation would be very useful for agricultural purposes and interesting applications are plentiful. For example, more efficient irrigation schemes could be designed, based on remotely sensed root zone water content estimates. Furthermore, root zone water availability could contribute to detecting water stress in an early stage, allowing mitigation of its potential catastrophic effects.

1-2 Microwave remote sensing of the land surface

Remote sensing techniques are increasingly important for the study of land surface. Advantages are that remote sensing techniques provide data on a large scale and are non-destructive. Most remote sensing techniques are based on the fact that all materials emit radiation as a function of their temperature, if higher than the absolute zero (0 K). Emitted radiation can be separated in different band widths, for which different sensors are susceptible (radar, visible radiation, thermal radiation, infrared, etc.). Several missions exist that monitor the earth surface using optical, thermal or microwave remote sensing. Microwaves have three main advantages over other types of remote sensing. First, microwaves have the ability to penetrate canopies and soils, providing volumetric information that is not available with visible frequencies (e.g. when a 'normal' photo is taken, you only see the vegetation crown). Second, microwave signals are strongly sensitive to water content in soil and vegetation and can therefore be used as indicators of water status. Third, microwaves can continue with cloud cover and at night [17], not being disturbed by clouds, water vapor and aerosols. Retrieving soil moisture above densely vegetation areas is however not yet possible. Vegetation affects microwave emission by absorbing or scattering emitted radiation from the soil. Furthermore, vegetation emits own radiation. Hence, the key in retrieving soil moisture with microwaves is to understand how vegetation affects microwaves and how that correlates to soil moisture.

Passive and active microwave remote sensing

Microwave remote sensing can be divided in two techniques, i.e. passive and active techniques. Passive techniques only detect naturally emitted radiation from a certain body (soil, vegetation), which is expressed in brightness temperature. Active techniques send out a signal, of which the backscatter is detected again. Active microwave measurements are expressed in the power ratio, which is the ration between the sent signal and the detected backscatter.

Passive microwave sensing measures the emitted natural radiation from vegetation. Passive microwaves are generally very weak. However, the microwaves arriving at the earth's surface from the sun is negligible. Therefore, microwave radiometer measurements are not contaminated by reflected solar contribution. Emitted microwaves are very sensitive to changes in water content and provides information related to the surface temperature and dielectric properties and hence contains information about the soil water content.

Active microwave is all about backscattering (reflection) of microwaves in the direction of incidence. A generated microwave signal is fired at the target surface, after which the signal is scatter back to a detector (normally at the same location the the signal generator). Backscatter signal is the combination of surface scattering and volume scattering, which is the absorbed and scattered signal as microwaves pass through different layers of vegetation [18]. Scattering is influenced by texture, dielectric constant, geometry, emissivity and polarization (in the following sections the dielectric constant and polarization will be briefly discussed). Also the structure of canopy plays a significant role. Microwave backscattering is not sensitive to chemical composition or pigmentation of leaves, but mainly to physical structure and the dielectric constant (and hence water content) (e.g. [19]). The parameter that determines the characteristics of the returned microwave signal is the backscatter cross section σ, or normalized backscatter coefficient σ^0 in case of vegetation.

Polarization of microwaves

The polarization of a microwave is the plane in which the electric field vector in the electromagnetic wave oscillates [18]. Naturally emitted microwave energy is often unpolarized, but becomes polarized after interaction with the environment. Active systems can generate waves of one particular orientation (i.e. horizontal or vertical). The way in which a polarized microwave interacts with a surface depends on the angle of polarization, the orientation and roughness of the surface and its dielectric constant. Polarimetry uses this to discriminate different types of targets. Polarimetric microwave systems send out microwaves with horizontal or vertical polarization and detects the horizontal or vertical component in the return signal. A polarized wave incident on a depolarizing target, e.g. full forest canopy, returns a signal containing polarizations other than the incident. For example, when the incident wave is horizontal (H), the return signal may contain contain a vertical component (V), which is called HV-polarization. Likewise, HH, VV and VH combinations can be distinguished. Because of the different polarimetric responses of vegetation, different vegetation types can be differentiated (e.g. [20],[21]).

Microwave remote sensing

Microwaves (MW) are on the longer end of the wavelength spectrum [10e^{-3}m - 1 m] and interact with the magnetic dipoles in material. Another advantage of microwaves is that because of the long wavelengths, microwaves are not scattered by atmospheric gasses or water drops. Radiation traveling through the atmosphere may be scattered by interaction with particals, depending on the size of the matter and the wavelength. Water droplets are large compared to visible radiation and scatters. However, for microwaves water droplets are relatively small and will not be affected by their presence in the atmosphere. This allows microwaves to reach the earth surface even on days with cloud cover, which is a big advantage over other remote sensing techniques.

For remote sensing of vegetation, the most common frequency band widths are the L-band (f = 1-2 GHz, λ = 12-30cm) and the C-band (f = 4-8 GHz, λ = 3.75-7.5cm) [18]. Both frequency ranges are most sensitive to different parts of vegetation. L-band (longer wavelength) penetrates deeper through canopies and soil, and is more sensitive to trunks and branches of

vegetation. C-band senses water in only the top 2-3 cm of the soil and is mainly sensitive to vegetation components (e.g. leaves).

Canopy is a complex heterogeneous volume consisting of components of different sizes, shapes and orientations. Individual scattering components consist of leaves, stems, branches, trunks and the soil. Canopy is so complex and dense that it can be modeled as a volume, composed of random idealized identical objects, leading to an average behavior [22].

Influence of vegetation

Both passive and active microwave remote sensing techniques are sensitive to vegetation. Radar is particularly sensitive to vegetation (e.g.[23],[24],[25]). The presence of vegetation results in two-way attenuation of a reflected signal by the soil, contributes to total backscatter by means of surface and volume scattering by the canopy and scatters signals reflected from the soil [26]). Therefore it is chosen to only investigate the influence of vegetation on active remote sensing, i.e. radar.

Since the beginning of the 1990s, ESA's ERS-1 (1991 - 2000) and ERS-2(1995 - 2011) have gathered backscatter data on a global scale, which was later used to estimate soil moisture [27]. Both satellites operated at C-band vertical polarization and its backscatter can be linked to soil moisture through the dielectric constant [28]. The latter is based on the large contrast between dielectric constants of water and dry soil (factor 20). However, in vegetated regions low correlations were found between ERS backscatter and soil moisture [28]. It was argued that this was the result from dense vegetation cover, through which C-band radar has only low penetration capabilities.

NASA's upcoming Soil Moisture Active Passive (SMAP) mission will bring new opportunities, since this satellite is equipped with L-band instruments (radiometer/radar). L-band has greater penetration of vegetation and should be able to provide an improved soil moisture product with higher quality. However, L-band instruments can only detect changes in the upper 5cm of the soil [29], while one is actually interested in the soil moisture content of the root zone. Furthermore, vegetation is considered an obstruction for signal retrieval. In vegetated ares, the signal detected by the radiometer or radar is influenced by both soil and the vegetation. Above areas exceeding a certain vegetation water content (i.e. 5 kg m^{-2}, [29]), the error in soil moisture retrieval increases dramatically. This means that dense forests and 35 % of the non-frozen soil surface are excluded from soil moisture retrieval.

Vegetation: Barrier or new source of information?

Rather than considering vegetation as a barrier to retrieval, Steele-Dunne *et al.* [30] posed the question: Can vegetation be considered as a source of information on water availability?

Work by [31] showed that the diurnal variation in ascending and descending overpass satellite signal corresponded with the onset of water stress in West Africa. It was suggested that the C-band radar backscatter was influenced by the variation in water status of vegetation.

Results from numerical modeling as presented by Steele-Dunne et al. [30] showed that backscattering of different polarizations of L-band are influenced by different aspects (e.g. L-band HV polarization react to variations of leaf dielectric constant, co-polarized L-band

reacts to trunk dielectric constant). In this study, the MIMICS model was used [26], which required geometrical and dielectric parameters of the modeled surface area. Although the results from this study were promising, field observations are required to validate these modeling results.

Current challenges are plentiful, e.g. investigating how vegetation influences the dielectric constant, how the dielectric constant influences backscattering and which information can be retrieved from an observed backscatter signal. As discussed, dielectric parameters are a main driver of radar backscatter. However, until now only few studies have presented typical numbers for vegetation. Other studies have determined dielectric constants of vegetation, e.g. [26], [32] and [33] observed diurnal variation in trunk dielectric constant. Furthermore, the dielectric constant of leaves has been monitored (e.g. [34]). However, the diurnal variation of the dielectric constant of vegetation, and leaves in particular, is still unknown. It is suggested that water stress has a significant influence on the dielectric properties of vegetation, which it its turns affects radar backscatter. This study presents a time series of diurnal leaf dielectric properties. This will provide the missing link between water stress, dielectric properties of leaves and radar backscatter. Revealing this connection will be a great step in exploring the possibilities of using vegetation as an indication for water availability in the root zone.

For this thesis maize was measured, because from a remote sensing point of view this is an interesting crop. It is a plant that uses a relatively large amount of water and gains a lot of biomass during a growing season. Because of the big changes in biomass on both a daily and seasonal scale, maize can have significant influence on radar backscatter.

1-3 The dielectric constant of vegetation

The dielectric constant is a fundamental property of all materials. The strength of interaction between microwaves and a material is determined by the dielectric constant and is an important determinant of emissivity of a material. The dielectric constant is a complex number. The real part determines the propagation characteristics of the energy as it passes through the material. The imaginary part determines the energy losses. In a heterogeneous material, e.g. soil or vegetation material, the complex dielectric constant is a combination of all individual dielectric constants of the constituent parts (e.g. water, air). Other factors that influence the dielectric constant are temperature, salinity and wavelength.

The dielectric constant of leaves is governed by water content and salinity [35]. In combination with the shape and orientation it controls the scattering and emission by a vegetation canopy. The dielectric constant of leaves mainly depends on the water inside the leaf. Water can be divided in 'free' and 'bound' water. Free water is water that does not tightly binds to its environment and can therefore move freely through vegetation. Bound water on the other hand does bind with its environment, causing an inability to move through the plant of change easily change its orientation. Water possesses a permanent electric dipole moment. When an electric field is applied, a water molecule will orient so its dipole moment is aligned with the field [36]. The time it takes for a water molecule to orient in that direction is a function of the interaction with the environment and temperature. One can expect that this time is significantly higher for bound water (which binds with its environment) compared to free water. According to [36] bound water has similar dielectric properties as ice. Bonds are strong

at low moisture levels, since free rotation of water molecules is impeded (bound water phase). When the moisture content increases, molecules are further from the vegetation cell surface and can rotate more freely (free water phase). An increase in vegetation water content comes with an increase of free water, which leads to an increase in dielectric constant, [34],[37].

In the last decades, several studies presented dielectric constant values for vegetation (e.g. [34], [37], [38]), soil ([39], [40], [41]) and cheese [42]. However, no long time series of dielectric constant of vegetation exist. As suggested by [30], dielectric behavior of vegetation should be studied by conducting in-vivo dielectric measurements of vegetation. To learn about the diurnal variation of leaf dielectric properties and how it varies during periods of low water availability, this study focuses on retrieving dielectric constant times series of leaves, which will be linked to vegetation water content.

1-4 Maize

Maize is one of the world's most grown crops and is cultivated all around the globe. Maize is a cold-intolerant C4 crop with a shallow root system that generally does not grow deeper than 1 m below the surface ([43],[44]). The optimal growing temperature of maize lays between 25° to 35° and although C4 plants are water efficient, the production and growth of maize can severely be affected by water stress [45],[46].

Like any other plant, maize plants aim to produce as much biomass as possible given the meteorological and environmental circumstances. Biomass is produced via photosynthesis, a process in which light is used to convert CO_2 and water into sugar and oxygen. Gas exchange of CO_2 and O_2 takes place in the leaves via the stomas, which are opened during the day. However, the leaves contain water, which evaporates when the stomas are opened (transpiration), leading to a decrease in leaf water content. Leaf water content is the main control of leaf turgor pressure (firmness of a leaf). Decreasing leaf water content will result in a lower turgor, causing leaves to lose rigidity (wilting leaves). In the diurnal stomatal closure cycle of maize, the transpiration is the highest around noon and decreases to a minimum during night ([47]). According to Hsiao [48], availability of CO_2 and light have a complex effect on leaf turgor. During night the turgor pressure decreases, which results in stomatal movement (i.e. closure) to prevent further damage.

The life of a maize plant can be separated in two main growing stages: (1) the vegetative and (2) the reproductive stage.

Vegetative stage consists of the phases in which maize is growing and developing leaves. With sufficient resources available, a maize plant develops 1 or 2 leaves per week. The phase of the plant is named after the amount of visible leaves, which reaches a maximum of approximately 17. The final vegetative phase is tasseling, which is when the last branch of tassel is visible, but silks have not yet emerged. By then, plants have normally reached their maximum height.

From then on, maize continues with the reproductive stage. After the silking, blister, milk, dough and dent phase, the plant reaches physiological maturity. Depending on the type of maize, the total life cycle lasts between 2.5 and 4 months.

Influence of water stress on maize

The aim of this research was to investigate the effects of water stress on maize. By determining certain signatures it might be possible to detect water stress in the field with the dielectric measurements (and eventually radar). Maize is affected by water stress in various way. Cakir [49] reported that, based on a 3-year study, the vegetative growth is strongly affected by water stress, e.g. plant height growth decreases when water stress occurs early in the vegetative phase. Up to the first 5 weeks, maize is rather drought tolerant [50], but during the late vegetative stage and tasseling, water stress caused leaf size to decrease. Moreover, loss of lower leaves occurs earlier. This period has most influence on both the development of a maize plant as on the eventual yield. Stomatal closure is the main cause for transpiration decline as water stress develops [48], leading to a stop in development. According to [51], the growth stop can be explained by a lack of turgor pressure in the leaves, which is a result of a decrease in leaf water content. Leaf water content has a faster response to water stress compared to the water content in the stalks. Igathinathane *et al.* [52] found that when maize experiences a period of water stress, the leaves are first to show a 'critical' drop in water content. It can take a number of days before a drop with the same order of magnitude is detected in stalk water content. Therefore, leaf water content is in fact a very good measure of water stress. It responds fast to water stress and is very representative for the degree to which plant production is stagnated.

What if we could detect this critical drop in leaf water content with radar? This would be of importance for both soil moisture and vegetation. The critical drop in leaf water content indicates water stress in the root zone. Besides, knowing whether maize fields are on the onset of water stress could be of great use for crop management strategies. This study is a first step in exploring the possibilities of using vegetation as a source of information for soil moisture and vegetation monitoring with microwave remote sensing missions.

1-5 Scope of this research

There are many open questions regarding microwave remote sensing of vegetation, which must be addressed before we can consider using radar to monitor vegetation water stress. This MSc thesis will only focus on a very small piece of the puzzle. Understanding diurnal variation of leaf dielectric constant would be a significant step forward in understanding the influence of vegetation on radar backscatter and how we could possibly use radar for vegetation and soil moisture monitoring.

This scope of this study is two-folded. First, this study will investigate how the dielectric properties of leaves vary on a daily basis. A time series of AM and PM values of leaf dielectric properties obtained from the field will be presented. Second, a first step will be made in exploring the possibilities of using vegetation as a source of information for microwave remote sensing, for both soil moisture as vegetation monitoring.

If it is possible use satellite radar imagery to determine the water status of vegetation, this information could be used to quantify the amount of water available in the root zone and the presence of water stress. Not only would this be very interesting for agricultural purposes (e.g. vegetation water status monitoring), this will also yield new hydrological insights.

1-6 Research questions

To cover the described challenges, the following research questions are formulated.

> What controls the dielectric constant of vegetation and how does it vary on a diurnal basis?
>
> How does water stress affect the dielectric properties of vegetation?
>
> How does vegetation influence radar backscatter?

1-6-1 Hypotheses

What controls the dielectric constant of vegetation and how does it vary on a diurnal basis?

It is expected that water content is the main driver for changes in dielectric constant. The dual-dispersion model [36] and the datasets used to develop it, indicate that water content is the main driver. We expect to see that as leaf water content changes in response to water stress, that there will be a change in dielectric properties. It is expected that leaf water content, and therefore the dielectric constant, is higher at 6AM than at 6PM. During the day, leaf water content will decrease as vegetation will evaporate.

How does water stress affect the dielectric properties of vegetation?

Water stress implies that water availability decreases. This might lead to two observable consequences. First, the diurnal difference in water content will be higher, since vegetation will not be able to replenish its water content during the day. This will lead to a larger difference between the morning and afternoon dielectric properties of vegetation. Secondly, as the general vegetation water content goes does as water stress prolongates, the dielectric constant should show a similar decrease in time.

How does vegetation influence radar backscatter?

Previous studies have shown diurnal patterns in radar backscatter above vegetated areas (e.g. [53]). Radar backscatter depends on the different dielectric properties of the observed area. Lower frequencies (e.g. L-band) have a longer wavelength and will penetrate further through the same canopy than a higher frequency radar. Therefore it is expected that backscatter at lower frequencies will mainly be sensitive to soil moisture. However, at all frequencies the total backscatter is a combination of a contribution by vegetation and soil moisture. Higher frequencies will not fully penetrate vegetation, leading to volume and surface scatter by the canopy. Therefore it is expected that at higher frequencies the dielectric constant of vegetation will be the main source of influence on radar backscatter. During periods of water stress this will mean that the retrieved signal above a vegetated area decreases. Water stress causes lower water availability, leading to a lower dielectric constant of vegetation. With increasing frequency, radar observations are less sensitive to soil moisture and more sensitive to vegetation water content.

1-7 How to read this thesis

The Methods chapter contains a description of the measurement techniques and tools are used for measuring the dielectric properties of vegetation, meteorology and quantifying water stress. It also contains an overview of the models used to simulate radar backscatter above a vegetated area. In Chapter 3 (Results and discussion) all findings will be presented. First, an overview of the situation in the field will be given (i.e. meteorological circumstances). Second, a quantification of water stress will be presented. Third, that the dielectric measurements as conducted in the field will be shown and discussed. Finally, the outcome of the modeling exercises are presented. Chapter 4 includes the conclusions from this study and recommendations for further research.

Chapter 2

Methods

2-1 Study area

The fieldwork of this study was conducted at the University of Florida Plant Science Research and Education Unit, located in Citra, FL (N 29.41°, W 82.18°). Measurements were made as part of the MicroWEX-11 experiment. The location of Citra can be seen on the map in Fig. 2-1.

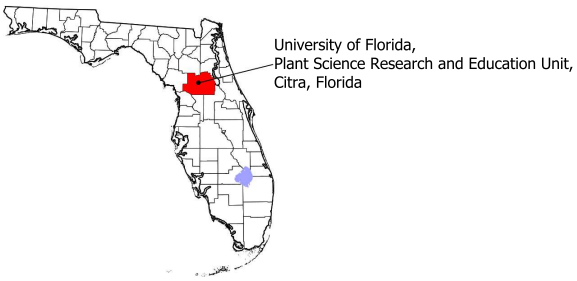

Figure 2-1: Location of study site at Citra shown on the map of Florida, USA

2-2 Meteorological conditions

Citra is located in central Florida, which has a humid subtropical climate (Cfa), according to the Köppen climate classification [54]. This climate is characterized by hot, humid summers and mild winters. From October to May precipitation is generally significantly lower (dry season), compared to June to September (wet season). The average annual rainfall is 1334 mm and the yearly maximum and minimum average temperatures are 27.9°C and 15.1°C, respectively [1]. Hurricanes strike Florida between almost every month of the year. However,

[1] http://climatecenter.fsu.edu/

most hurricanes (75% of the total) occur between August and October. Meteorological data was measured at the Citra fieldwork site, which will be discussed later in this chapter.

2-3 Vegetation

Maize plants (*Zea mays L.*) were grown from seeds on the research facility of the University of Florida. Maize was planted on a field of 183 x 183m, in rows with 1 m spacing with a density of approximately 5 plants per meter. Irrigation was applied mainly at the end of September. Table 2-1 shows the applied irrigation amounts and their respective dates. No further irrigation events were planned to induce water stress on the measurement location. This was only the case for the area where the dielectric measurements were done. On the rest of the MicroWEX fieldwork site, irrigation was still applied throughout the experiment. Plants received unobscured sunlight. The growth of plants was restricted only by competition between the plants. The growing period was 78 days.

Table 2-1: Dates and mounts of irrigation events at dielectric measurements study site

Date	Amount [mm]
24-Sep-12	12
25-Sep-12	12
27-Sep-12	24
28-Sep-12	36
29-Sep-12	12

2-4 Measuring the dielectric properties of vegetation

One of the objectives of this study is to gain insight in the diurnal variation of the dielectric constant of vegetation. Therefore, it was necessary to conduct dielectric measurements in the field. Various techniques have been presented to measure the dielectric constant of vegetation, however with varying suitability for field applications. For this study several requirements to a measurement technique were formulated. First of all, measurements of vegetation dielectric constant needed to be conducted in-vivo (non-destructive), in order to retrieve a diurnal pattern. Secondly, various locations on individual leaves needed to be measured. This was necessary to study the variation of the dielectric constant along the leaf and between leaves. Finally, time consuming methods were not favorable. Since it was aimed to compare measurements between different points and leaves, measurements should be conducted after each other as rapid as possible. Because of these constraints, most existing methods of measuring the dielectric constant were considered unsuitable.

For example, Shrestha *et al.* [55] and Franchois *et al.* [56] used a semi-rigid coaxial cable, with which the bulk dielectric constant of vegetation material was measured. This is a destructive method and was therefore not used in this study. El-Reyes and Ulaby [35] present a method in which coaxial probes are used to measure the dielectric constant. However, this method requires a time consuming calibration procedure, making it unattractive to use it for

fast measurements in the field. Tan [57], Sarabandi and Ulaby [58] and Chung [59] placed vegetation samples in a waveguide, which was connected to a VNA to determine the dielectric constant. However, this method is difficult to apply in the field for in-vivo measurements. Burke *et al.* [38] used Impulse Time Domain Transmission (ITDT) to measure complex dielectric permittivity of vegetation. Their method is non-invasive and in-vivo, however the applicability in the field has yet to be tested. Atmospheric turbulence influences dielectric measurements, making repeatable results difficult to obtain and is therefore not suitable of the fieldwork of this study. Sancho-Knapik *et al.* ([60],[61]) used a microwave digital patch antenna to determine the relative water content of in-vivo popular leaves. This methods was not yet tested under field conditions. Menzel *et al.* [62] used microwave resonators to determine biomass of alive vegetation using a cavity resonator by relating the shift in center frequency to the change in water content. The methods presented by Sancho-Knapik *et al.* ([60],[61]) and Menzel *et al.* [62] do not yield results from which the dielectric constant can be determined and are hence not used in this research.

In this study the measurement technique developed by Steele-Dunne *et al.* [63] was used. An electromagnetic wave is transmitted through a microstrip line resonator. The dielectric constant of the measured sample will modify the capacitance between the stripline and the ground plane, which changes the resonant frequency and the reflectivity of the stripline. Therefore, the change in resonant frequency of the sensor can be used to monitor changes in leaf dielectric properties. To obtain the most accurate results, the microstrip resonator was placed horizontally. Most leaves do not have a perfectly flat surface. When a leave is just placed on the sensor, the possibility exists that only an air bubble is measured. To prevent this, the leaf was placed between two Teflon blocks with a thickness of 1 cm. This created a layered measurement setup with a block of Teflon, the sensor, the leaf and another block of Teflon. Also, Teflon has known constant dielectric properties, making the experiment more reproducible. The measurement setup is presented in Fig. 2-2.

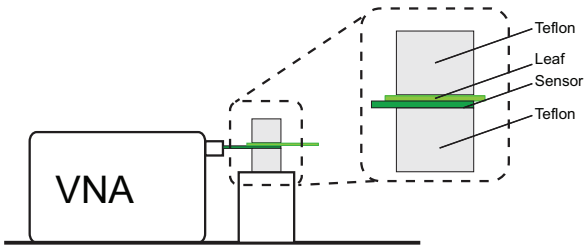

Figure 2-2: Setup used for the dielectric measurements

All measurements were conducted using a ZVH8 Cable and Antenna Analyzer (ZVH8, 100kHz to 8GHz, Rohde & Schwarz, Mnchen, Germany) with the K42 Vector network Analysis and K40 Remote Control option. The VNA sends out the electromagnetic wave to the microstrip line and measures the reflected signal. Fig.2-3 illustrates how the reflected signal changes with leaf water content. As can be seen, the resonance frequency, magnitude and width of the dip changes as a leaf dries out. A single leaf with known gravimetric moisture content was measured four times as it dried out. When the leaf was wet ($M_g = 0.5560$) the measured reflected signal shows a sharp, narrow dip around 3.5 GHz. After drying out ($M_g = 0.2801$) the dip is wider, flatter and shifted all the way to 3.7 GHz. This clearly shows that a decrease in leaf water content results in an increase of the resonant frequency of the sensor at that leaf.

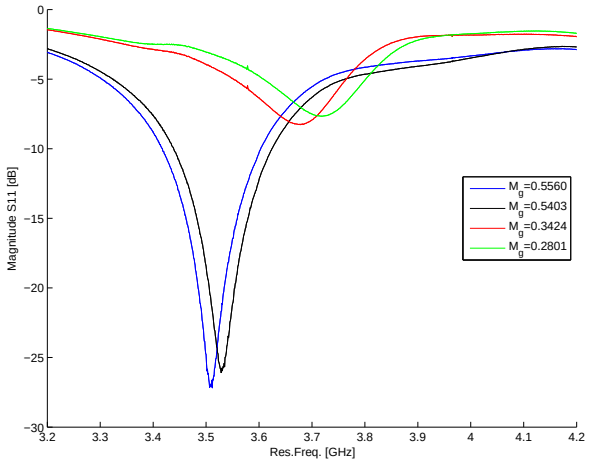

Figure 2-3: Resonant frequency vs. bulk leaf gravimetric moisture content of a single maize leaf at position 1 (collar) for 4 different water statuses, measured under lab conditions with an angle of 45°

Measurements were performed manually. Each measurement registered the magnitude [dB] and phase [°] of the reflection coefficient S11 at 1201 points between 2.1 and 4.1GHz. From 8 to 19 October 2012 dielectric measurements were done at 6AM and 6PM. The interval of twelve hours was chosen to match the gap between satellites overpass times (e.g. ERS: 10AM and 10PM [31], SMAP: 6AM and 6PM [29]). 6AM is just before the onset of dawn, meaning that no transpiration has yet taken place and the vegetation moisture content can hardly get any higher. Therefore this is a good time to measure the morning dielectric properties of vegetation. The highest transpiration rate (and hence lowest vegetation water content) takes place between noon and 3PM. Given the time it takes to execute the dielectric measurements (1 hour for three leaves), it is difficult to obtain measurements that are representative for one moment in time. At 6PM, the onset of sunset, the transpiration rate has gone down, but the water content is still very low (after a day of transpiration). Measuring at 6AM and 6PM clearly shows the difference between the pre-dawn morning water content and the declined water content at the end of the day. Also considering the launch of SMAP in the near future (6AM and 6PM overpass times), dielectric measurements at these times will be very useful in explaining the diurnal difference in radar backscatter.

For all dielectric measurements, the following procedure was used. For every leaf, seven measurements were taken. First, a measurement of the Teflon block only was taken. This was done to be able to check the background noise ans consistency of the measurements in time, since Teflon should yield the same results. Five measurements were taken on the leaf. Three were taken along the middle nerve of the leaf, at the collar, in the middle of the leaf and at the tip of the leaf. In the middle of the leaf, two more measurements were taken, one on each side of the blade. Finally, a measurement was taken of air only. Fig. 2-4 illustrates the measurement points on the leaves. Measurements were taken perpendicular at 90° and at 45° to the leaf.

Lab experiments were conducted to show the relation between bulk gravimetric moisture content and resonance frequency. The bulk gravimetric moisture content was determined by weighing and drying all leaves of one maize plants. The dielectric measurements were

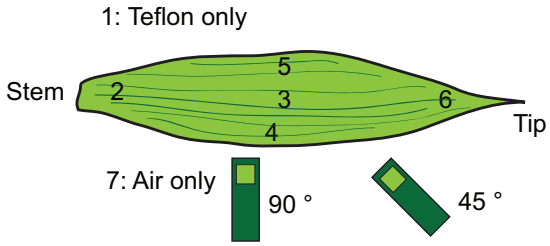

Figure 2-4: Measurement points on leaf as used for the Citra field measurements, including the 90° and 45° measurement orientation of the microstrip line resonator.

conducted on the same leaf. In Fig. 2-5 the results can be seen for measurements taken at an angle of 45°. This clearly shows that the resonance frequency increases with a decreasing gravimetric moisture content of the maize leaf. Also, the reliability of a single measurement has been checked by measuring the same point on a maize leaf multiple times. This yielded an average standard deviation $\eta = 0.6\text{e}^{-2}$GHz at 90° and $\eta = 1.3\text{e}^{-2}$GHz at 45°. In Fig. 2-5 it can be seen that the error of the tip resonant frequency at a bulk gravimetric moisture content of 0.5560 is significantly higher that other errors. This is due to the fact that the error bars in Fig. 2-5 are based on three identical measurements. If one of those measurements is not executed correctly, the values can deviate strongly. For example, if the location is slightly different from the previous measurements or the leaf does not completely covers the measurement window of the sensor, this yields deviated measurements. Although in general the standard deviation is low, this points out the importance of careful application of the measurement procedure.

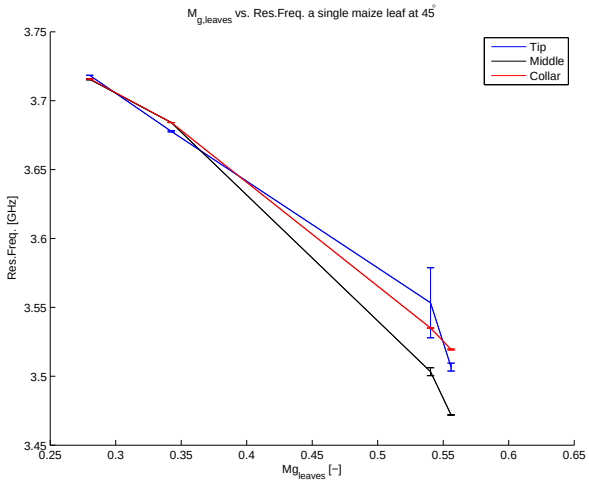

Figure 2-5: Resonant frequency vs. bulk leaf gravimetric moisture content for three positions (tip, middle and collar) on a single leaf measured under lab conditions under an angle of 45°, including error bars that represent one standard deviation.

2-4-1 Vegetation sampling

To link the dielectric measurements to vegetation water content, vegetation samples were taken. This was done at the same time as the dielectric measurements. Vegetation water content has been measured daily at 6AM and 6PM from 24 September to 19 October. On 11 and 12 October, vegetation samples were taken every 3 hours. A destructive method was used, meaning that two maize plants were cut, weighed, dried and weighed again. Drying was done in a $70°C$ oven, in which the vegetation samples were placed for 5 days. The vegetation samples were divided in leaves and stems. Weights were determined for the total of all leaves and stems respectively of the two maize plants. From the wet and dry weights, both the gravimetric moisture content and the volumetric moisture content could be determined, according to the following equations.

$$M_g = \frac{m_{fresh} - m_{dry}}{m_{fresh}} \tag{2-1}$$

$$VWC = \eta[(m_{fresh,leaf} - m_{dry,leaf}) + (m_{fresh,stem} - m_{dry,stem})] \tag{2-2}$$

In which M_g is gravimetric moisture content, VWC the volumetric moisture content, m_{fresh} the weight after the plant is cut, m_{dry} the dry weight and η the number of plants per m.

The vegetation sampling and dielectric measurements were done on different leaves. Although the water content might slightly differ, it was assumed that the destructive samples were taken from plants that were representative for the fieldwork site (including the plants on which the dielectric measurements were done).

2-4-2 Trend analysis

A trend analysis was performed to quantify the variations in the vegetation water content and the sensor's resonant frequency. Using Spearman's rank test, the data series was tested on the absence of trends for several confidence boundaries. Not only does that reveal the presence or absence of a trend, but also with how much confidence that can be concluded. By comparing the order of appearance and the magnitude of the measurements, it was checked whether the trend within the data series lies within certain confidence boundaries. A more complete description of Spearman's rank test can be found in Appendix A.

2-5 Water stress

Water stress has a large impact on vegetation (e.g. [46],[49]). Increasing water stress affects the moisture distribution within the plant, which can be seen in the leaf water content. To use the dielectric measurements as a measure of water stress, it was necessary to quantify water stress as it occurred. This was done using two methods. First, a water balance was made of the sample area in the field, in which the water stress was expressed as the evaporation deficit. Second, the soil water tension was measured at different depths. Both methods will be explained in the following sections.

2-5-1 Water balance

To quantify the water stress occurring at the study site, a water balance was made using the following equations:

$$\frac{dS}{dt} = P + I - E_{max} - Q \tag{2-3}$$

$$E_{max} = E_{ref} \cdot K_c \tag{2-4}$$

with soil moisture change $\frac{dS}{dt}$, precipitation P, irrigation I, maximum evaporation E_{max}, Penman-Monteith reference evaporation E_{ref}, crop factor K_c and runoff Q. At the study site all parameters were measured, except for the runoff. In this case, a positive runoff means that not all precipitation and irrigation can infiltrate or be evaporated and hence runs off. A negative runoff however, means that there is not enough water available for the crops to match the theoretical evaporation. In other words, this is the evaporation deficit and will be used as a quantification of water stress.

Meteorological data

Meteorological data was retrieved from the Florida Automated Weather Network (FAWN) [2]. FAWN is a network of 36 weather stations all across the state of Florida and is managed and maintained by the University of Florida. The data used in this study was from the Citra weather station (N 29.41058°, W 82.17021°, elevation 18.3 m above MSL), located on the same University of Florida grounds as where all field data was collected. All data was obtained from 1 August to 31 October with a reporting frequency of 15 minutes. Air temperature and relative humidity was measured at a height of 2 m above ground level using a CS215-L temperature and relative humidity sensor (Campbell Scientific, Inc., Logan,UT, USA). Soil temperature was measured at 10 cm depth using a 107-L temperature sensor (Campbell Scientific, Inc., Logan, USA). Precipitation was measured with a WaterLOG H-340SDI tipping bucket (Xylem Inc., Logan, USA) at a height of 2 m. Solar radiation was measured with a LI200x silicon photovoltaic pyranometer (Campbell Scientific, Inc, Logan, USA). Wind speed was measured with a Vaisala 425A ultrasonic anemometer (Vaisala Oyj, Helsinki, Finland). Daily reference evaporation was provided by FAWN, which was calculated using Penman-Monteith [64].

Evaporation

Maximum evaporation was calculated by multiplying the FAO Penman-Monteith [65] reference evaporation (based on [64]) by a crop factor. Reference evaporation was provided my FAWN. To calculate maximum evaporation for maize, FAO crop factors for maize were used ([65]), which take into account the different growing stages of maize.

[2] http://fawn.ifas.ufl.edu/

Soil moisture

On the experimental site, the soil moisture profile was measured every 5 minutes at seven depths (0.02 m, 0.04 m, 0.08 m, 0.16 m, 0.32 m, 0.64 m and 1.2 m). For every measurement, the total amount of water was determined in the first 1.2m of the soil by multiplying the soil moisture content value by the reach of each sensor. These values were summed to arrive at the total moisture in the soil at a given moment in time. It was assumed this is representative for the root zone throughout the whole experiment. Although it is acknowledged that the roots of maize did not reach these layers from the very beginning, at the moment at which precipitation stopped and water stress arose the maize was yet fully developed. Based on the latter the assumption was made that maize was able to take water up from the entire first 1.2m of the subsoil. To calculate $fracdSdt$, the daily change in soil moisture was calculated, based on the difference in midnight values.

2-5-2 Soil water tension

Soil water tension has been measured from 11 September to 19 October using two UMS T4e Pressure Transducer Tensiometers (UMS GmbH, Mnchen, Germany). One was installed at 50 cm depth with an angle of 35° with respect to the vertical and one was installed at 30 cm depth with an angle of 40°. UMS Tensiometers use a thin wafer piezoresistive pressure transducer to measure water tension. The resistance of the transducer changes as it is deformed by the pressure difference across it. Data was logged every minute using a CR1000 logger (Campbell Scientific, Inc., Logan, UT, USA).

2-6 Radar backscatter modeling

This study investigated the effect of vegetation on radar signals of various configurations (i.e. frequencies, polarizations, incidence angles). The expected output is two-folded. In soil moisture retrieval, vegetation is considered a barrier. This study aims to show what happens to this barrier and its significance when there is an increasing presence of water stress. For higher frequencies it will be investigated if the diurnal difference in vegetation water content causes a change in the total backscatter that is large enough to measure. The approach consists of two parts, (1) for the ranges observed in the field, a sensitivity analysis of radar backscatter to vegetation water content and soil moisture and (2) modeling a time series of backscatter using the observed field data.

2-6-1 The water-cloud model

Within active microwave soil moisture retrieval, semi-empirical and empirical models, and change detection approaches are frequently used. Radar is influenced by a vegetation by three main mechanisms [66]: direct backscatter from plants, direct backscatter from soil and multiple scattering between soil and vegetation. Additionally, the direct soil backscatter is attenuated by the vegetation, in both ways. The water cloud algorithm [67] assumes that a canopy can be represented by a cloud of water droplets (within the microwave region), based on the assumption that the vegetation dielectric constant is dominated by the dielectric

constant of water. Within a volume of air, leaves are represented by water drops, with a dielectric constant (real part) varying between the value for dry vegetation (2-3) ([37],[34]), and water (80) [68]. Another important aspect of the water cloud approach is that it ignores the second and higher-order contributions, originating from multiple scattering between soil and vegetation. During a radar double or multi-bounce, the signal's polarization is often changed. This effect is not taken into account in this approach. This means that predictions of radar backscatter based on the water-cloud model are a conservative underestimation of the signal that can be retrieved in the real world ([69],[70]). Neglecting the higher-order effects, backscatter above a vegetated area is composed of two contributions,(1) attenuation of the soil surface scattering component and (2) scattering of the vegetation elements (leaves, stems, branches).

Attema & Ulaby (1978)

The water-cloud model as proposed by [67] is described with the following equations

$$\sigma^0 = C \cdot [1 - exp(-\frac{D \cdot W \cdot h}{cos\theta})] + A \cdot exp(\frac{B \cdot m_s \cdot D \cdot W \cdot h}{cos\theta}) \tag{2-5}$$

$$W = \frac{(m_w - m_d)n}{h} \tag{2-6}$$

Where σ^0 is the total backscatter above a vegetated surface, A, B, C and D are (to be calibrated) vegetation and soil parameters, θ is the incidence angle of the modeled radar setup, m_w and m_d are the respective wet and dry weights of the bulk vegetation sample, W is the water content per unit volume [kgm^{-3}], m_s is the soil moisture and h is the plant height. Backscatter is determined as the power ratio between the sent and retrieved signal.

Vegetation and soil parameters have to be determined by means of calibration. For a given radar configuration, the water-cloud model can be calibrated using ground data. This includes vegetation type, radar configuration (i.e. frequency, polarization, angle of incidence) and soil type. Therefore, the applications of the water cloud model for new situations is limited. There are few calibration studies for corn grown on sandy soils (as in this study). However, it was possible to model radar backscatter for a number of very interesting radar configurations, i.e. C-, L-, X-, K_u- and K_a-band. C- and L-band are mainly interesting considering their usage within past, current or planned soil moisture retrieval missions. The higher frequencies are interesting for potential use of direct vegetation monitoring applications.

Over time several authors have adjusted, enhanced and expanded Attema & Ulaby's water-cloud model [67]. In this study several modified versions of the water-cloud model were used (see Table 2-2), which will all briefly be explained.

Ulaby *et al.* (1984)

Ulaby *et al.* [66] expanded the water-cloud model by separating total vegetation backscatter in different contributions by leaves and stalks. The set of equations to describe their modified water-cloud model are presented below.

Table 2-2: Specifications of radar configurations model with the water-cloud model

Author	Band	Frequency [GHz]	Polarization	Incidence angle	Sensitivity analysis	Bare soil modeling
Ulaby *et al.* (1984)	X	8.6	VV	50	Y	Y
	Ku	13.0	VV	50	Y	Y
	Ku	17.0	VV	50	Y	Y
	Ka	35.0	VV	50	Y	Y
Dabrowska-Zielinkska *et al.* (2007)	L	1.8	HH	35	Y	Y
	C	5.3	VV	23	Y	Y
Joseph *et al.* (2010)	C	4.8	HH & VV	15	N	Y
	C	4.8	HH & VV	35	N	Y
	C	4.8	HH & VV	55	N	Y

$$\sigma^0_{tot} = \sigma^0_{leaf} + \sigma^0_{stalk} + \sigma^0_{soil} \tag{2-7}$$

$$\sigma^0_{leaf} = A_{leaf}[1 - exp(\frac{-B_{leaf}V_1}{h_1})][1 - \gamma^2_{leaf}]cos\theta \tag{2-8}$$

$$\sigma^0_{stalk} = A_{st} \cdot V_2 \cdot \frac{h_2}{h} \cdot \gamma^2_{leaf} \tag{2-9}$$

$$\sigma^0_{soil} = C_s \cdot m_s \cdot \gamma^2_{leaf} \cdot \gamma^2_{stalk} \tag{2-10}$$

$$\gamma^2_{leaf} = exp(-2\alpha_{leaf} \cdot sec\theta \cdot V_1) \tag{2-11}$$

$$\gamma^2_{stalk} = exp(-\alpha_{st} \cdot V_2 \cdot \frac{h_2}{h}) \tag{2-12}$$

As can be seen, the vegetation backscatter consists of two parts, the contribution from the leaves and from the stalks. The leaf backscatter σ^0_{leaves} is a function of vegetation parameters A_{leaf} and B_{leaf}, vegetation descriptor V_1, height of the leaves h_1 [m] leaf attenuation factor γ^2_{leaf} and angle of incidence θ [rad]. The stalk contribution is dependent on vegetation parameter A_{st}, vegetation descriptor V_2, total plant height h, stalk height h_2 [m] and leaf attenuation factor γ^2_{leaf}. Plant height h is the total height of the plant, which can be divided in a part where there are no leaves (h_2) on the stalk and where there are leaves (h_1). The soil backscatter depends on soil parameters C_s, soil moisture content m_s, and leaf and stalk attenuation factors γ^2_{leaf} and γ^2_{st}. The leaf attenuation factor is a function of vegetation parameters α_{leaf}, the angle of incidence θ and vegetation descriptor V_1. Attenuation by the stalks can be computed with the vegetation parameter α_{st}, vegetation descriptor V_2, plant height h and stalk height h_2. Fig. 2-6 shows h_1, h_2 and h. h_1 is the height of the plant where leaves are growing. h_2 is the height were no leaves are growing and the only scatterer is the stalk. h is the total height of the plant.

Figure 2-6: Used plant height descriptors h_1, h_2 and h. Figure taken from *Ulaby et al.* (1984).

In this approach V_1 and V_2 are taken equal, both being the total bulk vegetation water content. Furthermore, it is assumed that h_1 and h_2 both equal h, due to an absence of more detailed data.

As vegetation descriptors V_1 and V_1 different definitions have been presented by various authors. In previous studies the vegetation water content (VWC) (e.g. [24], [71] and [72]) or LAI (e.g. [73], [74]) is used to determine V_1 and V_2. Dabrowska-Zielinska *et al.* [75] compared the use of LAI, VWC and LWAI (LAI multiplied by the ratio between the mass of water in the vegetation and the wet biomass). It was concluded that VWC is well performing as a vegetation descriptor in the water-cloud model. Since VWC was measured during the fieldwork campaign, and will be used as the vegetation descriptor during the modeling exercise of this study. In previously reported application of the water-cloud model, it was assumed that V_1 equals V_2, for which the "bulk" vegetation water content used (VWC of the entire plant).

Modified Ulaby *et al.* (1984)

Here, a modified water-cloud model, based on Ulaby *et al.* [66] is proposed. Ulaby *et al.* [66] assumes that vegetation descriptors V_1 and V_2 are equal and uses a value of total bulk VWC to express this. However, during the measurement campaign VWC of leaves and stalks were determined separately, as were h_1 and h_2. Therefore a modified model is used, in which V_1 equals the leaf VWC and V_2 equals the stem VWC. Besides the real values for h_1 and h_2 were used. The proposed modified model is formulated with the following equations.

$$\sigma^0_{tot} = \sigma^0_{leaf} + \sigma^0_{stalk} + \sigma^0_{soil} \tag{2-13}$$

$$\sigma^0_{leaf} = A_{leaf}[1 - exp(\frac{-B_{leaf}V_{leaf}}{h_1})][1 - \gamma^2_{leaf}]cos\theta \tag{2-14}$$

$$\sigma^0_{stalk} = A_{st} \cdot V_{stalk} \cdot \gamma^2_{leaf} \tag{2-15}$$

$$\sigma^0_{soil} = C_s \cdot m_s \gamma^2_{leaf} \cdot \gamma^2_{stalk} \tag{2-16}$$

$$\gamma^2_{leaf} = exp(-2\alpha_{leaf} \cdot sec\theta \cdot V_{leaf}) \tag{2-17}$$

$$\gamma^2_{stalk} = exp(-\alpha_{st} \cdot V_{stalk}) \tag{2-18}$$

Dabrowska-Zielinska *et al.* (2007)

Dabrowska-Zielinska *et al.* [75] used the water-cloud model to simulate C- and L-band radar backscatter. In their approach however, the water-cloud model was slightly modified, based on Prévot *et al.* [71] and Champion [76]. In their approach, the water-cloud model (the vegetation term in particular) is simplified further with the introduction of more calibration parameters.

$$\sigma^0_{tot} = \sigma^0_{veg} + \gamma^2 \sigma^0_{soil} \tag{2-19}$$

$$\sigma^0_{veg} = A V_1^E cos\theta (1 - \gamma^2) \tag{2-20}$$

$$\sigma^0_{soil} = 10 \cot^{10} log(C + D m_s) \tag{2-21}$$

$$\gamma^2 = exp(\frac{-2BV_2}{cos\theta}) \tag{2-22}$$

Where σ^0_{tot} is the total backscatter, σ^0_{veg} the vegetation backscatter, σ^0_{soil} the soil backscatter, γ^2 the two-way attenuation, A,B,C,D and E are vegetation and soil parameters, V_1 and V_2 are vegetation descriptors, m_s is the soil moisture and θ is the angle of incidence. All backscatter terms are determined as a power ratio. The difference with the water-cloud model of Ulaby *et al.* [66] is the reduction to only one attenuation term, taking into account effect of the entire plant, and the introduction of extra vegetation parameter E.

Dabrowska-Zielinska *et al.* [75] calibrated their model for two situations. First, they determined the parameters for a L-band radar at 1.8 GHz, HH polarized and with an incidence angle of 35°. Second, the parameters were determined for a C-band radar at 5.3 GHz, VV polarized and with an incidence angle of 55°. The used parameters are shown in 2-3. Due to the difference in incidence angle and polarization, it was not possible to make a clear comparison of the two bands of measurement. However, it was still expected that L- and C-band radar will show a difference in sensitivity. C-band has a wavelength of 6 cm, and will be more sensitive to vegetation components. L-band however, with a wavelength of 23 cm, will penetrate more of the canopy and into the soil. L-band is therefore expected to be less sensitive to vegetation water content, compared to C-band.

Joseph *et al.* (2010)

Joseph *et al.* [72] based their water-cloud soil moisture retrieval model on adjustments proposed by, among others, [77], [66] and [24]. Their model is described in the following equations.

$$\sigma^0_{tot} = \sigma^0_v + \gamma^2 \sigma^0_s \tag{2-23}$$

$$\sigma^0_v = (1 - \gamma^2) A \cdot V_1 cos\theta_i \tag{2-24}$$

$$\gamma^2 = exp(\frac{-2BV_2}{cos\theta}) \tag{2-25}$$

with total backscatter σ^0_{tot}, vegetation backscatter σ^0_v, soil backscatter σ^0_s, attenuation γ^2 and radar incidence angle θ_i. A and B are crop dependent parameters and V_1 and V_2 are vegetation descriptors. For the soil backscatter [72] used a different model, in contrary to a parameter based approach. Joseph *et al.* [72] used the Integral Equation Method (IEM) (e.g. Fung *et al.* [78]) to simulate surface scattering from bare soil. The parameters required to use IEM were not measured during the fieldwork campaign. Therefore the empirical bare soil backscatter model of Dubois *et al.* [79] was used instead. Therefore, the model as proposed by Jospeh *et al.* will only be used for dry soil time analysis. Instead of plugged in the IEM module, bare soil will be approximated using an empirical soil scattering model. This will be explained further on.

2-7 Sensitivity analysis

Radar backscatter is sensitive to the moisture content of both vegetation and soil. During the sensitivity analysis, we will investigate the degree to which radar backscatter of a certain frequency is influenced by vegetation and soil. The sensitivity will be determined by running the water-cloud model with soil moisture values between 0 and 0.2 [-] and vegetation water content values between 1.5 and 3.5 [kgm^{-2}]. These values were chosen to match the range as observed in the field. For every radar configuration, the total backscatter, including all individual contributions will be computed.

Table 2-2 presents the available parameters for certain radar configurations as presented by different authors. Ulaby *et al.* [66] calibration the water-cloud model at 4 different frequencies (8.6, 13, 17 and 35 GHz) all with VV polarization and at an equal angle of incidence of 50°. Dabrowksa-Zielinska *et al.* [75] calibrated 2 radar configurations, i.e. (1) a L-band radar with HH polarization and an angle of 35° and (2) a C-band radar with VV polarization and an angle of 23°. Both studies used a version of the water-cloud model in which soil backscatter was parameterized. Joseph *et al.* [72] calibrated C-band for HH and VV polarizations at 3 angles of incidence (15°, 35° and 55°). In the latter, the soil backscatter was not an integral part of the water-cloud model, and was modeled otherwise. For this study will therefore only compare the sensitivity of the radar configurations as reported by [66] and [75]. For radar backscatter modeling under dry soil conditions, all configurations will be used however. In this approach, only the vegetation backscatter module water cloud model will be used. For the dry soil backscatter, the empirical approach based on [79] will be used, which will be explained later on.

Based on [66] radar backscatter is modeled for 4 frequencies between X- and K_u band, with equal polarization and angle of incidence. Different microwave frequencies respond to different components when directed at a certain surface. With increasing wavelength, the penetration depth through vegetation cover increases. This will mean that for higher frequencies, the response above a vegetated area consists more of surface scattering. Lower frequencies can penetrate better through the canopy to and will therefore be more exposed to volume scattering.

Table 2-3 shows the vegetation parameters used here, based on [66]. It is assumed α_{st} is always equal to 0, resulting in an attenuation coefficient of 1 (no attenuation).

Table 2-3: Water-cloud parameters for the modeled radar configurations

Author	Radar parameters				Vegetation parameters						Soil parameters		
	Band	Freq.[GHz]	Angle [°]	Pol.	A	B	α	E	A_{st}	α_{st}	C_s	C	D
Ulaby *et al.*	X	8.6	50	VV	0.22	2.6	0.411		0.025	0	0.197		
(1984)	Ku	13	50	VV	0.27	2.8	0.444		0.029	0	0.185		
	Ku	17	50	VV	0.30	2.7	0.418		0.022	0	0.234		
	Ka	35	50	VV	0.36	2.0	0.360		0.034	0	0.133		
Dabrowska-Zielinska	L	1.8	35	HH	0.01	0.04		0.0				-14.8	15.9
et al. (2007)	C	5.3	23	VV	0.08	0.15		2.9				-14.3	6.6
Joseph *et al.*	C	4.8	15	HH	0.03	0.09							
(2010)			15	VV	0.01	0.13							
			35	HH	15.96	1.18E-04							
			35	VV	3.05	1.38E-04							
			55	HH	5.57	4.16E-04							
			55	VV	2.96	1.96E-04							

2-8 Dry soil time series

An aim of this research is to investigate the possibilities of vegetation monitoring, especially during periods of water stress. During water stress, water management is crucial, since even a short period of severe water shortage can already result in underdevelopment and eventually in a decreased yield. With this modeling exercise, the response to radar has been modeled during a period of water stress. Finding out how the diurnal difference in radar backscatter changes with frequency will give insight in possible applications of active microwave technology for vegetation monitoring.

2-8-1 Bare soil scattering

For dry soil conditions the approach slightly differs from the sensitivity analysis. To allow a fair comparison between the model output of different radar configurations, the vegetation and soil backscatter will be calculated separately. Vegetation backscatter will be determined based on the equations presented in the previous section, according to [66],[75] and [72]. Dry soil backscatter will be modeled using a different approach, i.e. a bare soil backscattering model as proposed by [79]. To arrive at the total backscatter, both contributions will be added again. This allows us to compare the influence of vegetation only, given a certain soil condition.

An empirical soil moisture backscattering approach was proposed by Dubois *et al.* [79], which expresses radar backscatter from bare soil. Using field data sets, an empirical model was formulated that describes HH or VV radar backscatter as a function of the angle of incidence, the frequency, the surface roughness and the dielectric constant of soil.

$$\sigma^0_{hh} = 10^{-2.75} \cdot \frac{cos^{1.5}\theta}{sin^5\theta} \cdot 10^{0.028\epsilon tan\theta}(khsin\theta)^{1.4} \cdot \lambda^{0.7} \tag{2-26}$$

$$\sigma^0_{vv} = 10^{-2.35} \cdot \frac{cos^3\theta}{sin^3\theta} \cdot 10^{0.046\epsilon tan\theta}(khsin\theta)^{1.1} \cdot \lambda^{0.7} \tag{2-27}$$

The equations above describe bare soil backscatter for HH and VV polarization, based on [79] and corrected by [80]. σ^0_{hh} and σ^0_{vv} are the HH and VV polarized backscatter, θ is the angle of incidence, is the dielectric constant of soil, k is the wave number and h is the surface roughness (RMS height). The data required were the dielectric constant of soil and the surface roughness. A single value of RMS height (h = 1cm) was assumed for the intire period. This value is based on reported values in the literature for similar conditions ([81],[82],[83] and [72]. Dobson *et al.* ([40],[41]) reported values of dielectric constant for dry sandy soil. For low soil moisture content, the value is equal for different frequencies. Dielectric constants varied between 2.8 and 4, for a soil moisture content [-] of respectively 0.023 and 0.08. Based on these values, the measured soil moisture content will be used to compute the time series of the soil dielectric constant.

2-8-2 Modeling time series

The main question of this modeling exercise is how changes in vegetation water content influences radar backscatter. Furthermore, we want to know whether there is a significant difference in backscatter due to water stress. Modeling of radar backscatter consisted of two parts: the contribution by vegetation and by soil. Combined, a time series of total backscatter from 22 September to 19 October 2012 was simulated for several radar configurations. The simulations were based on time series of soil moisture, vegetation water content and plant height as measured in the field.

The vegetation contribution to radar backscatter at L- and C- band was done using the water-cloud model as presented by Dabrowska-Zielinska *et al.* [75]. More C-band modeling was done using the water-cloud model as presented by Jospeh *et al.* [72], though with multiple angles of incidence (15°,35°,55°) and polarizations (HH, VV). Higher frequency modeling for X-, K_u- and K_a was done using the model presented by Ulaby *et al.* [66] and the modified model based on Ulaby *et al.* [66].

For all radar configurations, the same soil backscatter model was used, i.e. the empirical model presented by Dubois *et al.* [79].

Chapter 3

Results and Discussion

3-1 Meteorology

Fig. 3-1 presents the meteorological data measured at the study site in Citra. Citra is located in central Florida, which was a humid subtropical climate. Although storms can occur, no storm events were registered during the fieldwork campaign. After September it decreases again. A total precipitation of 300 mm fell in September and October, which is 25% higher than average (240mm total in September and October). Average temperatures in September and October are around 27° and 24° respectively. Air temperature was indeed measured around these averages. During the summer months, monthly precipitation is the highest. Air temperature decreases from 25-34° in September to 5-20° at the end of October. Similarly, soil temperature decreased from approximately 30° to 20°. Precipitation events occurred in September and the start of October, but stopped after 7 October. Relative humidity and net radiation also decrease in time. Reference evaporation was almost halved, from 4mm/d in September to 2mm/d at the end of October. Wind speed was quite constant over time, although it appears that there is an increase at the end of October. This meteorological data will be used to quantify water stress.

3-2 Soil moisture

Fig. 3-2 presents the measured soil moisture at the Citra fieldwork site, where data was gathered from 1 September to 21 October. It can be seen that the upper 0.30m is mostly dry. After a rain or irrigation event, the moisture content in the upper layer rises quickly, but most water directly infiltrates to lower layers. Most change in soil moisture content occurs between 0.3m and 0.8m. This is the zone where most root related action takes place (e.g. water uptake). At 1.2m the change in soil moisture is relatively low, because this probably below the root zone of the plants.

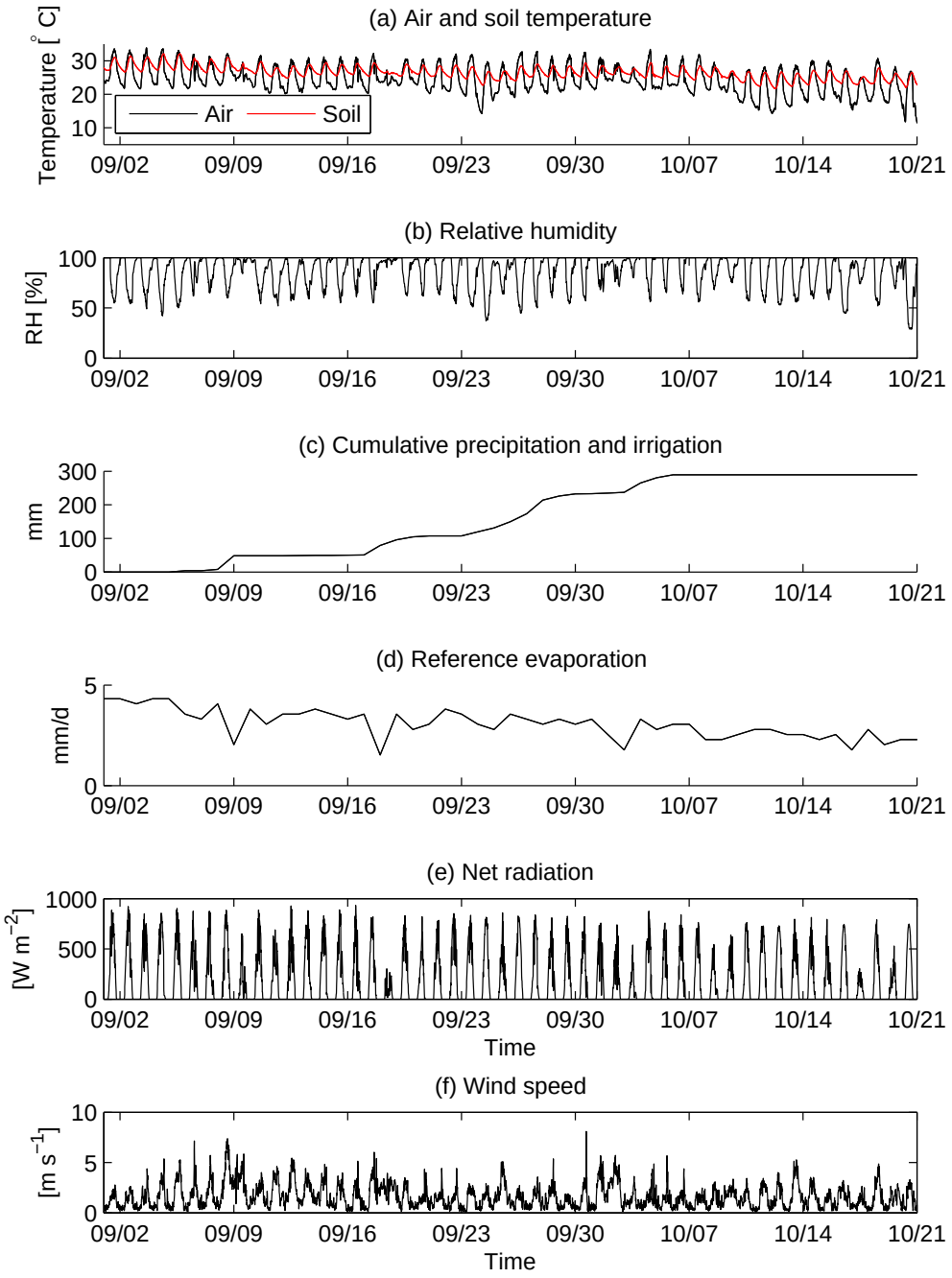

Figure 3-1: Meteorological measurements from 1 September to 21 October 2012 at Citra; (a) Air (at 2m above ground level) and soil temperature (at 10cm depth), (b) Relative humidity at 2m, (c) Daily precipitation, (d) Daily reference evaporation, (e) Net radiation and (f) Wind speed at 2m.

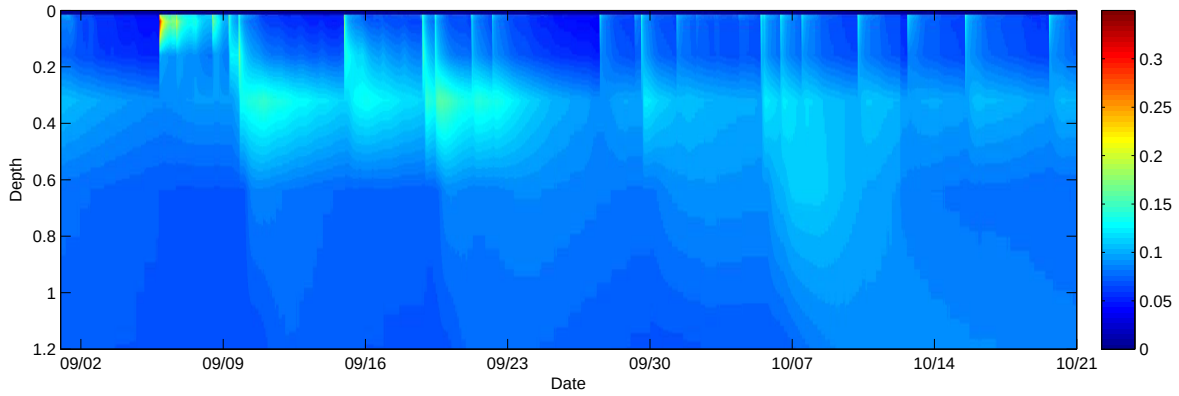

Figure 3-2: Soil moisture measured at the Citra fieldwork site from 1 September to 21 October at 6 different depths (0.02, 0.04, 0.16, 0.32, 0.64 and 1.2m).

3-3 Vegetation

3-3-1 Maize development

Maize development was monitored throughout the field experiment. The results are shown in Table 3-1. Maize developed at a rate of approximately two stages per week (i.e. two new leaves per week). The data in Table 3-1 are based on the plant for which the dielectric constant was measured, which was representative of the surrounding plants. Fig. 3-3 shows the development expressed in (a) the plant height, (b) the gravimetric moisture content M_g [-] and (c) the vegetation water content VWC [kg m^{-2}]. Fig. 3-3 (a) shows the height of the upper and the lower leaf, since these are important parameters for the modeling exercise. Height is considered the distance from ground level to the node where a leaf begins. The node of the upper leaf is not necessarily the highest point of the plant, which can be the stalk or tassel. Height measurements were taken by means of weekly destructive vegetation sampling, which means that the height is not the exactly the same height as the plant on which the dielectric measurements were conducted. However, based on observations the latter was not considered significantly different from the rest of the field.

One can see that the growth rate is the highest during stage V10. This corresponds with the literature ([84], [85]), which found that the time between the emergence of new leaves is shorter and the plant growing rate is relatively high. The grown maize was a crop with a short growing season. Therefore the maximum vegetative stage was reached after V11. As described in Chapter 2, other maize species can continue to stage V16. After the vegetative stage the crop height remained stable, with a maximum height of 1.4 m.

Table 3-1 presents the growing stage of maize as observed in the field. The determination of the growing stage was mainly done based on the number of leaves, which is shown as well. Starting from the tasseling phase the number of leaves was constant. Knowing the growth stage, one can determine the FAO K_c-factor [65]. Table 3-1 shows that at first the K_c-factor has a value of 0.3, which eventually increases to 1.2 at the end of the vegetative phase. Between stage 6 and 11, the K_c-factor linearly increases. During the productive phase the K_c-factor normally decreases again. This phase was not part of the measurement period.

3-3-2 Vegetation water content

Fig. 3-3 (b) shows the leaf and stalk water content at 6AM and 6PM, expressed in gravimetric moisture content of leaves and stalks. It can be seen that after 23 September, all values are decreasing, especially after 7 October. However, the AM leaf values show a remarkable pattern. From 8-12 and from 16-19 October, the 6AM leaf values increase over time.

Fig. 3-3 (c) shows a different pattern. Water content of stalks expressed as VWC first increases from 23 September to 7 October. However, after 7 October a declining pattern can be seen as well. The difference with M_g is that VWC is an absolute amount of water present [kg m^{-2}]. This means that when maize is growing, the absolute amount of water is most probably increasing, since the stalk is growing and more leaves emerge. The relative amount of water, M_g can still decrease though.

On most days, both M_g and VWC were higher in at 6AM compared to 6PM. This was expected since transpiration of maize occurs mainly during the day, with the peak transpiration rate around noon. This implies that M_g and VWC of maize should decrease between 6AM and 6PM. It should be taken into account that every measurement is based on different plants, since wet and dry masses were was determined using destructive methods. When a measurement was taken, it was always aimed to use plants that were representative for the study area. Plants that had a deviating amount of leaves, height, leaf size or damage were not considered as suitable sampling material. The plants were selected to ensure that they were representative of the corn in the study area. Nonetheless, some variability is inevitable.

Table 3-1: Growing stage and K_c factor of maize during the fieldwork in Citra

Date	No. leaves	Growing stage	FAO Kc-factor
19-Aug	0	VE	0.3
7-Sep	6	V6	0.3
13-Sep	7	V7	0.3
14-Sep	8	V8	0.44
19-Sep	9	V9	0.68
21-Sep	10	V10	0.77
1-Oct	11	V11	1.2
4-Oct	11	Tasseling (getting ears)	1.2
9-Oct	12	Tasseling/Silking	1.2
19-Oct	12	Silking	1.2

3-4 Water stress

3-4-1 Water balance

The terms of the water balance are shown in Fig. 3-4. Fig. 3-4 (a) shows the rainfall and irrigation. As discussion in Chapter 2, irrigation was stopped after September 29th. In the first week of October a number of rain events occurred. After October 7th however, no more rain nor irrigation was registered at the study site. In Fig. 3-4 (b) the maximum evaporation

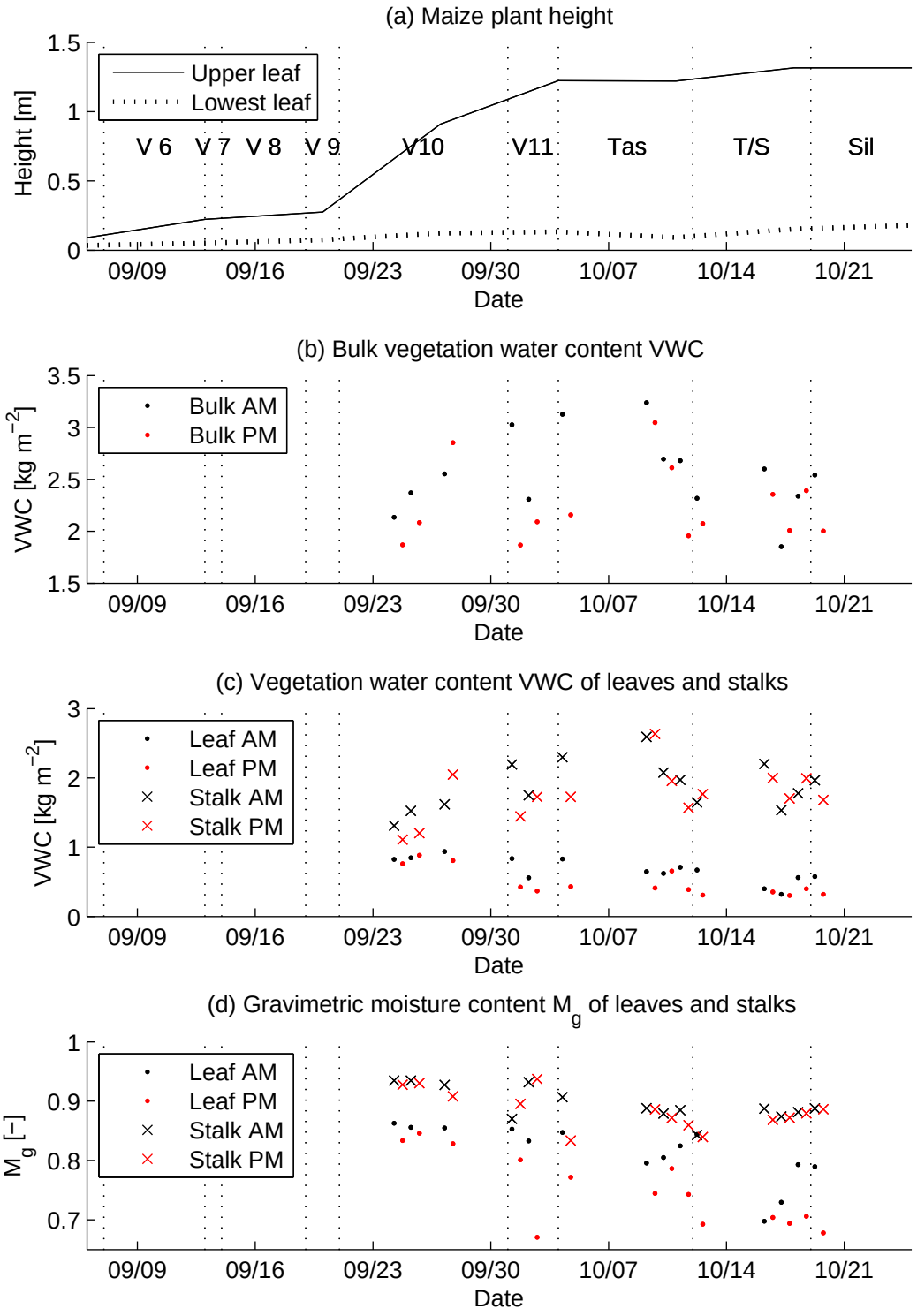

Figure 3-3: Vegetation development 1 Sep - 21 Oct 2012, including growing stages, (a) height of upper and lower maize leaves, (b) Bulk vegetation water content, (c) leaf and stalk vegetation water content - AM and PM leaf values show a negative trend - and (d) leaf and stalk gravimetric moisture content - AM and PM leaf values show a negative trend-

and calculated evaporation is plotted. The maximum evaporation means the theoretical maximum evaporation that would occur if water availability was not constrained (reference evaporation multiplied by the maize crop factor). From the water balance in Chapter 2 follows that during times of insufficient water, one can find an evaporation deficit. By subtracting the deficit from the maximum evaporation, one arrives at the calculated evaporation. Until October 7th the calculated evaporation was almost always equal to the maximum evaporation. Only on September 26th the calculated evaporation was very low. This makes sense since this was the only day between September 24th and October 7th without any rainfall or irrigation. The water balance only takes into account the external fluxes and not the internal water flow patterns of the maize. As follows from the results maize has a high water content, especially the stems. When insufficient water can be taken up from the soil, vegetation uses its own stock of water for transpiration. From 7 to 21 October the calculated evaporation was low again, around 1 mm/d. Fig. 3-4 (c) shows that the change in soil moisture is in the same order of magnitude as the calculated evaporation. Since no precipitation or irrigation occurred during this period, the change in soil moisture was the only source of water to be used for transpiration.

The quantification of water stress by means of the cumulative evaporation deficit is shown in Fig. 3-4 (d). Water stress was summed starting from 1 September. Until 7 October the water stress gradually, but slowly, increased. Between 7 and 21 October however, a large increase was observed (the evaporation deficit doubled). This corresponds with the absence of rain and irrigation.

3-4-2 Soil tension

In Fig. 3-4 (e) the soil water tension at 30cm and 50cm is shown. The first thing that can be noticed is that the tension is fairly higher at 0.3m compared to 0.5m. Furthermore, the steepness and the absolute value of the peaks is higher as well. One can see that on 26 September a high peak was observed in the soil water tension at both depths, followed by another rise in tension starting at 30 September. This can be seen in the evaporation deficit as well, since on 26 and 30 September the the deficit increases. After a rainfall event the tension decreases again, reaching a minimum of 20 [kPa]. From 7 October onwards, the evaporation deficit and the soil water tension at both depths show a sharp increase. This corresponds with the absence of rain or irrigation.

Fig. 3-4 (f) shows the soil moisture content at three depths, i.e. 0.04m, 0.64m and 1.2m. It can be seen that the upper layer reacts faster to rainfall events and drying out of the soil. The low values between 7 and 19 October correspond with observed values for dried out sandy soils from previous studies (e.g. [86], [87]). This corresponds with the observed values of soil water tension in the period of 7 - 19 October, according to the theoretical values found by [88],[89].

From the soil moisture profile it can be derived that the roots are located between 0.4m and 0.8m. Therefore the tensiometer at 0.5m can be considered as a good measure of water stress in the root zone.

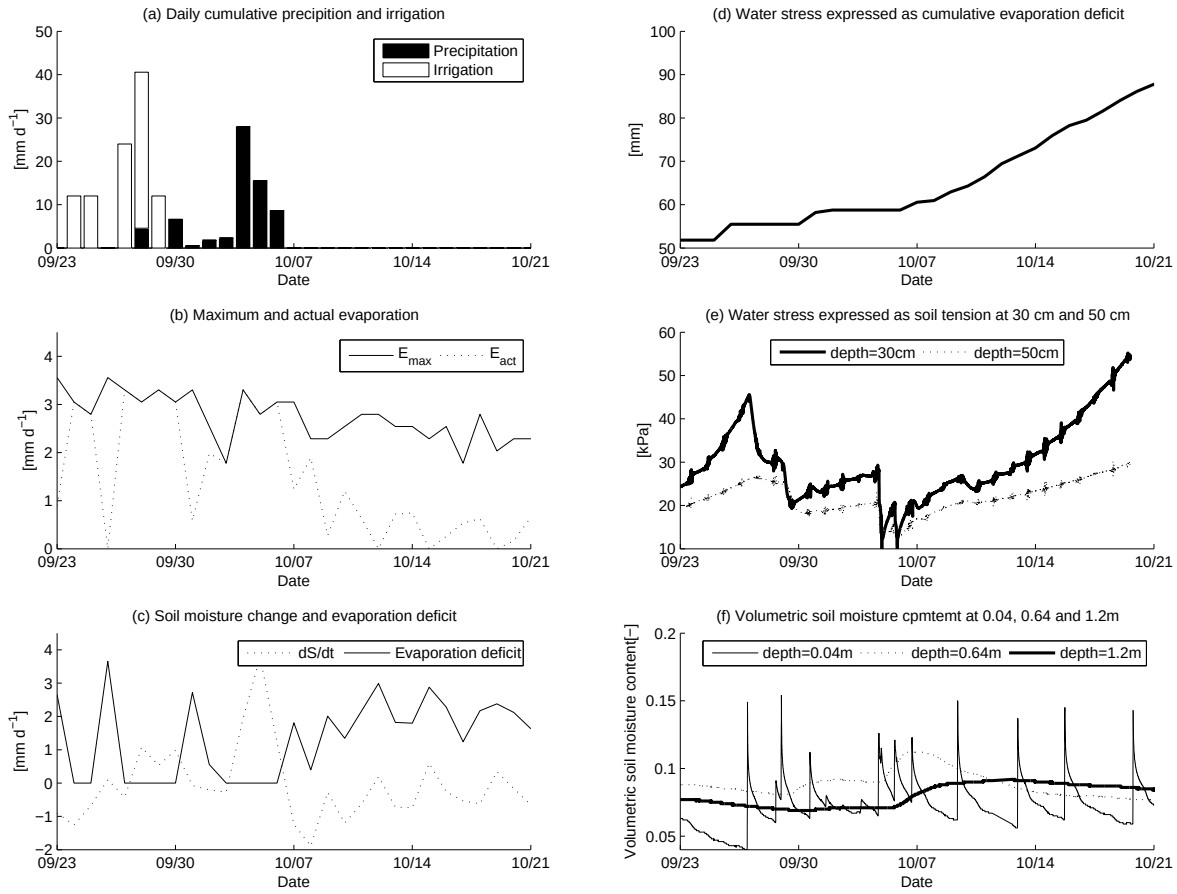

Figure 3-4: Water balance terms and quantification of water stress; (a) Precipitation and irrigation at Citra, (b) maximum and calculated evaporation at Citra, (c) soil moisture change and evaporation deficit, (d) water stress expressed as cumulative evaporation deficit, (e) water stress expressed as soil water tension and 30cm and 50cm depth and (f) soil moisture at 0.04m, 0.64m and 1.2m depth.

3-4-3 Summary and discussion

Water stress has been quantified using (1) a theoretical evaporation deficit and (2) the measured soil water tension. The results of both methods were useful, since similar patterns of increasing water stress were observed. The increase in evaporation deficit matched the increase in soil water tension. However, the magnitude of the soil tension peak at 30cm depth on 27 September does not coincide with an increase in evaporation deficit. This might be explained by a different soil water tension value lower in the root zone. According to Sharp [43] root distribution of maize can easily adjust to the absence or presence of water in certain layers (top soil / upper root zone/lower root zone). When water shortage in the upper soil layer occurs, water is taken from lower soil layers by the maize roots. During a decreasing root water uptake, transpiration decreases and stomatal resistance increases. Apparently water availability was low in the entire root zone after 7 October, since in that case the tension at 30cm and 50cm do show a similar pattern as the evaporation deficit. This can be seen in the soil moisture profile as well. Although at 1.2m the soil moisture content is slightly higher

than at 0.64m and 0.04m, almost no change was registered. This indicates little uptake of water by the roots and hence explains the increasing evaporation deficit. The soil tension at 50cm is considered a good estimate of root zone water tension, since from the soil moisture profile it can be seen that the roots are located between 0.4m and 0.6m depth. Observed soil moisture, soil water tension and calculated evaporation deficit all point at increasing water stress, the implications of which will be investigated in the following section.

3-5 Dielectric property measurements

In this study the resonant frequency of the microstrip line was used as a measure of the dielectric properties of maize leaves. As showed in Chapter 2, a change in leaf water content results in shift in resonant frequency of the sensor. When the leaf water content goes down, the resonant frequency of the sensor at that leaf increases. This section will discuss the time series of the resonant frequencies and its observed diurnal difference. Results will be presented from a trend analysis to quantify the variation in the dielectric properties and relate it to the vegetation water content.

3-5-1 Resonant frequency time series

From 8 to 19 October 2012, dielectric measurements were conducted on leaf 8, 10 and 12 of a single maize plant. During the entire measurement period leaf 12 was the upper leaf. At 6AM and 6PM, each leaf was measured ten times; at five locations and at two measurement orientations (see Chapter 2). To analyze the statistical significance of the results, the measurements were averaged in three ways: (1) an average of all 10 measurements per leaf, (2) an average of the blades (4 measurements) and veins (6 measurements) per leaf and (3) an average of the measurements at 90° (5 measurements) and at 45°. In this chapter only the results from (1) are presented and discussion. Results from (2) and (3) are similar and can be found in Appendix B.

Fig. 3-5 shows the averaged resonant frequency at leaf 8, 10 and 12, including error bars that represent 1 standard deviation. The mean and standard deviation were determined with all 10 measurements (five locations, two angles). The resonant frequency at leaf 8 shows a clear diurnal difference, as the afternoon resonant frequencies are higher than the morning values. This indicated that the leaf is losing water during the day and recovers at night. The order of magnitude of the diurnal difference lies within the range of 0.05-0.12GHz. Leaf 10 and 12 on the other hand show significantly smaller diurnal differences. Moreover, the afternoon values are not always higher than the morning values. This is interesting since it implies that leaves behave differently during a period of water stress.

Fig. 3-6 presents the diurnal difference (PM - AM) for both the vegetation water content and the resonant frequencies of leaf 8, 10 and 12, including a 1 standard deviation error bar. The diurnal difference in gravimetric moisture content is increasing over time. In time, the plants lose more water during the day, which indicates an increasing water stress. This can be seen in the diurnal difference in resonant frequency of the sensor at leaf 8 as well. Over time, the difference between AM and PM values is increasing, meaning that more water is transpired at leaf 8.

Leaves 10 and 12 show only little diurnal difference on all days. In the results from leaf 10 a similar (inverted) signal as leaf 8 can be seen however. The magnitude is smaller, but a matching wave shaped signal can be seen from 8 to 12 October. Especially the dip on 11 October was observed on both leaves. A decreasing frequency implies an increase in water content.

In Appendix A the results are shown of the other methods of averaging, i.e. over blade/vein and over a 90/45° measurement angle. The observed trends were similar. In general, it was observed that the resonant frequency and the diurnal difference of leaf number 8 increased in time. For leaves 10 and 12 the difference was small or non-existent.

3-5-2 Trend analysis of dielectric measurements and vegetation water content

To confirm of reject the hypothesis of an existing trend in bulk leaf water content and the resonant frequencies at the individual leaves (as shown in Fig. 3-5), an analysis was done on all times series of morning and afternoon resonant frequency time series as well as the diurnal difference. Likewise a trend analysis was performed on the vegetation time series.

The results of the trend analysis are presented in Table 3-2. For every data series, the confidence boundaries for the trend were determined.. The minimum confidence boundary value was arbitrarily set at 80%, meaning that lower values were not considerend a trend. This was done because one can always detect a trend in data series if one sets the confidence boundaries low enough.

It can be seen is that the AM and PM data series from leaf 8 show a positive trend with confidence between 87% and 99%. The PM values in particular show a positive trend with very high confidence (96-99%). Also the diurnal difference shows a positive trend with a high level of confidence (91%). The AM and PM values of the bulk leaf vegetation content (both M_g and VWC) show a negative trend with a confidence level between 84% and 98%. On leaf 10 trends are absent in the AM and PM values. The diurnal difference however shows a decreasing trend with a confidence level of 78%. Leaf 12 shows a positive trend in the AM values. No trend is present in the PM values. The diurnal difference of leaf 12 has a negative trend. Implications for the dielectric measurements and vegetation water content are discussed in the next section.

3-5-3 Summary and discussion

The data series of the vegetation water content and the resonant frequency at different leaves yielded interesting results. Apparently a lower bulk leaf water content accompanies a higher resonant frequency at leaf number 8. The question is now why there is such a different between the dielectric data series of the leaves and why a similar increase in frequency was not observed in leaves 10 and 12.

For vegetation sampling bulk measures were conducted. Leaf water content was determined by weighing and drying all leaves from two maize plants, so data on the moisture content of individual leaves were not available. Leaf 8 can be considered as an 'average' leaf. Placed approximately in the middle, higher (and newer) leaves were likely to contain more water. Lower (and older) leaves were drying out, without being replenished again. Therefore it might

Table 3-2: Presence of trends in the resonant frequency data series of the sensor at leaf 8, 10 and 12 and the bulk leaf gravimetric and vegetation water content, including level of confidence, "+" means a positive trend (increasing), "-" means a negative trend (decreasing), "n/a" means that no trend is present.

		AM	PM	PM - AM
Resonant frequency at leaf				
	8	+87%	+99%	+91%
	10	n/a	n/a	n/a
	12	+83%	n/a	-96%
Mg				
	Leaf	-84%	-98%	n/a
	Stem	n/a	n/a	n/a
VWC		n/a	n/a	n/a
	Leaf	-89%	-87%	n/a
	Stem	-89%	n/a	n/a

be reasonable to assume that the bulk leaf moisture content is actually representative for the moisture content in leaf 8.

The difference between data series of different leaves are probably caused by plant physiological effects: (1) influence of the age and position of leaves and (2) protection measures of certain leaves by maize plants.

Several studies have been published on the effect of water stress on individual leaves.

Syvertsen [90] investigated the effect of aging on the leaf water potential. Leaves with a high leaf water potential are better capable of retaining water. Field measurements revealed that older leaves show a decrease in minimum leaf water potential. This could explain the difference between the data series of different leaves. According to Syvertsen [90], older leaves have a lower capability of retaining water, implying that during the day more water is lost. The minimum potential of old leaves are more likely to be lower the value where turgor is lost. The latter causes the stomatas to stay open at times where younger leaves are better able to close the stomatas (e.g. during water stress).

Dwyer and Stewart [91] found that older maize leaves have lower stomatal resistance and a lower photosynthetic rate. This means that the diurnal change in water status is lower compared to younger leaves. A lower stomatal resistance results in more water loss since it takes less energy to evaporate water. Also, the photosynthetic rate is the highest in the leaves around the main ear. Jordan *et al.* [92] reported that water stress first affects lower leaves, by mean of an increase in stomatal resistance. During persistent water stress, the effects proceeds to upper leaves. Furthermore, they reported that stomatal closure is a result of of depressed leaf water potential. According to Turner and Incoll [93], Turner and Begg [94] and Turner ([95], [96]), stomatal resistance of maize leaves are higher at lower leaves near the bottom. Holgren *et al.* [97] and Slatyer and Bierhuizen [98] on the other hand found that photosynthesis (and hence change in leaf water status) increases with leaf age. According to them, lower (older) leaves should have higher diurnal difference in water content caused by higher photosynthetic rates. Brown and Rosenberg [99] found that leaves with lower illumination (lower leaves) have generally higher photosynthetic rates. Beardsell and Cohen

[100] related stomatal resistance in maize to the level of abscisic acid (ABA), which both increases during water stress. ABA is a plant hormone, which controls the amount of water that is lost through stomas as a response to drought.

What we know is that the upper leaves 10 and 12 show little diurnal variation compared to leaf 8. Leaf 8 is a lower and older leaf with less illumination. Leaf 10 and 12 were fully exposed to solar radiation. A diurnal difference in resonant frequency implies a change in leaf water status, since that is the main driver of the dielectric properties. Low diurnal difference in the upper leaves is probably the result of low photosynthetic rates. The latter can either be caused by high stomatal resistance or a depleted leaf water status. The bulk leaf water content cannot confirm or reject any of the proposed causes. Measurements of leaf water status (thickness, leaf water content, leaf water potential) of individual leaves would give more insight it what processes are governing. However, it is likely that the stomatal resistance of the upper leaves was higher. The absolute values of the resonant frequency was generally lower in leaf 10 and 12 compared to leaf 8, which indicates a higher water content. This is in correspondence with field observations, which did not suggest that the upper leaves had a lower water content than leaf 8. In that case the released ABA caused the upper leaves to retain more water, together with an increase of the stomatal resistance.

Another interesting influence could be the presence of ears. During this study the main (and only) ear was located between leaf 6 and 8. This would explain the high photosynthetic rate of leaf 8 and hence the significantly larger diurnal difference in resonant frequency.

The trend analysis suggests that a decrease in bulk leaf water content can be associated with an increase in resonant frequency in leaf 8. Leaf 10 probably arrived at a level of minimum water content. ABA protected leaf 10 from further depletion of water content, leading to a stable water content and an absence of a trend in resonant frequency. Leaf 12 shows two trends, an increasing resonant frequency in the morning measurements and a decreasing diurnal difference. It is likely that in the afternoon leaf 12 reaches its minimum water content, after which ABA is activated to control further loss of water. Longer time series are required to see whether the resonant frequencies reaches stable values and the diurnal difference indeed goes to 0 (like leaf 10).

Summarizing, leaf 8 showed a trend of increasing resonant frequency. This is caused by a lower water content in that particular leaf. The diurnal difference also increased, indicating a rise in photosynthetic rate. The latter corresponds with the presence of the main ear around leaf 6-8 and a theoretical lower stomatal resistance on lower leaves. In leaf 10 and 12 the photosynthetic rate is probably minimized by ABA to protect the leaves from damage due to a too low water content. Therefore, the photosynthetic rate and hence the diurnal difference in resonant frequency was decreased.

To fully understand the measured dielectric properties of leaves, it is required to gain more insight in what drives the water status of individual leaves during water stress. It would be useful to further investigate of vertical moisture distribution and the effects of ears on photosynthesis. For next measuring campaigns it might interesting to measure various indicators of leaf water/drought status, e.g. leaf thickness, leaf water potential, photosynthetic rate and the amount of ABA.

3-6 Water cloud model simulations of radar backscatter above a vegetated surface

3-6-1 Sensitivity analysis of radar backscatter to soil moisture and vegetation water content

The sensitivity to soil moisture and vegetation water content for several radar configuration was determined using the water cloud model [67]. This modeling exercise was performed so show the effect that vegetation has on radar backscatter and that more detailed data on vegetation moisture content and/or dielectric constant would be beneficial for understanding radar backscatter from vegetated surfaces. Values of soil moisture and VWC were based on the measured values from the field. During the measurement campaign, soil moisture values between 0.04 and 0.2 [-] were registered. The measured total bulk vegetation water content values were all within the range of 1.5 to 3.5 kgm^{-2}. In the following sections the results of C- and L-band (based on [75]) and X-, K_u-,K_a (based on [66]) will be presented and discussed.

L-band (Dabrowska-Zielinska *et al.* 2007)

Fig. 3-7 presents the results of the sensitivity analysis for a L-band radar configuration (1.8 GHz, HH polarized). The total backscatter was calculated using Eq. 2-19 - 2-20. It consists of two terms, i.e. the contribution by vegetation and the attenuated soil contribution. The vegetation backscatter is a function of VWC and soil backscatter depends on soil moisture. The attenuated soil backscatter is influenced by VWC as well, since the canopy decreases the signal through two-way attenuation. A higher VWC results in a lower transmissivity, and higher attenuation. Total backscatter is therefore a function of both VWC and soil moisture.

Fig. 3-7 (a) presents the vegetation backscatter as a function of VWC. Also it shows the range of the soil moisture backscatter contribution. It can be seen that up till a VWC of 2.6 kgm^{-2} the soil backscatter term is higher than the vegetation contribution. Between 2.6 and 2.8 kgm^{-2} the order of magnitude is about the same, but for higher VWC values it is mainly the vegetation water content that determines the total backscatter. Fig. 3-7 (b) shows the soil backscatter as a function of soil moisture. A high soil moisture results in a high backscatter. This can also be seen in Fig. 3-7 (d), since up to a VWC of 2.6 kgm^{-2} the total backscatter is mainly in the range of the soil contribution. At higher VWC values, vegetation water content takes over as the governing influence on total backscatter.

L-band radar penetrates further into soil and canopy compared to higher frequencies. Therefore L-band is very useful for measuring soil moisture. The results presented here illustrate that in a dry soil the variation is total backscatter is mainly due to variation in vegetation water content. Apparently, in the lower range of soil moisture content, this particular L-band backscatter (35°, HH) is mainly sensitive to VWC. Please not that this modeling exercise is based on one L-band configuration only.

C-band (Dabrowska-Zielinska *et al.*, 2007)

The C-band modeling results are shown in Fig. 3-8. Fig. 3-8 (a) shows the vegetation backscatter as function of VWC, including the range of the soil backscatter contribution.

At VWC values lower than 1.8 kgm^{-2} the soil contribution is higher than the vegetation contribution. For higher values of VWC, the soil and vegetation contributions are in the same range. This can be seen in Fig. 3-8 (d), which shows that total backscatter is equally influenced by VWC and soil moisture for VWC values higher than 1.8 kgm^{-2}.

X-, K_u- and K_a-band (Ulaby *et al.*, 1984)

Fig. 3-9 to 3-12 show the modeling results for 8.6, 13, 17 and 35 GHz. In this modeling approach it was possible to simulate leaf and stalk backscatter separately, in addition to the attenuated soil signal. Vegetation backscatter consists of the contributions of leaves and the stalk. Stalk backscatter decreases with an increasing VWC, in contrast to leaf backscatter. This is due to attenuation caused by the leaves, decreasing the measured signal from stalks. The order of magnitude of stalk backscatter is significantly lower than leaf backscatter for all frequencies. This means that mainly leaves determine the vegetation backscatter.

The attenuated soil signal is strongly dependent on VWC. The highest soil contribution occurs at times when VWC is very low, because the two-way attenuation is small. The order of magnitude of the soil backscatter is lower than vegetation at all frequencies. The attenuated soil backscatter is even smaller, making only a relatively small contribution to the total backscatter.

At higher frequencies the sensitivity of total backscatter to VWC increases. E.g. at 35GHz, the total backscatter is mainly sensitive to vegetation backscatter. This can be explained by the fact that at higher frequencies, backscatter mainly consists of surface scattering instead of volume scattering. The microwaves cannot easily penetrate the canopy and are hence mainly sensitive to leaf water content of the upper leaves. Furthermore, the absolute value of the modeled retrieved signal is higher at higher frequencies. This is because of similar reasons. When no volume scattering takes place, the total reflected signal is generally higher.

This sensitivity analysis showed that total backscatter at higher microwave frequencies is mainly determined by the contribution of vegetation. Since vegetation is almost only determined by leaf backscatter, this exercise shows that it is almost only the leaves that determine radar backscatter. This shows the importance of understanding how leaf dielectric properties vary with water stress and influence radar backscatter.

3-6-2 Backscatter time series simulations

L-band (Dabrowska-Zielinska *et al.* 2007)

Fig. 3-13 presents the simulated radar backscatter time series for a L-band radar configuration (HH polarization, 35°). For the computations the total bulk VWC was used, which lead to a similar pattern in backscatter. The difference between the maximum and minimum computed values is 7 dB. It can be seen that from 23 September to 7 October the signal is increasing in similar fashion as the total VWC. After 7 October the signal is decreasing. The results show a decreasing trend in PM values and no trend in AM values in the period from 7 to 19 October, as can be seen in Table 3-3.

Table 3-3: Observed diurnal difference and presence of trends (+ for positive, - for negative, n/a for no trend) including confidence boundaries for all modeled radar configurations. Trend was determined for the period from 8 to 19 October 2012.

Author	Band	Frequency	Polarization	Incidence angle	Diurnal difference	Trend					
		[GHz]		[$\^circ$]	[dB]	AM		PM		PM-AM	
						+/-	Confidence	+/-	Confidence	+/-	Confidence
Ulaby	X	8.6	VV	50	0.03	-	96		n/a		n/a
et al. (1984)	Ku	13.0	VV	50	0.02	-	96		n/a		n/a
	Ku	17.0	VV	50	0.02	-	96		n/a		n/a
	Ka	35.0	VV	50	0.06	-	96		n/a		n/a
Modified Ulaby	X	8.6	VV	50	0.8	-	94	-	82		n/a
et al. (1984)	Ku	13.0	VV	50	0.8	-	89	-	82		n/a
	Ku	17.0	VV	50	0.8	-	89	-	82		n/a
	Ka	35.0	VV	50	0.9	-	94	-	82		n/a
Dabrowska-Zielinkska	L	1.8	HH	35	0.4	-	96		n/a		n/a
et al. (2007)	C	5.3	VV	23	2.1	-	96		n/a		n/a
Joseph	C	4.8	HH	15	0.3	-	96		n/a		n/a
et al. (2010)	C	4.8	HH	35	1.1	-	96		n/a		n/a
	C	4.8	HH	55	1	-	96		n/a		n/a
	C	4.8	VV	15	1.1	-	96		n/a		n/a
	C	4.8	VV	35	1.1	-	96		n/a		n/a
	C	4.8	VV	55	1.1	-	96		n/a		n/a

C-band ((Dabrowska-Zielinska *et al.* 2007))

Fig. 3-13 presents the simulated radar backscatter time series for a C-band radar configuration (VV polarization, 23°). The pattern is similar to the backscatter computed for L-band. The difference between the maximum and minimum simulated backscatter value is approximately 2.5 dB. It can be seen that from 23 September to 7 October the signal is increasing in similar fashion as the total VWC. After 7 October the signal is decreasing. The results show a decreasing trend in AM values and no trend in PM values in the period from 7 to 19 October, as can be seen in Table 3-3.

C-band at different polarizations and incidence angles (Joseph *et al.* 2010)

Fig. 3-14 presents the results for the 6 radar configuration calibrated by [72]. The pattern is similar to other results that used the same input data. A similar trend was found in the PM values, in contrary to the AM values where no trend was found. The only difference is the change in magnitude, depending on the polarization and angle of incidence. In general, HH configurations have higher backscatter then VV configurations. In Fig. C-4 backscatter is plotted against VWC for all combinations of incidence angle and polarization. One can see here that 15° has the highest backscatter, followed by 55° and 35°. The latter is interesting, since normally microwave backscatter decreases with a higher incidence angle [18]. The path length through vegetation increases as the incidence angle increases ([101],[102],[103]). A longer path length causes more interaction with the vegetation and hence more attenuation of the signal. No clear reason was found why the backscatter at 55° is higher than at 35°.

X-, K_u- and K_a-band (Ulaby *et al.* 1984)

Fig. 3-15 presents the modeled radar backscatter time series for high frequencies (8.6 - 35GHz). In general the AM values are higher that the PM values, which is caused by a higher vegetation water content. Table 3-3 shows the order of magnitude of the diurnal

difference of the predicted total backscatter, which is between 0.02 and 0.06 dB. This is not a very high diurnal difference. Furthermore, no trend is present in the backscatter, which was expected. Given a decreasing vegetation water content and an increasing water stress, one would expect that his has influence on the radar backscatter.

X-, K_u- and K_a-band (modified Ulaby *et al.* 1984)

A different response is calculated with the modified water cloud model. In the latter, leaf and stalk vegetation water content values were used as input data, instead of bulk vegetation water content. In Fig. 3-16 it can be seen that the AM values are again higher than the PM values. The extra information about the water status of leaves and stalks resulted in a decreasing radar reflected in both the morning and afternoon. In Table 3-3 it is shown that both the AM and PM data series show a clear negative trend. This can be explained by decreasing leaf water content, which has a high impact on radar backscatter at high frequencies. The diurnal difference has the order of magnitude of 0.8 dB, which is significantly higher. The backscatter simulated with the modified water cloud model shows better correlation with the trend in water stress and leaf water content. This suggests that modeling including additional detail might be useful.

3-6-3 Summary and discussion

The results of the sensitivity analysis suggest that L-band radar might be more sensitive to VWC than to soil moisture, at least in the range of respectively 1.5 - 3.5 kgm^{-2} and 0.04 - 0.2. This interesting for future L-band satellite missinos. For example, NASA's SMAP mission will use L-band radar for soil moisture retrieval. According to [29] and [104], soil moisture retrieval is not significantly influenced by vegetation water content for VWC values lower than 5 kgm^{-2}. In this study, the variability in VWC was higher than the variability in soil moisture. From the sensitivity analysis it could be seen that at for low soil moisture values, it is mainly the vegetation that influences the total backscatter at L-band.

Higher frequencies might be applicable for vegetation water status monitoring. At all frequencies (8.6, 13, 17 and 35 GHz), the total backscatter was sensitive to VWC. As soil moisture content increases, the sensitivity to soil moisture increases as well. A constraint however can be the observable difference in magnitude of the backscattered signal. However, if diurnal differences of a low order of magnitude (0.01 - 0.1 dB) can be measured, this would mean it is possible to observe the effects of water stress on vegetation.

For the modeled time series of all different radar configurations, the absolute value of the backscatter, the diurnal difference and the difference in backscatter between high and low soil moisture content did vary. At high frequencies (8.6 - 35 GHz), the diurnal difference is very low and it is debatable whether this difference can actually be measured in the field. The modeled time series for most radar configurations did not show very different patterns. The pattern was equal and in all configurations a negative trend was observed in the PM values. For all tested radar configurations it was seen that vegetation has a significant influence in the total backscatter. Furthermore, the temporal pattern of VWC can be seen in all modeled radar backscatter time series as well. This shows that apparently it is not very important at which frequency a vegetated surface is measured.

The modified water-cloud model yielded very interesting results. By using the separate vegetation water content values for leaves and stems, the simulated backscatter was very different to that obtained using Ulaby *et al.* [66]. Although still in the high frequency range, the diurnal difference was higher (0.8 dB). Using the modified water-cloud model the effects of water stress on radar backscatter were very clear. A decreasing trend in backscatter was observed, coinciding with a similar increase in water stress. The modified water-cloud modeling approach shows the benefits of using detailed data instead of bulk values. As it was showed in the sensitivity that radar backscatter at high frequencies is mainly influenced by leaf backscatter, taking this into account allows more accurate backscatter modeling. The modified water-cloud model showed the possibilities of vegetation monitoring with high frequency microwaves. When more detailed models and data are taken into account, it could be possible to use high frequency microwave backscatter as an indication for water stress.

One limitation in this study is the dependency on calibrated parameters in order to predict backscatter. Calibration studies are very specific (e.g. location, crop, radar configuration), making the amount of applicable parameters sets rather limited. Using this approach lowers the freedom to investigate how different radar polarizations, e.g. cross polarization, frequencies or incidence angles respond to certain vegetation and soil water content. Furthermore, most parameter sets have been calibrated only once, without ever being checked again by other authors. Although at first sight the circumstances of [66],[75] and [72] look similar to the fieldwork site in Citra, FL, there still might exists non reported differences. A solution for this issue might be to calibrate the water-cloud model during a next fieldwork campaign. Firstly, this would allow us to test the the modeled time series produced in this research. Secondly, this would provide a parameter set specifically for Citra, which could be used in further research.

Another possible improvement is the use of more detailed model to simulate radar backscatter (e.g. MIMICS [26]). Benefits are that this will account for all backscatter terms, including multi-bounce scattering. Also, it would be possible to include field measurements of the dielectric constant. A multi layer model would for example give more insight in how much backscatter would actually occur for a given radar configuration. During the field campaign dielectric measurements were taken at three levels in the canopy. It would be useful if we could include the observed vertical distribution in the backscatter model. The full potential of high frequency microwaves for vegetation water status monitoring will be revealed when more detailed models and data are used. However, the modified water-cloud model already showed the possibilities are promising.

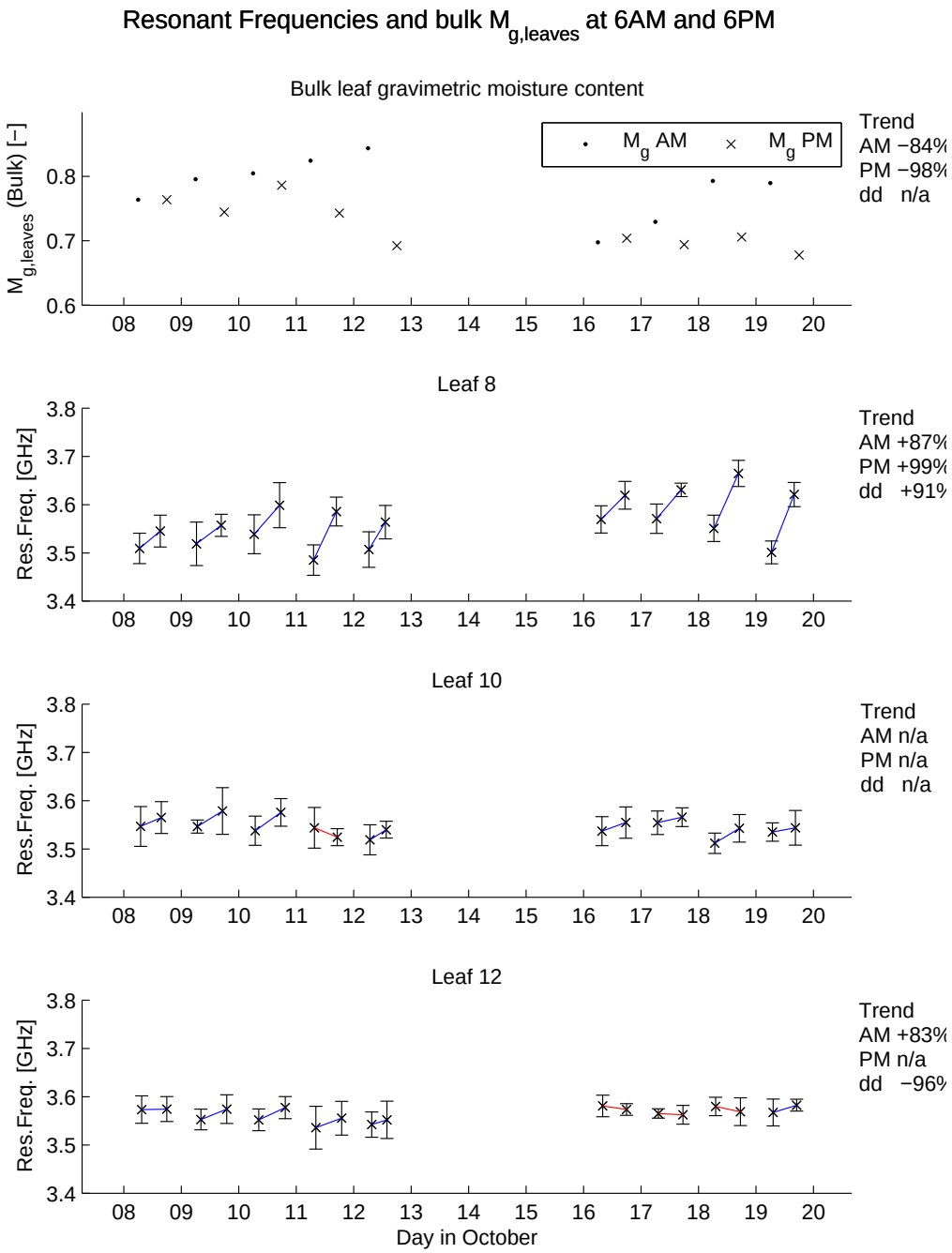

Figure 3-5: Bulk leaf water content and resonant frequencies of the microstrip line sensor at leaf 8, 10 and 12 in time, averaged over all measurements per leaf. Including confidence of the presence of trends, "+" indicates an increasing trend, "-" indicates a decreasing trend and "n/a" indicates no trend. Blue and red lines respectively indicate an increase and decrease of resonant frequency during the day.

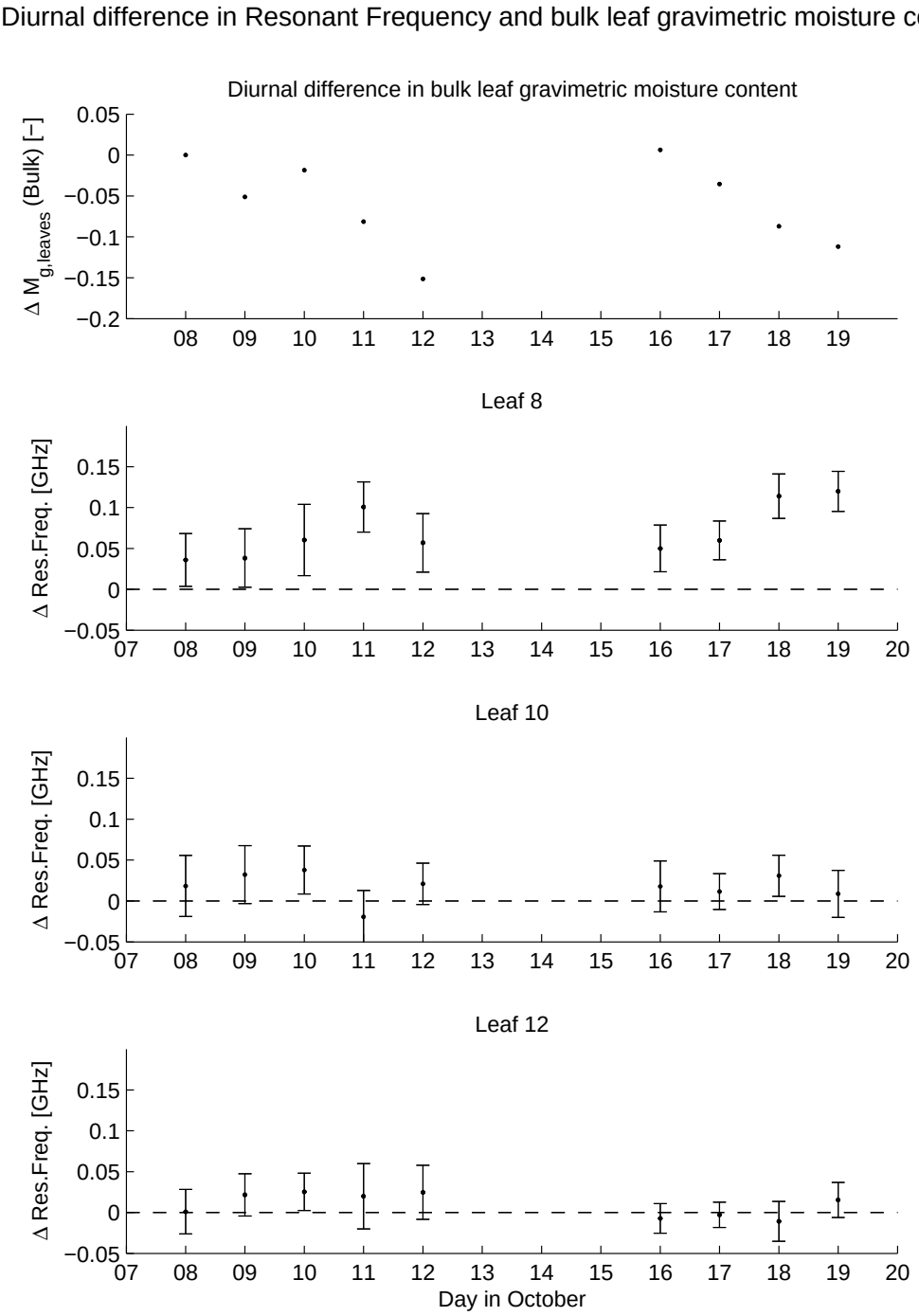

Figure 3-6: Diurnal difference (PM - AM) of gravimetric moisture content and of the resonant frequency the microstrip line sensor at leaf 8, 10 and 12, averaged over all measurements per leaf.

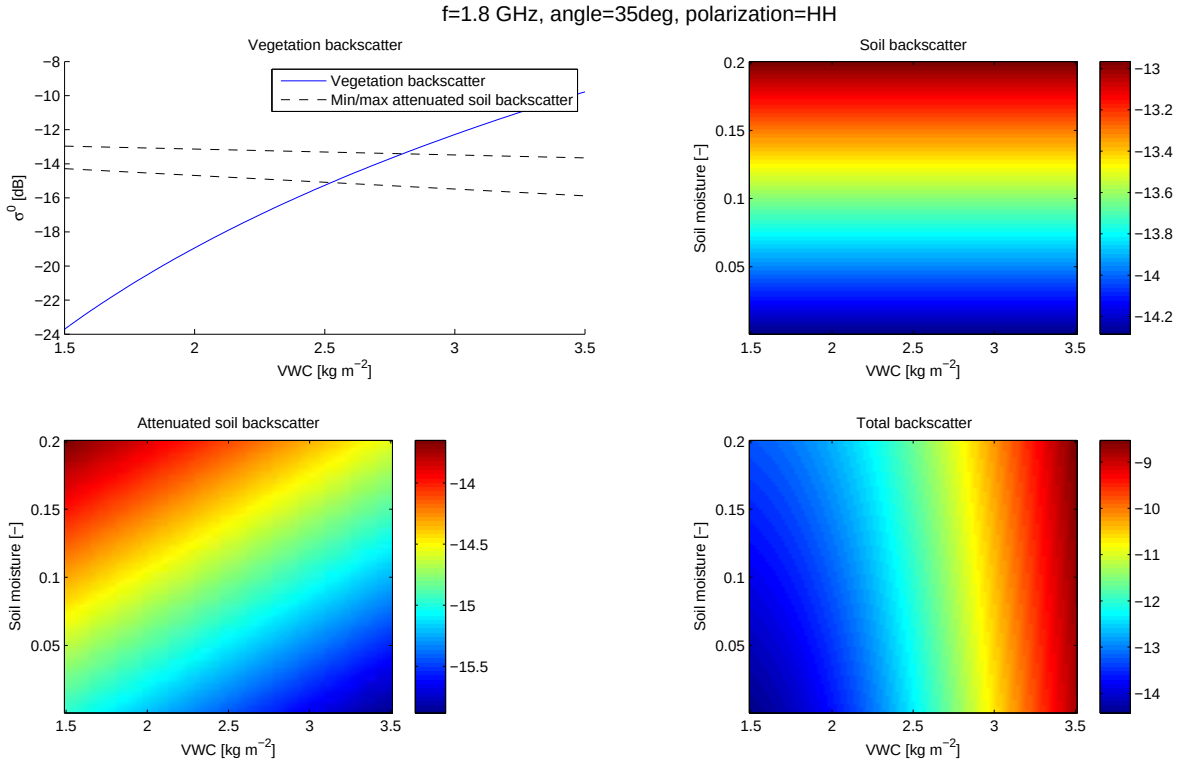

Figure 3-7: Sensitivity of L-band to soil moisture and vegetation water content based on Dabrowska-Zielinska *et al.* (2007); (a) leaf backscatter, (b) soil backscatter, (c) attenuated soil backscatter and (d) total backscatter.

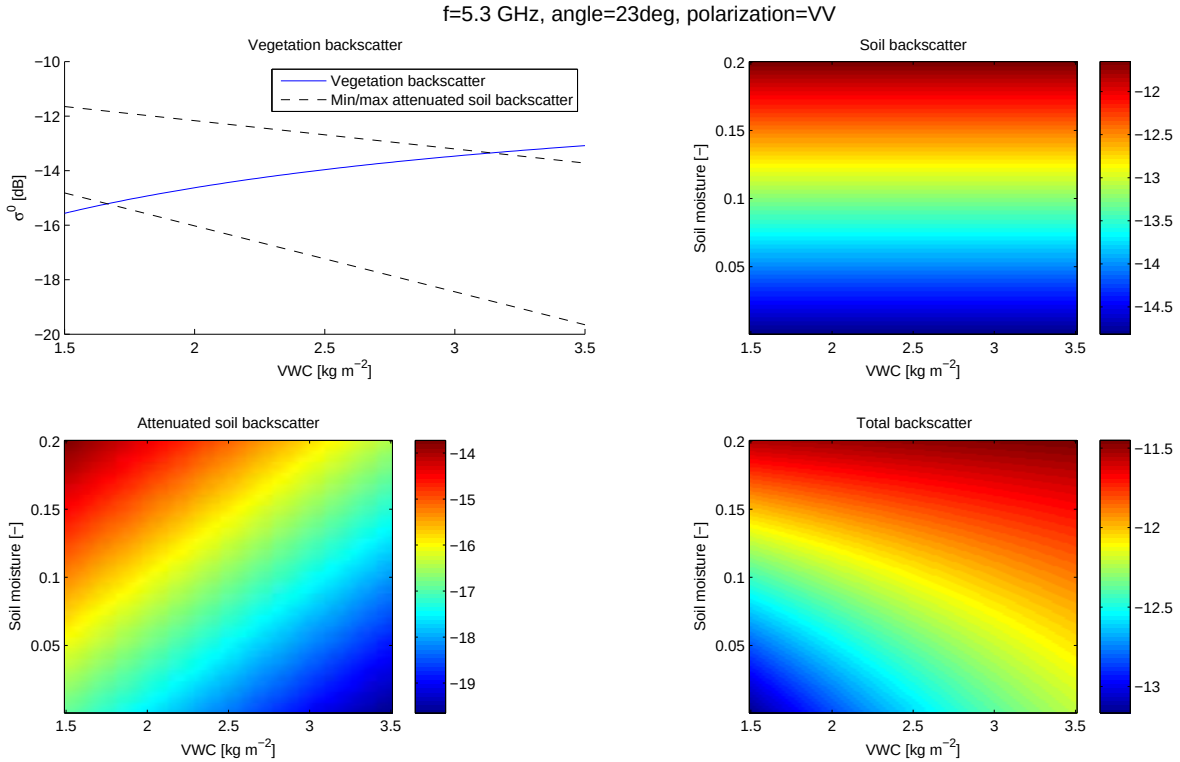

Figure 3-8: Sensitivity of C-band to soil moisture and vegetation water content based on Dabrowska-Zielinska *et al.* (2007); (a) leaf backscatter, (b) soil backscatter, (c) attenuated soil backscatter and (d) total backscatter.

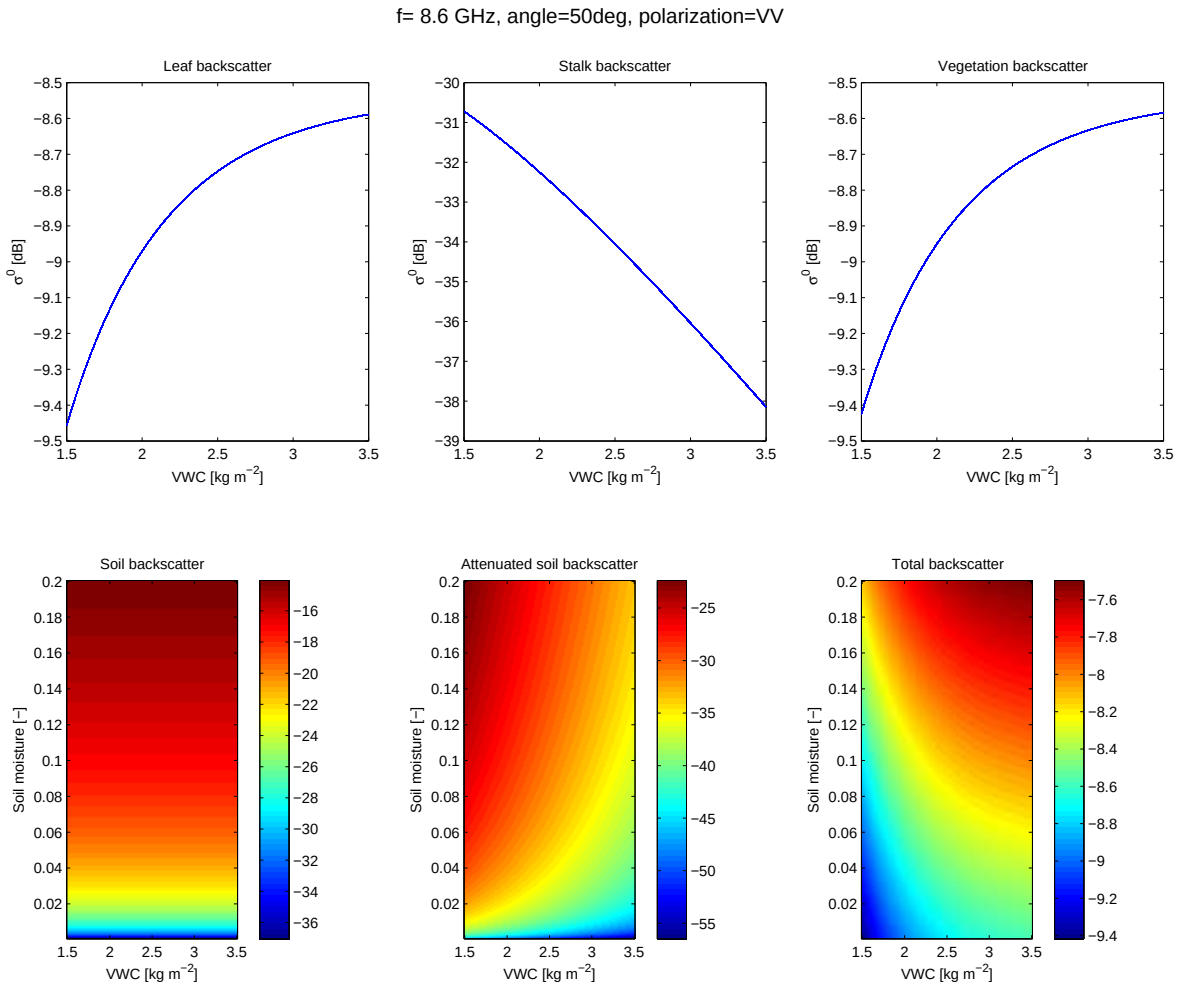

Figure 3-9: Sensitivity of X-band (8.6 GHz) radar to soil moisture and vegetation water content based on Ulaby *et al.* (1984); (a) leaf backscatter, (b) stalk backscatter, (c) total vegetation backscatter, (d) soil backscatter, (e) attenuated soil backscatter and (f) total backscatter.

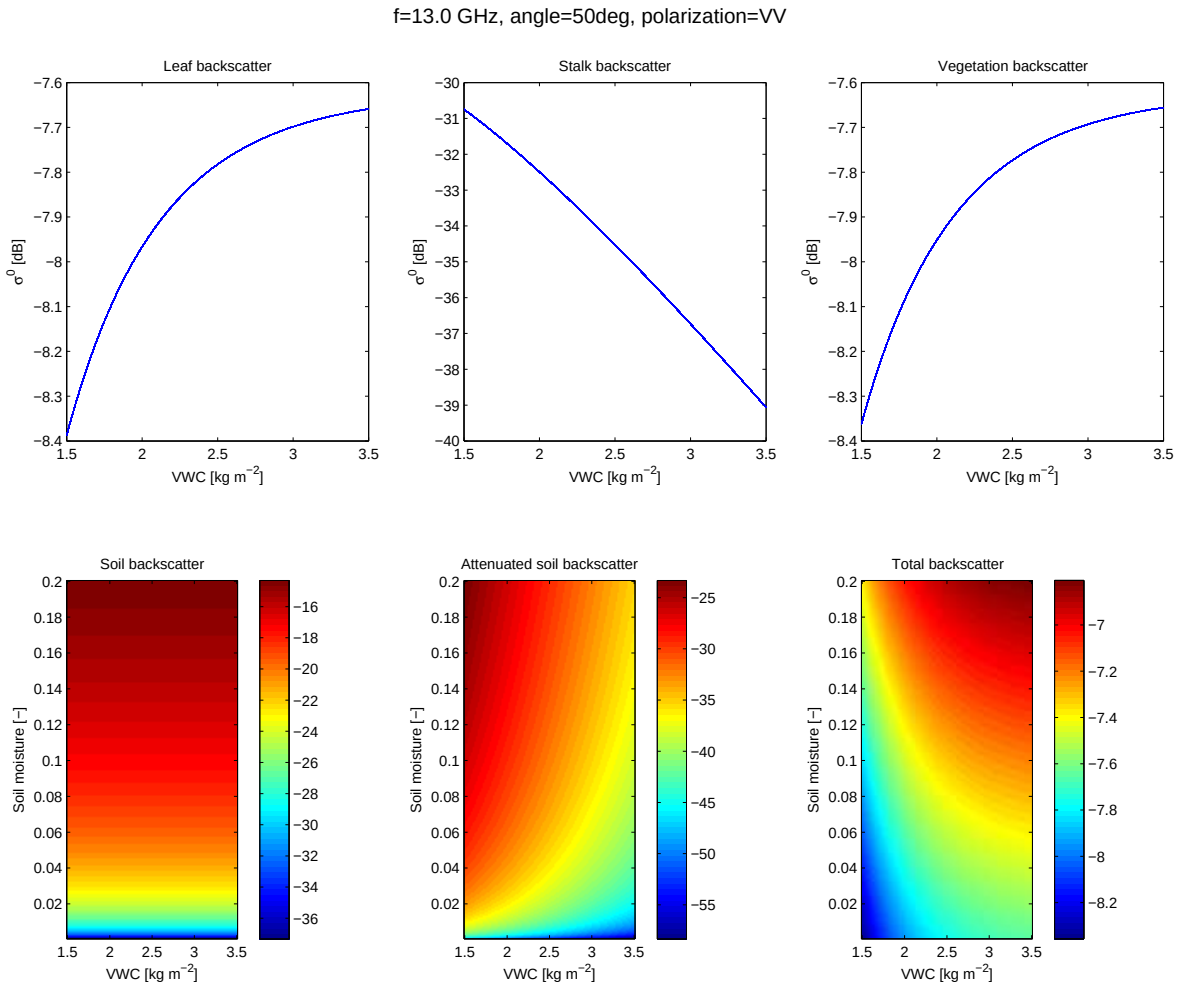

Figure 3-10: Sensitivity of K_u-band (13 GHz) radar to soil moisture and vegetation water content based on Ulaby *et al.* (1984); (a) leaf backscatter, (b) stalk backscatter, (c) total vegetation backscatter, (d) soil backscatter, (e) attenuated soil backscatter and (f) total backscatter.

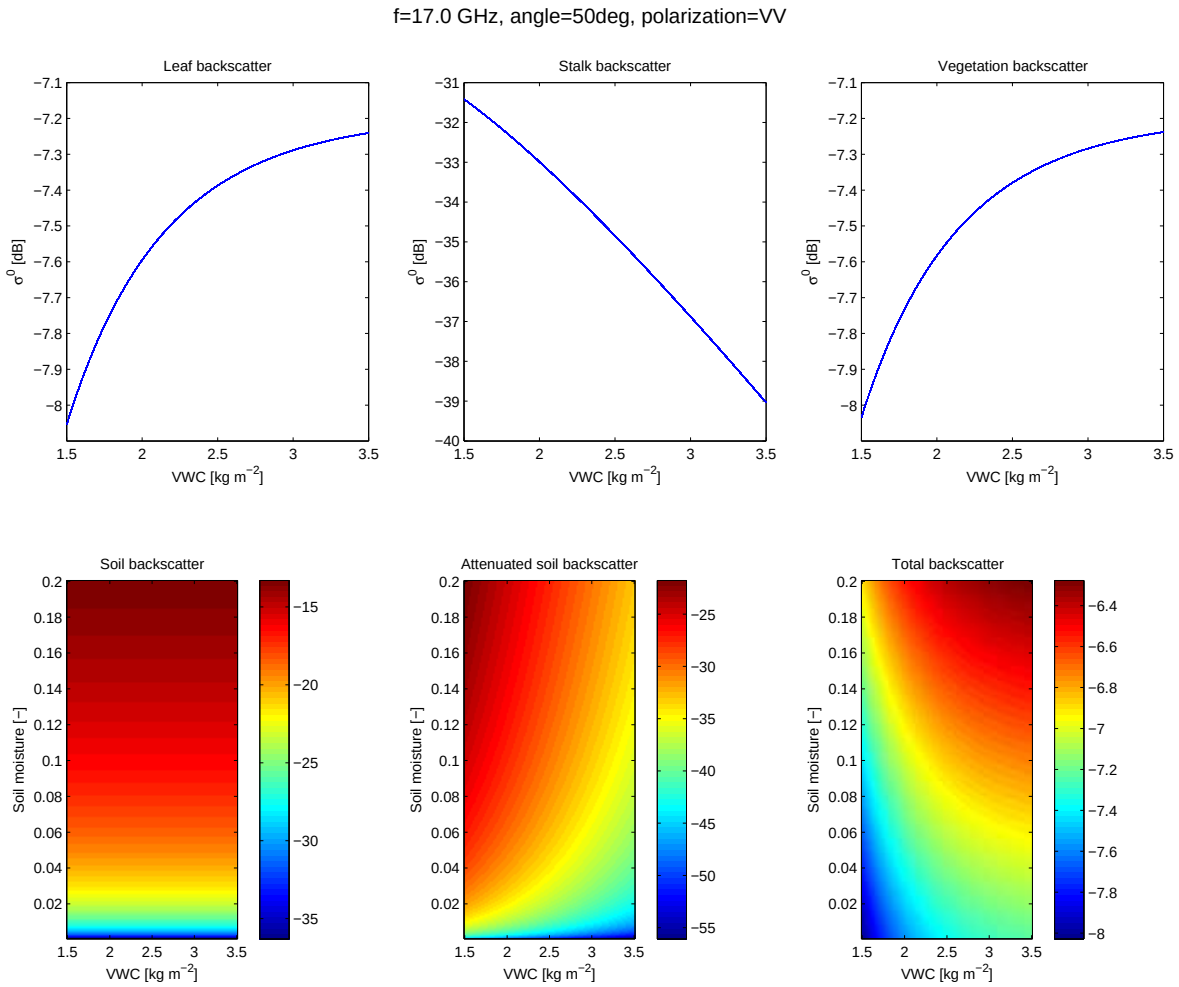

Figure 3-11: Sensitivity of K_u-band (17 GHz) radar to soil moisture and vegetation water content based on Ulaby *et al.* (1984); (a) leaf backscatter, (b) stalk backscatter, (c) total vegetation backscatter, (d) soil backscatter, (e) attenuated soil backscatter and (f) total backscatter.

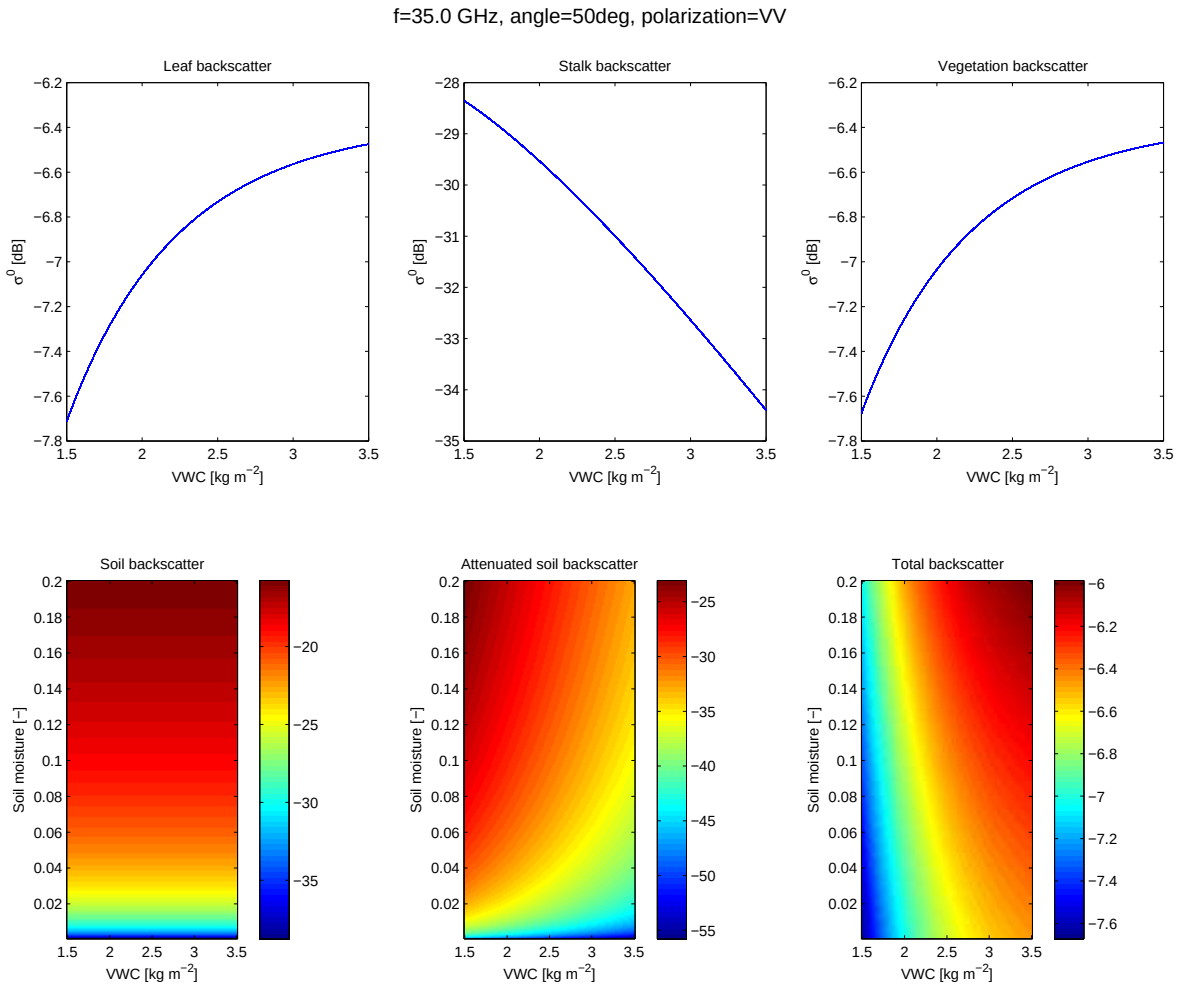

Figure 3-12: Sensitivity of K_α-band (35 GHz) radar to soil moisture and vegetation water content based on Ulaby *et al.* (1984); (a) leaf backscatter, (b) stalk backscatter, (c) total vegetation backscatter, (d) soil backscatter, (e) attenuated soil backscatter and (f) total backscatter.

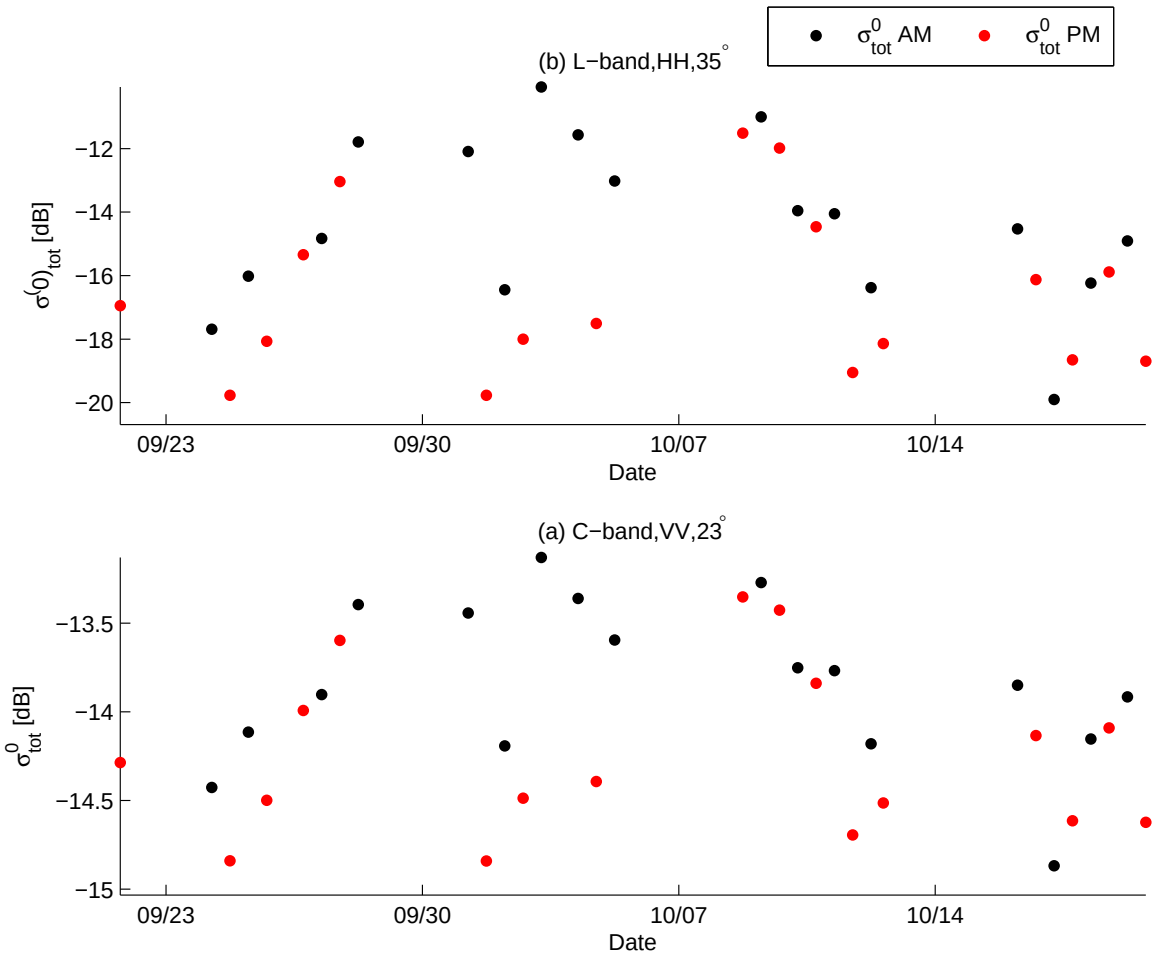

Figure 3-13: Total modeled radar backscatter time series ising Joseph *et al.* (2010) at AM and PM for (a) L-band VV polarized with an incidence angle of 35° and (b) C-band HH polarized with an incidence angle of 23°.

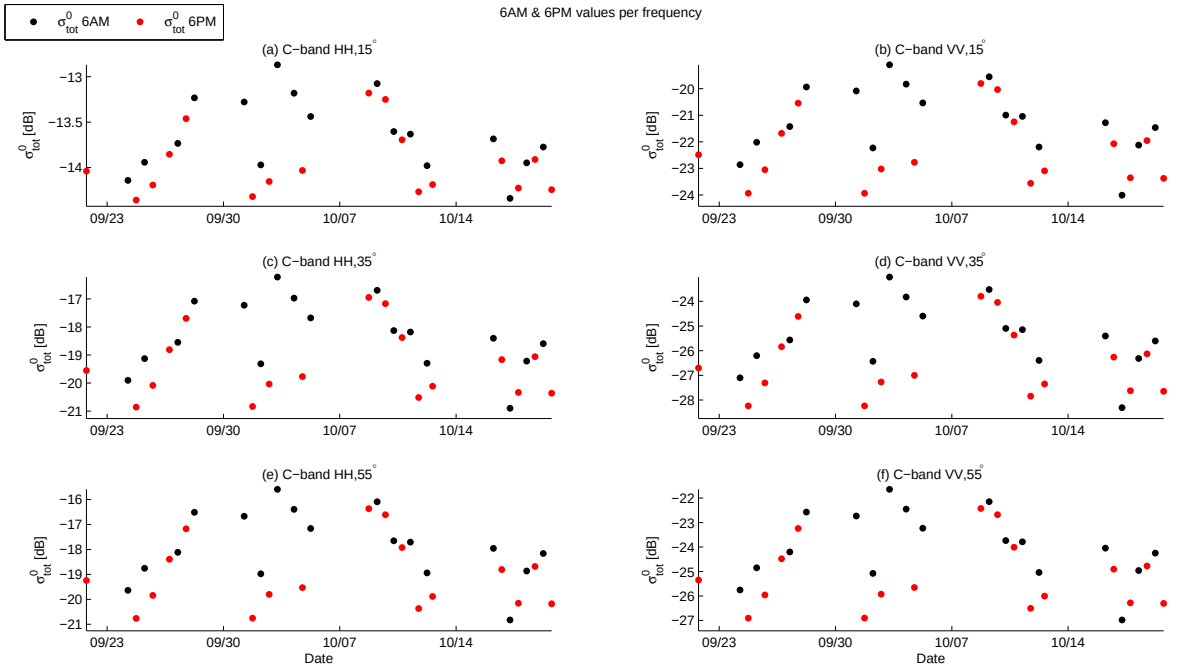

Figure 3-14: Total modeled radar backscatter times series using Jospeh *et al.* (2008) for C-band st different polarizations (HH and VV) and incidence angles (15°, 35°, 55°)

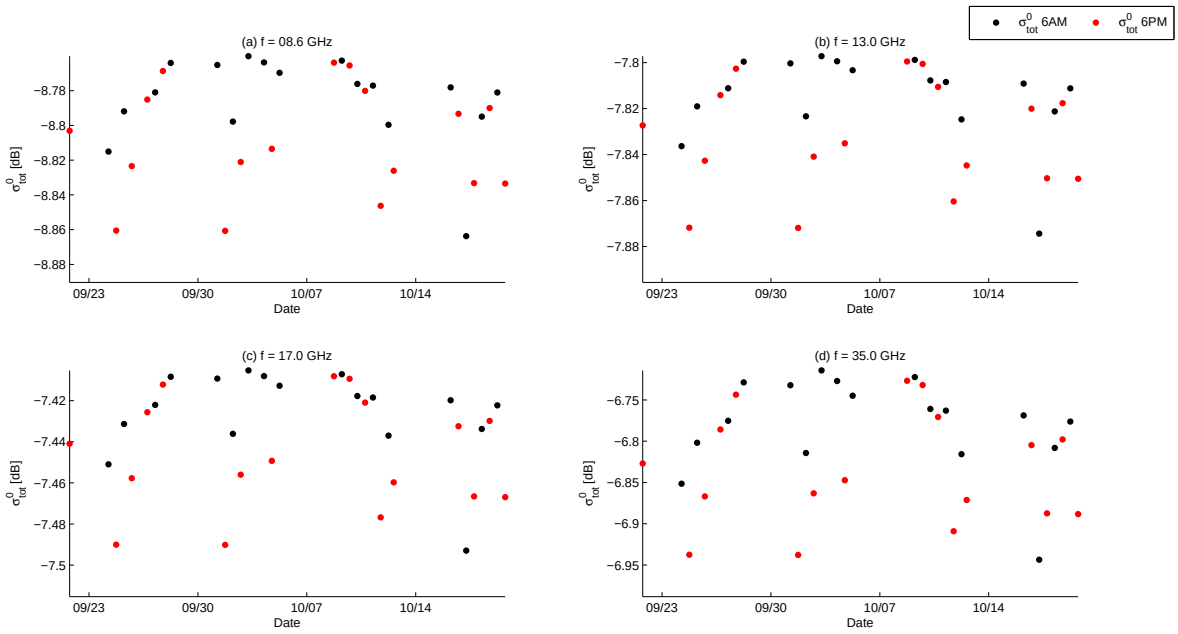

Figure 3-15: Total modeled radar backscatter time series using Ulaby *et al.* (1984) for:(a) 8.6 GHz X-,(b) 13GHz and (c) 17 GHz K_u- and (d) 35GHz K_a-band

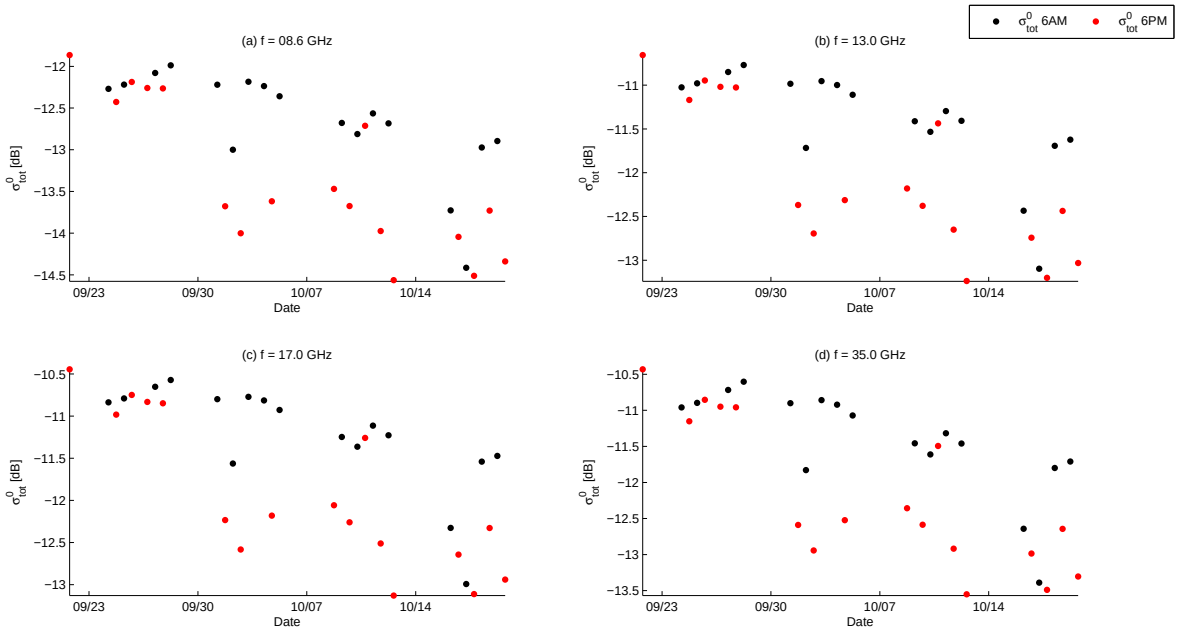

Figure 3-16: Total modeled radar backscatter time series using modified Ulaby *et al.* (1984) for X-, K_u- and K_a-band

Chapter 4

Conclusions and recommendations

4-1 Conclusions

From 19 August to 19 October 2013 maize was grown and measured. From 24 September to 19 October, diurnal measurements were done of the leaf and stalk water content. Starting at 7 October, the bulk leaf water content showed a negative trend with a confidence of 84% and 98% at AM and PM, respectively, indicating an increase in water stress.

Lab experiments clearly showed the relation between leaf water content and resonant frequency of the sensor. A decrease in leaf water content results in a lower dielectric constant. This was observed in the field as well, where a decrease in bulk leaf water content during the day corresponded with an increase in resonant frequency at the maize leaves.

Dielectric properties of 3 leaves were measured from 7 to 19 October 2013. Leaf 8, 10 and 12 showed different behavior in time. Leaf 8, located around the main ear of the plant, showed a clear diurnal pattern. Between 6AM and 6PM the resonant frequency generally increased, corresponding with a decrease in bulk leaf water content between morning and afternoon. The values of the resonant frequency of leaf 8 at 6AM and 6PM, as well as the diurnal difference, showed an increasing trend with a high level on confidence (87%-99%). This coincided with the negative trend in leaf water content and the increase of water stress (evaporation deficit and soil water tension) in time. Lab experiments showed the relation between resonant frequency of the sensor and leaf water content. Based on the latter, the shift in in resonant frequency as observed in the field is caused by a decrease in leaf water content.

Water stress was quantified by calculating the evaporation deficit and by measuring the soil water tension at 30cm and 50cm depth. Both the evaporation deficit as the soil water tension increased from 7 to 19 October 2013. It is therefore concluded that water stress increased during the measured period, which affected the water status of the maize plants.

Leaf 10 and 12, the upper maize leaves, showed a different response to water stress compared to leaf 8. Various plausible options were given to explain this difference. First, vertical

moisture distribution in maize plants can explain the field measurements. With a theoretical maximum photosynthetic rate around leaf 8 (main ear), a maximum diurnal difference in leaf water content and hence in resonant frequency can be expected. Second, the upper leaves are the first leaves were the vegetation water control mechanisms are activated (e.g. release of ABA). These mechanisms prevent leaves from losing to much water by stabilizing the water content and hence the resonant frequency.

This study showed that vegetation has a complex response to water stress. The field measurements confirm observations from previous studies. As other processes are governing in leaf 8, 10 and 12, a different response in resonant frequencies was measured. Hormones are released in the upper layers to retain water and decreasing the photosynthetic rate. Transpiration by leaf 8 is crucial for the reproductivity of maize (location main ear), which was observed in an increasing diurnal difference in resonant frequency.

The destructive vegetation sampling data and the measured soil moisture were used to perform two modeling studies. First, a sensitivity study of radar backscatter to vegetation water content and soil moisture was conducted. Second, backscatter time series for different frequencies, polarizations and incidence angles were simulated.

For L-,C-,X-,K_u- and K_a-band the sensitivity to soil moisture (ranging from 0 to 0.2 [-]) and vegetation water content (ranging from 1.5 - 3.5 kg m^{-2}) was determined. This showed that at L-band (1.8 GHz, HH, 23°), for low soil moisture content values (< 0.2 [-]) and VWC values between 2.5 and 3.5 kgm^{-2}, vegetation is the main contributor to total backscatter. This is mainly interesting for upcoming soil moisture remote sensing missions (e.g. NASA's SMAP), which assume that soil moisture retrieval is not significantly obstructed by vegetation for low vegetation water content values (< 5 kg m^{-2}).

At higher frequencies radar backscatter was mainly influenced by vegetation water status. Since higher frequencies are less capable of penetrating through canopy, high frequency backscatter mainly consists of canopy surface scattering instead of volume scattering. This brings interesting possibilities for vegetation water status monitoring using high frequency radar configurations. In this study the only variable in high frequency configurations was the frequency. More water-cloud parameters are required to investigate the effect of polarization and incidence angle, in order to find an optimal vegetation monitoring radar setup.

Time series analysis for high frequency radar configurations showed that using the standard water cloud model only a little diurnal difference in backscatter was simulated (0.05 dB). However, a modified water-cloud modeling approach, in which the separate values of leaf and stem water content could be used, yielded a diurnal difference of 0.8 dB. It would be beneficial to simulate more field measurements, using both the conventional (bulk vegetation water content only) and the proposed improved model (leaf and stalk water content separately). The latter would give more insight in the validity of the proposed improvements, after which it can be concluded whether vegetation water status monitoring at high frequencies is possible. However, the results from the modified water-cloud modeling are promising for potential vegetation water status monitoring applications. This study showed that when more detailed data are available and can be using in backscatter models, radar backscattering shows similar trends as water stress increases and leaf water content decreases. This approach modeled an observable effect of water stress on radar backscatter, which is promising for future development of vegetation water status monitoring applications.

4-2 Recommendations

The results of this study are promising and showed that there is a high potential for microwave vegetation monitoring. This is a first step however, and more detailed observations and models are required to explore the full potential.

The two methods (water balance model and measured soil water tension) to quantify water stress yielded satisfactory results. Both the evaporation deficit (based on a water balance) and soil water tension showed a similar pattern and rising trend between 7 and 19 October. However, the mechanisms of water uptake are complex during periods of water stress. Therefore it would be interesting to investigate the possibilities of quantifying water stress of the measured vegetation. For example, soil water tension could be measured at different points of the root zone. Maize roots can reach depths up to 1 m, where a different water status can be found compared to the upper layers. When soil water tension is measured here as well, in addition to soil moisture, a tension profile can be made, which indicates whether vegetation was indeed taking less water up. Soil moisture by itself does not necessarily indicate that root are able to actually take it up.

For next measurement campaigns it would be valuable to measure the leaf water content of individual leaves. During the fieldwork of this study this was not done, which made it impossible to directly link the resonant frequency to leaf water content. Lab measurements showed a clear relation between water content and resonant frequency. However, for quantitative applications the measurements should be calibrated in the field on the vegetation species of interest.

Another suggestion for vegetation sampling is to determine the vertical moisture distribution in the measured plant over time. Several explanations for the differences in dielectric measurements were found in this study, which were related to vertical moisture distribution. For example, the hypothesis that the main ear results in higher photosynthetic rates in the surrounding leaves could be good explanation for the difference in dielectric properties of the measured leaves.

Since vegetation can react in various complex ways, it is not easily found out how the dielectric properties are changed. It would be interesting to measure other vegetation parameters as well. For example, vertical distribution of the photosynthetic rate over time could give a great insight in how leaves are responding to water stress. This could show whether the photosynthetic rate is indeed going down in the upper leaves, as a result of higher stomatal resistance or released ABA hormones.

To better understand the implications on vegetation remote sensing, it is recommended to use a more detailed model to simulate radar backscatter above a vegetated area. Although the water cloud model yielded interesting results, it is too parsimonious to fully understand the measurement results and their effect on radar backscatter. The water cloud model only uses bulk vegetation water status, incidence angle and soil moisture as input. Just by replacing the bulk vegetation water content for separate values of leaf and stalk water content showed interesting modeling results. Providing a more detailed description of vegetation had a significant impact on simulated backscatter. Though validating this approach is still necessary, it shows how selection of vegetation parameters influences the model outcome. By using a more physically based model, one could better understand how different vegetation parts (leaves, stalks, branches) contribute to backscatter. Acknowledging it is not an effortless exercise to

gather more data in the field, it is required in order to arrive at a understanding of what information is captured in radar backscatter.

With the dataset acquired in this study, an additional interesting modeling exercise is recommended. It would be interesting to simulate backscatter using a multi layer model, that can take into account the three levels at which dielectric properties were measured (i.e. leaf 8, 10 and 12).

Eventually it would be beneficial to gain insight in the stalk dielectric properties as well. Although their contribution to total backscatter was minor in the high frequency results from this study, for a better understanding of the diurnal difference in radar backscatter it is required to gain more insight in the dielectric behavior of vegetation as a whole, including stalks.

This study showed that vegetation response is more complex than is often assumed in radar backscatter models. Especially during periods of water stress, vegetation does not react as a homogeneous volume of leaves. Field observations are needed to understand how vegetation behaves during times of declining water availability. Besides, without validation data numerical models are of no use if one wants to understand the mechanisms behind radar backscatter above real life vegetated areas.

This study showed that the effect that water stress has on vegetation is noticeable in the leaf dielectric properties. For water stress monitoring applications one is interested whether the 'critical drop' in vegetation water content and turgor pressure can be detected. The critical drop is a sign of irreversible damage, affecting the crop growth and yield ([48],[105]). During the fieldwork the critical drop did not occur yet. Therefore it would be interesting for further research to measure for a longer period during which water stress is (more severely) induced. Knowing how the critical drop is visible in the dielectric properties and in radar backscatter would contribute to determine whether a water stress monitoring system based on microwave remote sensing would be valuable.

For this thesis only the implications for active microwave remote sensing (i.e. radar) was investigated. However, a few passive microwave missions are currently in service or planned. The acquired dataset from this fieldwork might be used as well to model what signal might be sensed by active microwave sensors. The planned SMAP mission has both active and passive L-band sensors. Understanding more about how sensitive L-band sensors are to soil moisture and vegetation water content could lead to new insights about possible applications for soil moisture and vegetation water status monitoring.

Further research is required before all possibilities of soil moisture and vegetation monitoring using active microwave remote sensing are explored. This study has presented interesting results that hopefully stimulate follow up research projects. The eventual possibility to monitor water status of soil and vegetation on a global scale with high accuracy will lead to plentiful innovative applications that will contribute to improving the state of the world. Vegetation water status monitoring will improve efficient irrigation scheduling and increased food security. Accurate soil moisture retrieval will facilitate precise flood and drought prediction and enhanced weather forecasting. Hopefully this research will function as a stepping stone for new developments in the near future.

Appendix A

Spearman's rank test

Spearman's rank test [106] was applied to test for the absence or presence of trends. This statistical test compares the order of appearance and the magnitude of data points. For example, if both the order of appearance and the magnitude are ranking in a similar ascending fashion, one may conclude that a trend is present. In Spearman's rank test, the ρ-value is determined, which functions as a test statistic. Given certain confidence boundaries, one can subsequently confirm of reject the null hypothesis (no trend is present) using the Student's t-distribution.

In short, the ρ-value is determined using the following equations

$$\rho = 1 - \frac{6\Sigma d_i^2}{n(n^2-1)} \tag{A-1}$$

$$d_i = x_i - y_i \tag{A-2}$$

Where x_i is the rank of the data according to the order of appearance, y_i is the rank of the data based on its magnitude.

A trend is present when ρ lies outside of predefined test values, given a certain confidence boundary. Table A-1 shows the test values for certain confidence boundaries.

Table A-1: Student's t-distribution for 8 samples for given confidence boundaries

Student's t-distribution for 8 samples										
50%	60%	70%	80%	90%	95%	98%	99%	99.5%	99.8%	99.9%
0.706	0.889	1.108	1.397	1.860	2.306	2.896	3.355	3.833	4.501	5.041

Appendix B

Dielectric measurements

This section shows the results of the dielectric measurements, averaged per vein/blade and per incidence angle (45°/90°). As can be seen in Fig. B-1 and B-2 the patterns do not deviate much from the results obtained by averaging over all points. For leaf 8 the AM and PM values and diurnal difference increase, indicating a decrease in moisture content. Leaf 10 and 12 show only a small diurnal difference and the AM and PM values keep a relatively constant value. This indicates that water more retained instead of being evaporated (higher stomatal resistance, decrease in photosynthetic rate).

The only deviating aspects is the missing data of the blade of leaf 12 after 12 October, Fig. B-1. The blade was not measured between 12 and 19 October because it would have involved positioning the leaf in a way that may have caused permanent damage.

Recall that an increase in resonant frequency indicates a decrease in leaf water content and dielectric constant.

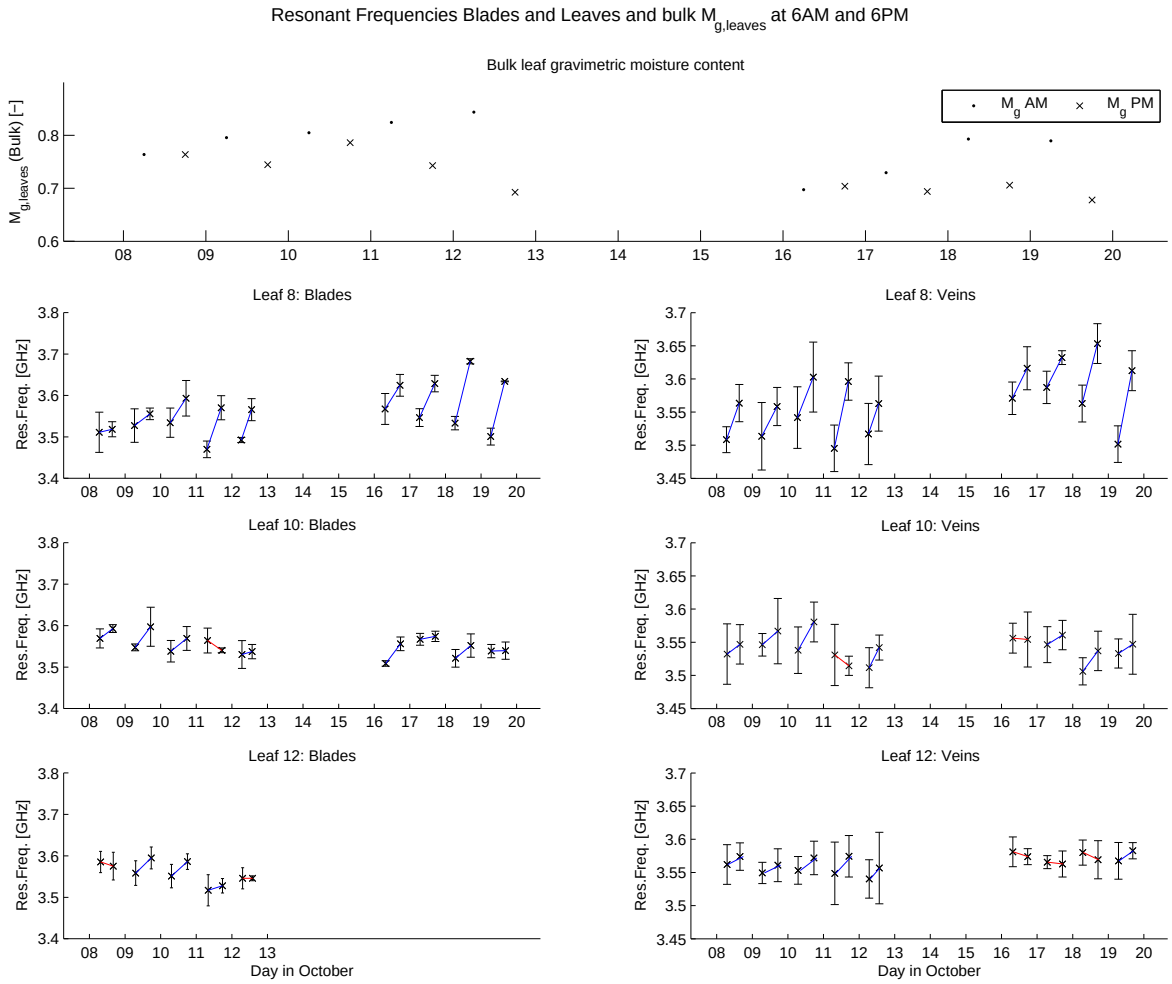

Figure B-1: Upper: Bulk leaf water content as function of time.. Lower figures: resonant frequencies of the microstrip line sensor at leaf 8, 10 and 12 in time, averaged per leaf over blade and vein measurements. Blue and red lines respectively indicate an increase and decrease of resonant frequency during the day.

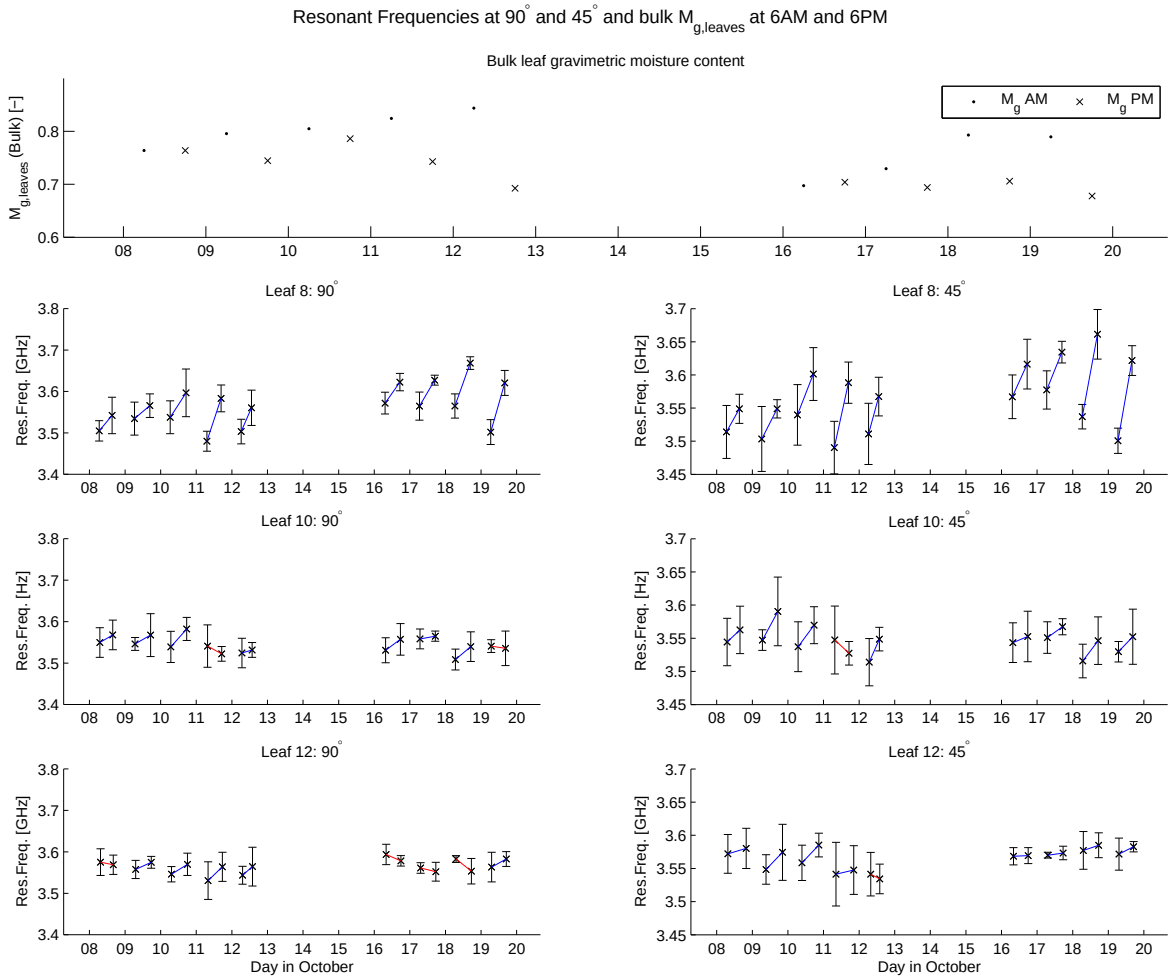

Figure B-2: Upper: Bulk leaf water content as function of time.. Lower figures: resonant frequencies of the microstrip line sensor at leaf 8, 10 and 12 in time, averaged per leaf over 90° and 45° measurements. Blue and red lines respectively indicate an increase and decrease of resonant frequency during the day.

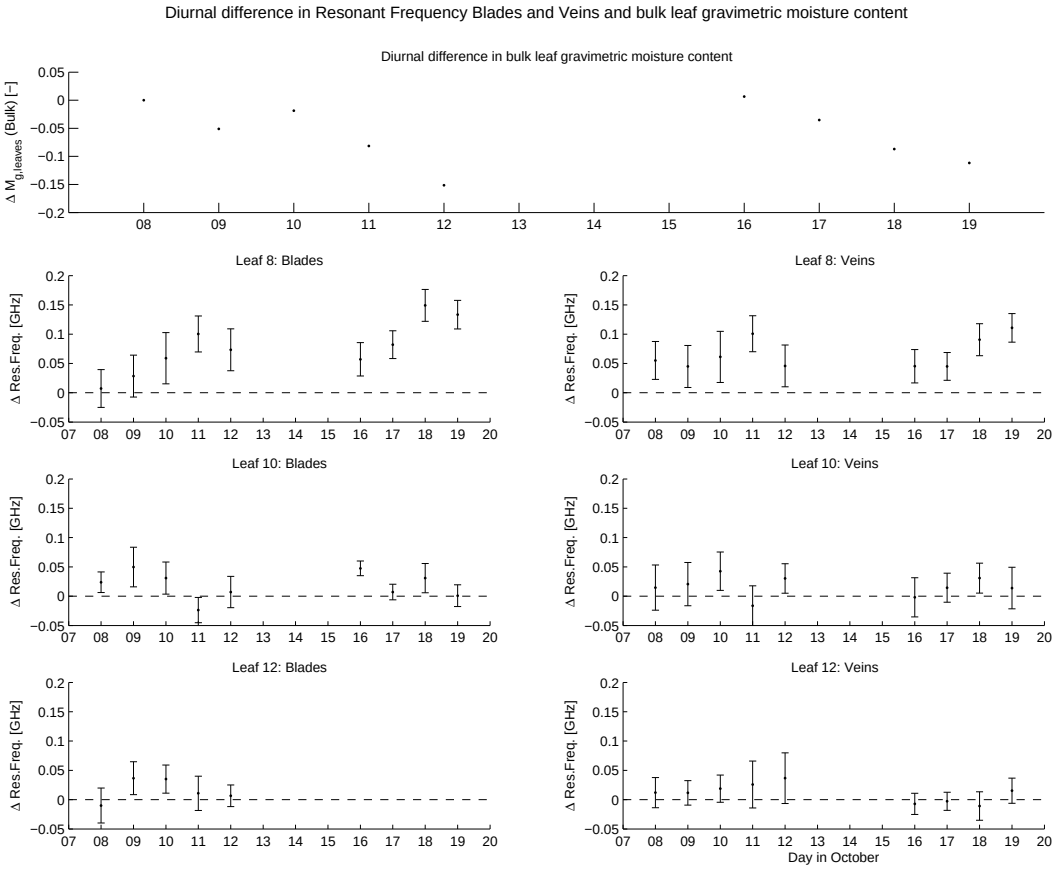

Figure B-3: Upper: Diurnal difference in bulk leaf water content as function of time. Lower figures: Diurnal difference in resonant frequencies of the microstrip line sensor at leaf 8, 10 and 12 in time, averaged per leaf over blade and vein measurements. Blue and red lines respectively indicate an increase and decrease of resonant frequency during the day.

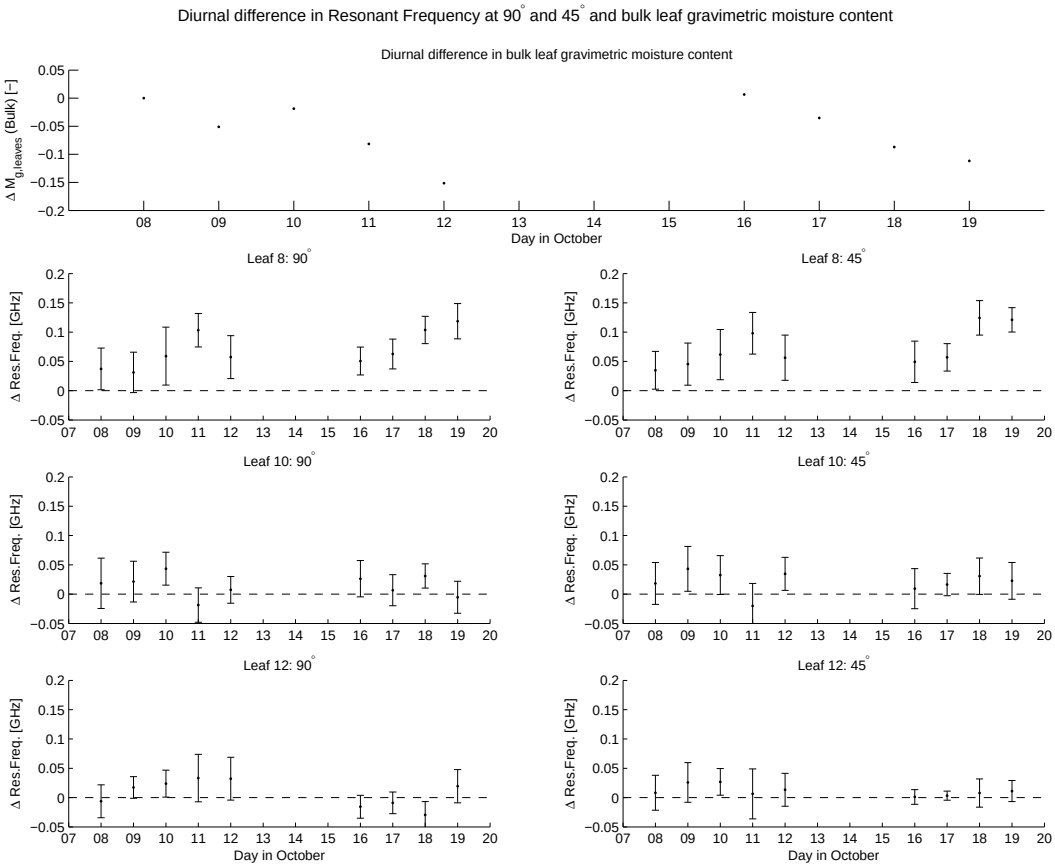

Figure B-4: Upper: Diurnal difference in bulk leaf water content as function of time.. Lower figures: Diurnal difference in resonant frequency of the microstrip line sensor at leaf 8, 10 and 12, averaged over 90° and 45° measurements per leaf.

Appendix C

Water-cloud model results

In this section the modeling results for all radar frequencies can be found.

For both the Ulaby *et al.* [66] and the modified Ulaby *et al.* model, the frequency is plotted against total backscatter Fig. C-1 and C-2, for three values of vegetation water content (observed minimum, observed maximum and observed mean). These figures show that at higher frequencies the magnitude of the observed backscatter increases. For the improved modeling approach however, the highest backscatter is not found for the highest frequency. This is explained by the fact that during the maximum bulk water content, the leaf water content was not at its maximum. The difference in backscatter between the minimum and maximum measured soil moisture is approximately 2.5 dB, which is is significantly higher than for the conventional modeling approach (Fig. C-1).

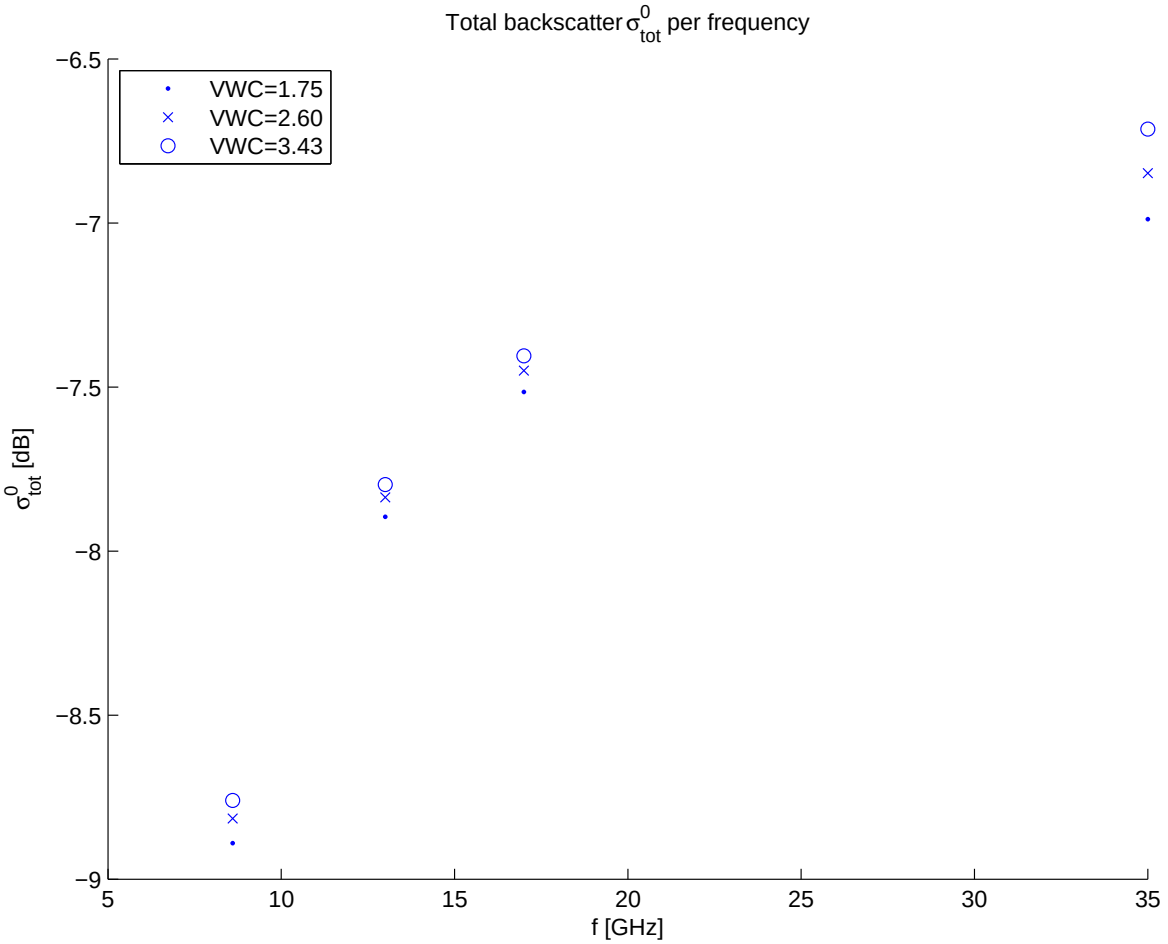

Figure C-1: Frequency vs. total backscatter for X- (8.6 GHz), K_u- (13, 17 GHz) and K_a-band (35 GHz) , based on maximum, minimum and average vegetation water content, modeled with the water-cloud model presented by Ulaby *et al.* (1984)

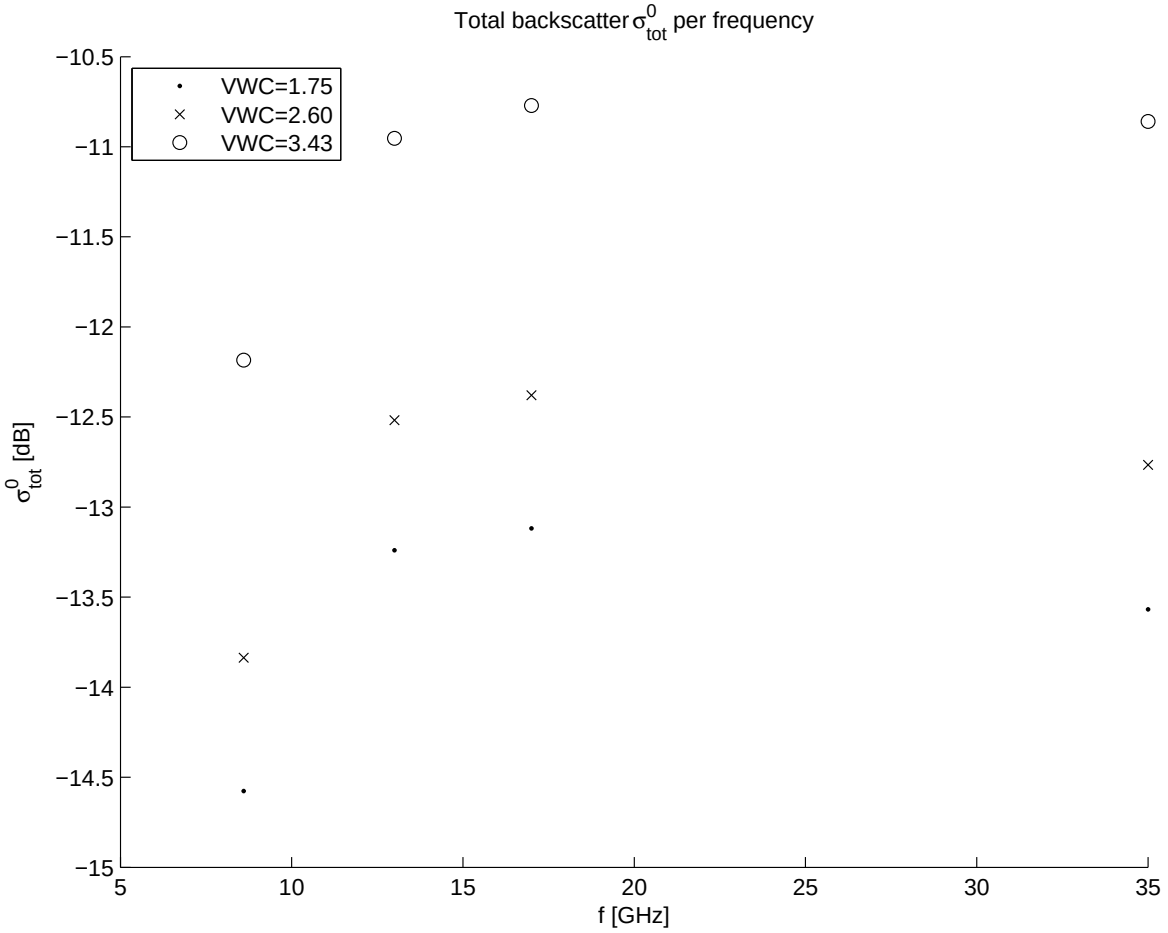

Figure C-2: Frequency vs. total backscatter for X- (8.6 GHz), K_u- (13, 17 GHz) and K_a-band 35 GHz), based on maximum, minimum and average vegetation water content, modeled with modified Ulaby *et al.* (1984) water-cloud model

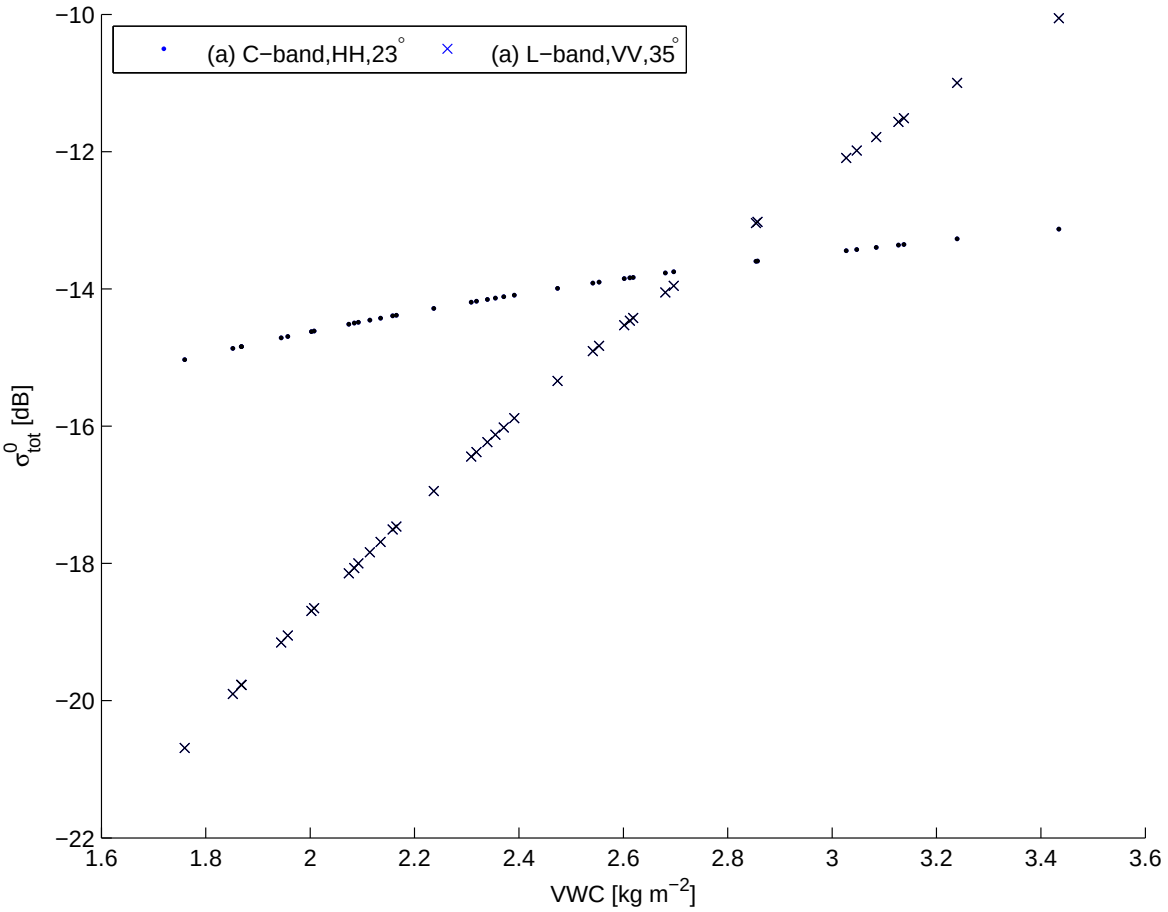

Figure C-3: Frequency vs. total backscatter for C-band (5.3 GHz)(HH,θ=23°) and L-band (1.8 GHz)(VV,θ=35°), modeled with the water-cloud model presented by Dabrowska-Zielinska *et al.* (2007)

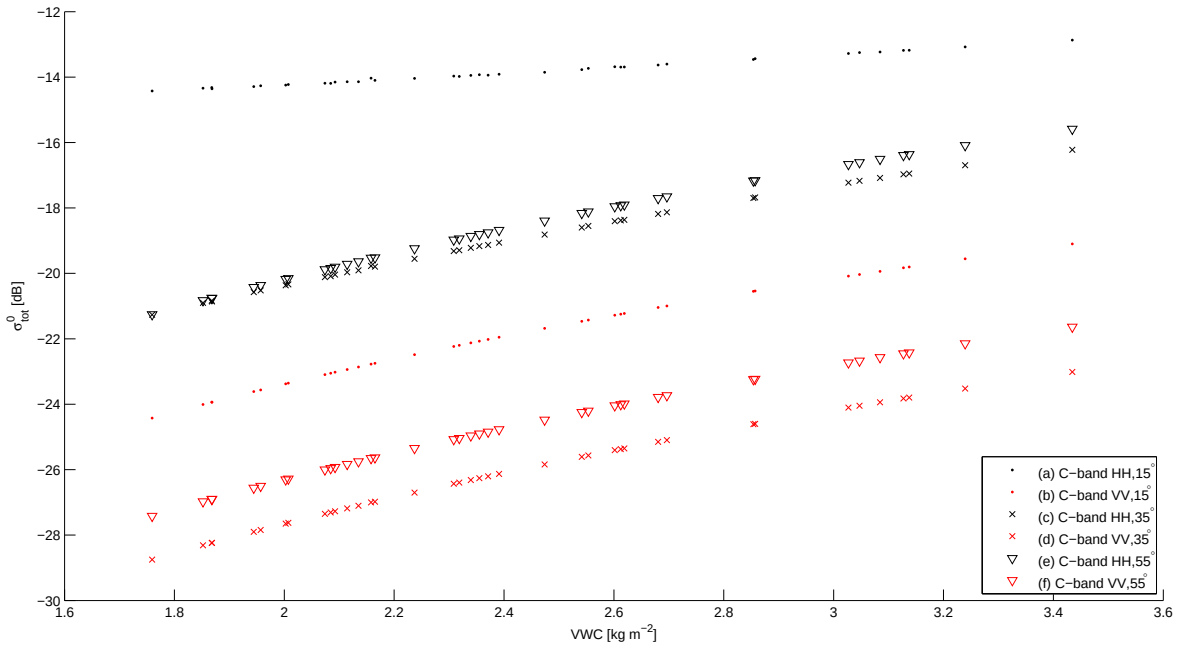

Figure C-4: VWC vs. σ^2_{tot} for C-band (4.75 GHz) at VV and HH polarization and an incidence angle of 15°, 35° and 55° modeled with Jospeh *et al.* (2008).

Bibliography

[1] D. Hillel, *Evironmental Soil Physics*. Academic Press, San Diego, 1998.

[2] Y. H. Kerr, J. Font, P. Waldteufel, and M. Berger, "The soil moisture and ocean salinity mission SMOS," *Earth Observation Quarterly*, vol. 66, pp. 18–25, 2000.

[3] R. Koster, S. Mahanama, T. Yamada, G. Balsamo, M. Boisserie, P. Dirmeyer, F. Doblas-Reyes, C. Gordon, Z. Guo, J. Jeong, D. Lawrence, Z. Li, L. Luo, S. Malyshev, W. Merryfield, S. Seneviratne, T. Stanelle, B. van den Hurk, F. Vitart, and E. Wood, "The contribution of land initialization to subseasonal forecast skill: first results from the GLACE–2 Project.," *Geophys. Res. Lett.*, vol. 37, p. L02402, 2010.

[4] T. J. Jackson, "III. measuring surface soil moisture using passive microwave remote sensing," *Hydrological processes*, vol. 7, no. 2, pp. 139–152, 1993.

[5] D. Entekhabi and I. Rodriguez-Iturbe, "Analytical framework for the characterization of the space-time variability of soil moisture," *Advances in water resources*, vol. 17, no. 1, pp. 35–45, 1994.

[6] D. Entekhabi, I. Rodriguez-Iturbe, and F. Castelli, "Mutual interaction of soil moisture state and atmospheric processes," *Journal of Hydrology*, vol. 184, no. 1, pp. 3–17, 1996.

[7] S. I. Seneviratne, T. Corti, E. L. Davin, M. Hirschi, E. B. Jaeger, I. Lehner, B. Orlowsky, and A. J. Teuling, "Investigating soil moisture–climate interactions in a changing climate: A review," *Earth-Science Reviews*, vol. 99, no. 3, pp. 125–161, 2010.

[8] L. Alfieri, P. Claps, P. D'Odorico, F. Laio, and T. Over, "An analysis of the soil moisture feedback on convective and stratiformprecipitation," *J.Hydrometeorol.*, vol. 9, no. 2, pp. 280–291, 2008.

[9] C. Hohenegger, P. Brockhaus, C. Bretherton, and C. Schär, "The soil moisture–precipitation feedback in simulations with explicit and parameterized convection.," *J.Climate*, vol. 22, no. 19, pp. 5003 – 5020, 2009.

[10] K. J. Beven and K. Beven, *Rainfall-runoff modelling*. Wiley Online Library, 2001.

[11] W. Wagner, G. Bloschl, P. Pampaloni, J. Calvet, B. Bizzarri, J. Wigneron, and Y. Kerr, "Operational readiness of microwave remote sensing of soil moisture for hydrologic applications," 2007.

[12] M. Sivapalan, K. Takeuchi, S. Franks, V. Gupta, H. Karambiri, V. Lakshmi, X. Liang, J. McDonnell, E. Mendiondo, P. O'Connell, T. Oki, J. Pomeroy, D. Schertzer, S. Uhlenbrook, and E. Zehe, "IAHS Decade on Predictions in Ungauged Basins (PUB), 2003–2012: Shaping an exciting future for the hydrological sciences," *Hydrological Sciences Journal*, vol. 48, no. 6, pp. 857–880, 2003.

[13] M. Sivapalan, "Prediction in ungauged basins: A grand challenge for theoretical hydrology," *Hydrological Processes*, vol. 17, no. 15, pp. 3163–3170, 2003.

[14] H. Winsemius, B. Schaefli, A. Montanari, and H. Savenije, "On the calibration of hydrological models in ungauged basins: A framework for integrating hard and soft hydrological information," *Water Resources Research*, vol. 45, no. 12, p. W12422, 2009.

[15] I. Rodriguez-Iturbe, A. Porporato, F. Laio, and L. Ridolfi, "Plants in water-controlled ecosystems: active role in hydrologic processes and response to water stress: I. scope and general outline," *Advances in Water Resources*, vol. 24, no. 7, pp. 695–705, 2001.

[16] A. Porporato, F. Laio, L. Ridolfi, and I. Rodriguez-Iturbe, "Plants in water-controlled ecosystems: Active role in hydrologic processes and response to water stress: Iii. vegetation water stress," *Advances in Water Resources*, vol. 24, no. 7, pp. 725–744, 2001.

[17] T. Jackson, J. Schmugge, and E. Engman, "Remote sensing applications to hydrology: soil moisture," *Hydrological Sciences Journal*, vol. 41, no. 4, pp. 517–530, 1996.

[18] H. G. Jones and R. A. Vaughn, *Remote sensing of vegetation. Principles, techniques, and applications*. Oxford University Press, 2010.

[19] T. J. Schmugge, W. P. Kustas, J. C. Ritchie, T. J. Jackson, and A. Rango, "Remote sensing in hydrology," *Advances in water resources*, vol. 25, no. 8, pp. 1367–1385, 2002.

[20] M. L. Imhoff, "Radar backscatter and biomass saturation: ramifications for global biomass inventory," *Geoscience and Remote Sensing, IEEE Transactions on*, vol. 33, no. 2, pp. 511–518, 1995.

[21] J. Cimino, A. Brandani, D. Casey, J. Rabassa, and S. D. Wall, "Multiple incidence angle SIR–B experiment over Argentina: mapping of forest units," *Geoscience and Remote Sensing, IEEE Transactions on*, no. 4, pp. 498–509, 1986.

[22] I. Woodhouse, *Introduction to microwave remote sensing*. Taylor and Francis, 2006.

[23] S. Paloscia, G. Macelloni, P. Pampaloni, and S. Sigismondi, "The potential of C-and L-band SAR in estimating vegetation biomass: the ERS-1 and JERS–1 experiments," *Geoscience and Remote Sensing, IEEE Transactions on*, vol. 37, no. 4, pp. 2107–2110, 1999.

[24] R. Bindlish and A. Barros, "Parameterization of vegetation backscatter in radar-based soil moisture estimation," *Remote Sens. Environ.*, vol. 76, no. 1, pp. 130–137, 2001.

[25] P. Ferrazzoli, S. Paloscia, P. Pampaloni, G. Schiavon, S. Sigismondi, and D. Solimini, "The potential of multifrequency polarimetric sar in assessing agricultural and arboreous biomass," *Geoscience and Remote Sensing, IEEE Transactions on*, vol. 35, no. 1, pp. 5–17, 1997.

[26] F. Ulaby, K. Sarabandi, K. McDonald, M. Whitt, and C. Dobson, "Michigan microwave canopy scattering model," *International Journal of Remote Sensing*, vol. 11, no. 07, pp. 1223 – 1253, 1990.

[27] W. Wagner, G. Lemoine, and H. Rott, "A method for estimating soil moisture from ers scatterometer and soil data," *Remote Sensing of Environment*, vol. 70, no. 2, pp. 191–207, 1999.

[28] R. A. de Jeu, W. Wagner, T. R. Holmes, A. Dolman, N. Van De Giesen, and J. Friesen, "Global soil moisture patterns observed by space borne microwave radiometers and scatterometers," *Surveys in Geophysics*, vol. 29, no. 4, pp. 399–420, 2008.

[29] D. Entekhabi, E. Njoku, P. O'Neill, K. Kellogg, W. Crow, W. N. Edelstein, J. Entin, S. Goodman, T. Jackson, J. Johnson, J. Kimball, J. Piepmeier, R. Koster, N. Martin, K. McDonald, M. Moghaddam, S. Moran, R. Reichle, J. Shi, M. Spencer, W. W. Thurman, T. Leung, and J. van Zyl, "The Soil Moisture Active Passive (SMAP) Mission„" *Proceedings of the IEEE*, vol. 98, no. 5, pp. 704 – 716, 2010.

[30] S. C. Steele-Dunne, J. Friesen, and N. van de Giesen, "Using diurnal variation in backscatter to detect vegetation water stress," *Geoscience and Remote Sensing, IEEE Transactions on*, vol. 50, no. 7, pp. 2618–2629, 2012.

[31] J. Friesen, S. C. Steele-Dunne, and N. van de Giesen, "Diurnal Differences in Global ERS Scatterometer Backscatter Observations of the Land Surface," *Geoscience and Remote Sensing, IEEE Transactions on*, vol. 50, no. 7, pp. 2595–2602, 2012.

[32] K. McDonald, M. Dobson, and F. Ulaby, "Using MIMICS to Model L-band Multiangle and Multitemporal backscatter From a Walnut Orchard," *IEEE Trans. Geosci. and Remote Sensing*, vol. 28, no. 4, pp. 477 – 491, 1990.

[33] K. McDonald, R. Zimmermann, J. Way, and R. Oren, "An investigation of the relationship between tree water potential and dielectric constant," *IGARSS'92; Proceerding of the 12th Annual International Geoscience and Remote Sensing Symposium, Houston, TX*, pp. 523 – 525, 1992.

[34] F. T. Ulaby and R. Jedlicka, "Microwave dielectric properties of plant materials," *IEEE Transactions on Geoscience and Remote Sensing*, vol. 22, no. 4, pp. 406–415, 1984.

[35] M. El-Rayes and F. Ulaby, "Microwave dielectric spectrum of vegetation Part I: Experimental observations," *IEEE Transactions on Geoscience and Remote Sensing*, vol. 25, no. 5, pp. 541–549, 1987.

[36] F. T. Ulaby and M. A. El-Rayes, "Microwave dielectric spectrum of vegetation–Part II: Dual-dispersion model," *Geoscience and Remote Sensing, IEEE Transactions on*, no. 5, pp. 550–557, 1987.

[37] N. Carlson, *Dielectric constant of vegetation at 8.5 GHz,Technical Report 1903-5.* Ohio State University ElectroScience Laboratory,Columbus, Ohio, 1967.

[38] E. J. Burke, R. C. Harlow, and T. P. Ferre, "Measuring the dielectric permittivity of a plant canopy and its response to changes in plant water status: An application of impulse time domain transmission," *Plant and Soil*, vol. 268, pp. 132–133, 2005.

[39] J. R. Wang and T. J. Schmugge, "An empirical model for the complex dielectric permittivity of soils as a function of water content," *IEEE Transactions on Geoscience and Remote Rensing*, vol. GE-18, no. 4, 1980.

[40] M. C. Dobson, F. T. Ulaby, M. T. Hallikainen, and M. A. El-Rayes, "Microwave Dielectric Behavior of Wet Soil - Part II: Dielectric Mixing Models," *IEEE Transactions on Geoscience and Remote Sensing*, vol. 23, no. 1, pp. 35–46, 1985.

[41] M. C. Dobson and F. T. Ulaby, "Active microwave soil moisture research," *IEEE Transactions on Geoscience and Remote Sensing*, vol. 24, no. 1, pp. 23–36, 1986.

[42] M. El-Reyes, A. Mohammend, and F. Ulaby, "Microwave dielectric behavior of vegetation material," *Univ. Michigan Tech. Rep., RL-022132-3-T*, 1987.

[43] R. Sharp and W. Davies, "Root growth and water uptake by maize plants in drying soil," *Journal of Experimental Botany*, vol. 36, no. 170, pp. 1441–1456, 1985.

[44] K. Mekonnen, R. Buresh, and B. Jama, "Root and inorganic nitrogen distributions in sesbania fallow, natural fallow and maize fields," *Plants and Soil*, vol. 188, pp. 319–327, 1997.

[45] T. C. Hsiao and E. Acevedo, "Plant responses to water deficits, water-use efficiency, and drought resistance," *Agricultural Meteorology*, vol. 14, no. 1, pp. 59–84, 1974.

[46] O. Ghannoum, "C4 photosynthesis and water stress," *Annals of Botany*, vol. 103, pp. 635–644, 2009.

[47] E. Acevedo, E. Fereres, T. Hsiao, and D. Hendserson, "Diurnal growth trends, water potential and osmotic adjustment of maize and sorghum leaves in the field," *Plant Physiology*, vol. 64, pp. 476–480, 1979.

[48] T. C. Hsiao, "Plant responses to water stress," *Ann Rev. Plant Physiol.*, vol. 24, pp. 519–570, 1973.

[49] R. Cakir, "Effect of water stress at different development stages on vegetative and reproductive growth of corn," *Field Crops Research*, vol. 89, pp. 1–16, 2004.

[50] L. Evans, I. Wardlaw, and C. Williams, "Environmental control of growth," *Grasses and grasslands*, pp. 102–25, 1964.

[51] E. Acevedo, T. C. Hsiao, and D. Henderson, "Immediate and subsequent growth responses of maize leaves to changes in water status," *Plant Physiology*, vol. 48, no. 5, pp. 631–636, 1971.

[52] C. Igathinathane, A. Womac, S. Sokhansanj, and L. Pordesimo, "Mass and moisture distribution in aboveground components of standing corn plants," *Transactions of the ASABE*, vol. 49, no. 1, pp. 97–106, 2006.

[53] J. Friesen, "Regional vegetation water effects on satellite soil moisture estimations for West Africa," *Ecology and Development Series*, no. 63, 2008.

[54] W. P. Köppen, R. Geiger, M. Milankovitch, V. Conrad, W. Borchardt, K. Wegener, and A. Wagner, *Handbuch der klimatologie*, vol. 3. Gebrüder Borntraeger, 1930.

[55] B. Shrestha, H. Wood, and S. Sokhansanj, "Modeling of vegetation permittivity at microwave frequencies," *IEEE Transactions on Geoscience and Remote Sensing*, vol. 45, no. 2, pp. 342–348, 2007.

[56] A. Franchois, Y. Pineiro, and R. H. Lang, "Microwave permittivity measurements of two conifers," *Geoscience and Remote Sensing, IEEE Transactions on*, vol. 36, no. 5, pp. 1384–1395, 1998.

[57] H. Tan, "Microwave measurements and modelling of the permittivity of tropical vegetation samples," *Applied physics*, vol. 25, pp. 351–355, 1981.

[58] K. Sarabandi and F. Ulaby, "Technique for measuring the dielectric constant of thin materials," *Instrumentation and Measurement, IEEE Transactions on*, vol. 37, no. 4, pp. 631–636, 1988.

[59] B.-K. Chung, "Dielectric constant measurement for thin material at microwave frequencies," *Progress In Electromagnetics Research*, vol. 75, pp. 239–252, 2007.

[60] D. Sancho-Knapik, J. Gismero, A. Asensio, J. Peguero-Pina, V. Fernandez, T. Alvarez-Arenas, and E. Gil-Pelegrin, "Microwave L-band (1730 MHz) accurately estimates the relative water content in poplar leaves. A comparison with a near infrared water index (R1300/R1450)," *Agricultural and Forest Meteorology*, vol. 151, no. 7, pp. 827 – 832, 2011.

[61] D. Sancho-Knapik, J. J. Peguero-Pina, H. Medrano, M. D. Fariñas, T. G. Álvarez-Arenas, and E. Gil-Pelegrín, "The reflectivity in the s-band and the broadband ultrasonic spectroscopy as new tools for the study of water relations in vitis vinifera l.," *Physiologia Plantarum*, 2012.

[62] M. I. Menzel, S. Tittmann, J. Bühler, S. Preis, N. Wolters, S. Jahnke, A. Walter, A. Chlubek, A. Leon, N. Hermes, A. Offenhäuser, F. Gilmer, P. Blümler, U. Schurr, and H.-J. Krause, "Non-invasive determination of plant biomass with microwave resonators," *Plant, Cell & Environment*, vol. 32, no. 4, pp. 368–379, 2009.

[63] S.C.Steele-Dunne, G.A.Steele, T. Emmerik, and N. de Giesen, "A microstrip line resonator for in-vivo measurements of leaf water content through its effect on leaf dielectric constant," *(submitted)*.

[64] J. Monteith, "Evaporation and environment," in *Symp. Soc. Exp. Biol*, vol. 19, p. 4, 1965.

[65] R. G. Allen, L. Pereira, D. Raes, and M. Smith, "FAO Irrigation and drainage paper No. 56," *Rome: Food and Agriculture Organization of the United Nations*, pp. 26–40, 1998.

[66] F. Ulaby, C. Allen, G. Eger, and E. Kanemasu, "Relating the microwave backscattering coefficient to leaf area index," *Remote Sens. Environ.*, vol. 14, no. 1-3, pp. 113–133, 1984.

[67] E. Attema and F. Ulaby, "Vegetation modeled as a water cloud," *Radio Sci.*, vol. 13, no. 2, pp. 357–364, 1978.

[68] C. D. Myron, F. T. Ulaby, M. T. Hallikainen, and M. A. El-Rayes, "Microwave Dielectric Behavior of Wet Soil - Part Ii: Dielectric Mixing Models," *IEEE Transactions on Geoscience and Remote Rensing*, vol. GE-23, no. 1, 1985.

[69] M. A. Karam, A. K. Fung, R. H. Lang, and N. S. Chauhan, "A microwave scattering model for layered vegetation," *Geoscience and Remote Sensing, IEEE Transactions on*, vol. 30, no. 4, pp. 767–784, 1992.

[70] T. Le Toan, A. Beaudoin, J. Riom, and D. Guyon, "Relating forest biomass to SAR data," *Geoscience and Remote Sensing, IEEE Transactions on*, vol. 30, no. 2, pp. 403–411, 1992.

[71] L. Prévot, I. Champion, and G. Guyot, "Estimating surface soil moisture and leaf area index of a wheat canopy using a dual-frequency (C– and X– Bands) scatterometer," *Remote Sensing of Environment*, vol. 46, pp. 331–339, 1993.

[72] A. Joseph, R. van der Velde, P. O'Neill, R. Lang, and T. Gish, "Effects of corn on C– and L–band radar backscatter: A correction method for soil moisture retrieval," *Remote Sensing of Environment*, vol. 114, pp. 2417–2430, 2010.

[73] S. L. Durden, L. A. Morrissey, and G. P. Livingston, "Microwave backscatter and attenuation dependence on leaf area index for flooded rice fields," *Geoscience and Remote Sensing, IEEE Transactions on*, vol. 33, no. 3, pp. 807–810, 1995.

[74] Y. Inoue, T. Kurosu, H. Maeno, S. Uratsuka, T. Kozu, K. Dabrowska-Zielinska, and J. Qi, "Season-long daily measurements of multifrequency (K_a, K_u, X, C, and L) and full-polarization backscatter signatures over paddy rice field and their relationship with biological variables," *Remote Sensing of Environment*, vol. 81, no. 2, pp. 194–204, 2002.

[75] K. Dabrowska-Zielinksa, Y. Inoue, W. Kowalik, and M. Gruszcynska, "Inferring the effect of plant and soil variables on C- and L-band SAR backscatter over agricultural fields, based on model analysis," *Advances in Space Research*, vol. 39, pp. 139–148, 2007.

[76] I. Champion, L. Prevot, and G. Guyot, "Generalized semi-empirical modelling of wheat radar response," *International Journal of Remote Sensing*, vol. 21, no. 9, pp. 1945–1951, 2000.

[77] J. Álvarez-Mozos, J. Casali, M. Gonzalez-Audicana, and N. E. Verhoest, "Assessment of the operational applicability of RADARSAT–1 data for surface soil moisture estimation," *Geoscience and Remote Sensing, IEEE Transactions on*, vol. 44, no. 4, pp. 913–924, 2006.

[78] A. K. Fung, Z. Li, and K. Chen, "Backscattering from a randomly rough dielectric surface," *Geoscience and Remote Sensing, IEEE Transactions on*, vol. 30, no. 2, pp. 356–369, 1992.

[79] P. C. Dubois, J. van Zyl, and T. Engman, "Measuring soil moisture with imaging radars," *IEEE Transactions on Geoscience and Remote Sensing*, vol. 33, no. 4, pp. 915–926, 1995.

[80] P. C. Dubois, J. van Zyl, and T. Engman, "Corrections to "Measuring soil moisture with imaging radars"," *IEEE Transactions on Geoscience and Remote Sensing*, vol. 33, no. 6, p. 1340, 1995.

[81] Y. Oh and K. Sarabandi, "An empirical model and an inversion technique for radar scattering from bare soil surfaces," *IEEE Transactions on Geoscience and Remote Sensing*, vol. 30, no. 2, pp. 370–311, 1992.

[82] Y. Oh, "Quantitative retrieval of soil moisture content and surface roughness from multipolarized radar observations of bare soil surfaces," *IEEE Transactions on Geoscience and Remote Sensing*, vol. 42, no. 3, pp. 596–601, 2004.

[83] A. Joseph, R. van der Velde, P. O'Neill, and R. Lang, "Soil moisture retrieval during a corn growth cycle using L-band (1.6 GHz) radar observations," *IEEE Transactions on Geoscience and Remote Sensing*, vol. 46, no. 8, pp. 2365–2374, 2008.

[84] J. Hanway and S. Ritchie, "How a corn plant develops," *Special Report No. 48, Iowa State University*, 1984.

[85] E. Nafziger, *Illinois Agronomy Handbook*. University of Illinois, 2012.

[86] E. Buckingham, "Studies on the movement of soil moisture," *USDA Bur. Soils Bull.*, vol. 38, p. 61 pp, 1907.

[87] M. T. Van Genuchten, "A closed-form equation for predicting the hydraulic conductivity of unsaturated soils," *Soil Science Society of America Journal*, vol. 44, no. 5, pp. 892–898, 1980.

[88] M. T. van Genuchten and D. R. Nielsen, "On describing and predicting the hydraulic properties of unsaturated soils," *Annales Geophysicae*, vol. 3, no. 5, pp. 615–628, 1985.

[89] J. Simunek and M. van Genuchten, "Estimating unsaturated soil hydraulic properties from tension disc infiltrometer data by numerical inversion," *Water Resources Research*, vol. 32, no. 9, pp. 2683–2696, 1995.

[90] J. Syvertsen, "Minimum leaf water potential and stomatal closure in citrus leaves of different ages," *Annals of botany*, vol. 49, no. 6, pp. 827–834, 1982.

[91] L. Dwyer and D. Stewart, "Effect of leaf age and position on net photosynthetic rates in maize (Zea mays L.)," *Agricultural and forest meteorology*, vol. 37, no. 1, pp. 29–46, 1986.

[92] W. R. Jordan, K. W. Brown, and J. C. Thomas, "Leaf age as a determinant in stomatal control of water loss from cotton during water stress," *Plant Physiology*, vol. 56, no. 5, pp. 595–599, 1975.

[93] N. Turner and L. Incoll, "The vertical distribution of photosynthesis in crops of tobacco and sorghum," *Journal of Applied Ecology*, pp. 581–591, 1971.

[94] N. C. Turner and J. E. Begg, "Stomatal behavior and water status of maize, sorghum, and tobacco under field conditions I. At high soil water potential," *Plant physiology*, vol. 51, no. 1, pp. 31–36, 1973.

[95] N. C. Turner, "Stomatal behavior and water status of maize, sorghum, and tobacco under field conditions II. At low soil water potential," *Plant Physiology*, vol. 53, no. 3, pp. 360–365, 1974.

[96] N. Turner, "Adaptation to water deficits: a changing perspective," *Functional Plant Biology*, vol. 13, no. 1, pp. 175–190, 1986.

[97] P. Holmgren, P. G. Jarvis, and M. S. Jarvis, "Resistances to carbon dioxide and water vapour transfer in leaves of different plant species," *Physiologia Plantarum*, vol. 18, no. 3, pp. 557–573, 1965.

[98] R. Slatyer and J. Bierhuizen, "The influence of several transpiration suppressants on transpiration, photosynthesis, and water-use efficiency of cotton leaves," *Australian Journal of Biological Sciences*, vol. 17, no. 1, pp. 131–146, 1964.

[99] K. Brown and N. J. Rosenberg, "Influence of leaf age, illumination, and upper and lower surface differences on stomatal resistance of sugar beet (beta vulgaris) leaves," *Agronomy Journal*, vol. 62, no. 1, pp. 20–24, 1970.

[100] M. F. Beardsell and D. Cohen, "Relationships between leaf water status, abscisic acid levels, and stomatal resistance in maize and sorghum," *Plant Physiology*, vol. 56, no. 2, pp. 207–212, 1975.

[101] M. W. Lang, P. A. Townsend, and E. S. Kasischke, "Influence of incidence angle on detecting flooded forests using c-hh synthetic aperture radar data," *Remote sensing of environment*, vol. 112, no. 10, pp. 3898–3907, 2008.

[102] Y. Rauste, "Incidence-angle dependence in forested and non-forested areas in seasat sar data," *International Journal of Remote Sensing*, vol. 11, no. 7, pp. 1267–1276, 1990.

[103] L. L. Hess, J. M. Melack, S. Filoso, and Y. Wang, "Delineation of inundated area and vegetation along the amazon floodplain with the sir-c synthetic aperture radar," *Geoscience and Remote Sensing, IEEE Transactions on*, vol. 33, no. 4, pp. 896–904, 1995.

[104] N. N. Das, D. Entekhabi, and E. G. Njoku, "An algorithm for merging SMAP radiometer and radar data for high-resolution soil-moisture retrieval," *Geoscience and Remote Sensing, IEEE Transactions on*, vol. 49, no. 5, pp. 1504–1512, 2011.

[105] K. Subramanian, C. Charest, L. Dwyer, and R. Hamilton, "Arbuscular mycorrhizas and water relations in maize under drought stress at tasselling," *New Phytologist*, vol. 129, no. 4, pp. 643–650, 2006.

[106] C. Spearman, "The proof and measurement of association between two things," *The American journal of psychology*, vol. 15, no. 1, pp. 72–101, 1904.